UNIVERSITAT POLITÈCNICA
DE CATALUNYA
BARCELONATECH

Study of the exfoliation process in epoxy-clay nanocomposites

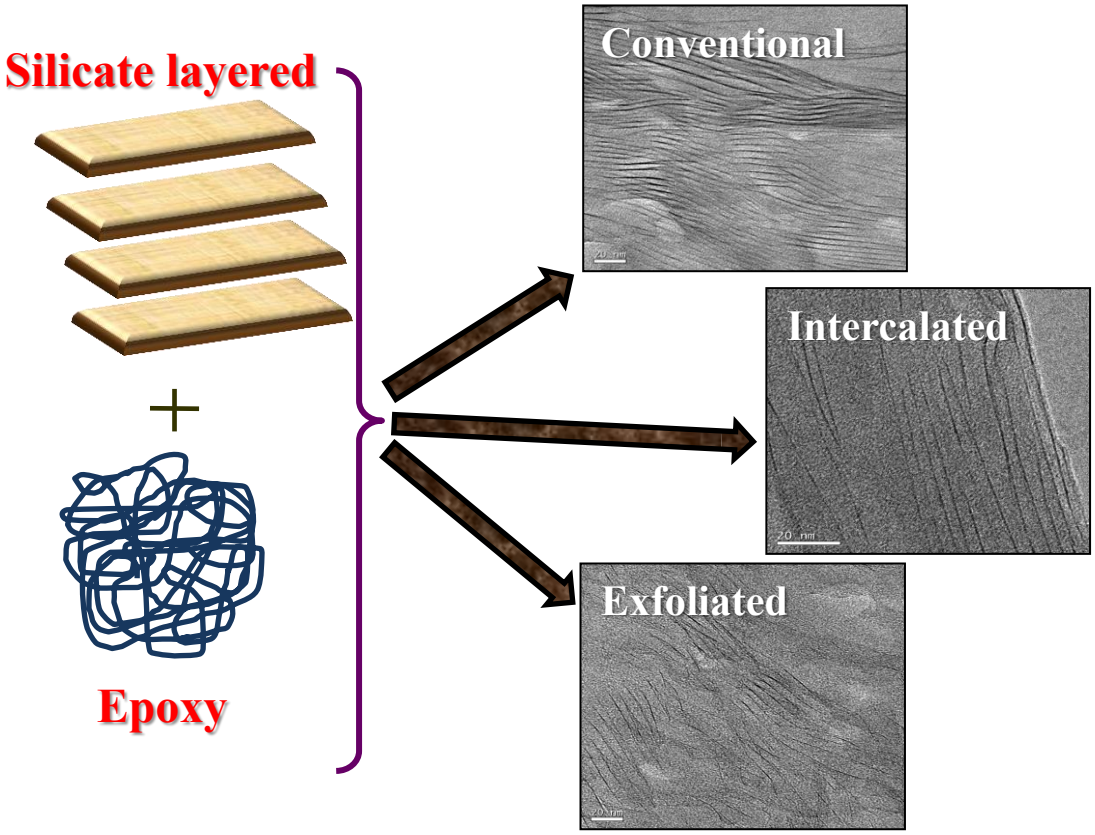

by

Fatemeh Shiravand

Presented to Mechanical Engineering, fluids and Aeronautic program (MFA) in Fulfilment of the Requirements for degree of Doctor Philosophy at the Universitat Politècnica de Catalunya, Barcelona, Spain

Spring 2014

UNIVERSITAT POLITÈCNICA DE CATALUNYA
BARCELONATECH

Doctoral thesis:

Study of the exfoliation process in epoxy-clay nanocomposites

Author: Fatemeh Shiravand

Supervisor: Prof. John M Hutchinson

Advisor: Dr. Yolanda Calventus Solè

Program of doctorate:

Mechanical Engineering, Fluids and Aeronautics (MFA)

Departament de Màquines i Motors Tèrmics (MMT)

School of Industrial and Aeronautical Engineering of Terrassa

Universitat Politècnica de Catalunya

April 2014-Terrassa

I cannot change the direction of the wind but I can adjust my sails to always reach my destination.

- Jimmy Dean -

Preface

Above all, I have to thank God who created us and gave us the mind to think and the ability to work.

I would like to express my gratitude to both my supervisor Prof. John M Hutchinson and my advisor Dr. Yolanda Calventus for their guidance, encouragement, support and constructive criticisms during my study.

Also, I wish to thank Dr. Frida Roman for her help in the operation of laboratory equipment and for her good advice.

Thanks are due to the staff of Autonomus University of Barcelona (UAB) especially Mr. Angel Alvarez, for their help with the transmission electron microscopy (TEM) and small angle X-ray scattering (SAXS), and also thanks to the staff, particularly Mr. Josep Palou and Mr. Francisco Jose Barahona Navarro, respectively, of the ETSEIAT(Escola Tecnica Superior de Enginyeries Industrial y Aeronautica de Terrassa), Universitat Politecnica de Catalunya (UPC), for providing scanning electron microscopy (SEM) facility and in the preparation of the samples for dynamic mechanical analysis.

Special thanks go to my dear colleagues at mechanic and thermic motor department (MMT) especially Pillar, Iria, Pere, Jose and Dr. Xavier Ramis, and also the colleagues in the Universitat Rovira i Virgili in Tarragona, especially Dr. Angel Serra and Dr. Xavier Fernandez for their advice and helpful suggestion through the course of my research and for providing the impact test facility.

Thanks to my dear friends, Amir and Maryam who help me in one way or another along the way.

I would like to thank my parents whom I dedicate this work, for their constant support and their invaluable love and unlimited patience and also my brother who encouraged me to go as far as I could in my studies.

Finally, and with all my heart, I would to show my gratitude to my husband, Hojjat, who is always cheering me up and supports me endlessly.

Barcelona-Terrassa
Spring 2014

Fatemeh Shiravand

Abstract

Cured epoxy resins are highly cross-linked polymers which are increasingly important in high performance engineering field due to the stiffness, high strength, heat resistance and solvent resistance. However, one major drawback is their poor resistance to impact and crack initiation. Consequently, there is a need to improve the toughness while maintaining desirable properties. Various approaches were suggested for improving the toughness including the addition of silicate layered clay.

The aim of this investigation is to develop the exfoliation process in the epoxy-silicate layered nanocomposites. It is generally considered that, in order to maximize the degree of exfoliation, the intra-gallery reaction, which is associated to the epoxy homopolymerization reaction between clay galleries, should occur before the extra-gallery reaction, which is related to the cross-linking reaction between epoxy groups and amines, hence for enhancement the rate of intra-gallery reaction, these different possibilities were considered to improve the exfoliation degree in cured nanocomposites as follow:

1. Select suitable cure temperature and curing program
2. Pre-conditiong the epoxy/clay mixture
3. Incorporation of the cationic initiator in clay galleries
4. Addition of the hyperbranched polymer to epoxy/clay mixture
5. Select the appropriate type of silicate layered clay

In support of these statements, TGAP (Araldite MY0510) as tri-functional epoxy resin, montmorillonite (Nanomer I.30E, MMT) as silicate layered clay and diamino diphenyl sulphone (Aradur 976-1, DDS) as curing agent were chosen as experimental system to study the influence of these strategies on improvement of the final nanostructure

The curing behavior and the thermal properties of epoxy silicate layered nanocomposites which is prepared based on the above procedures were separately examined with differential scanning calorimetry (DSC and TOPEM) and Thermogravimetric analysis (TGA) and also the fully cured nanostructure in each case is characterized by transition electron microscopy (TEM) and the x-ray scattering (SAXS) and moreover, the mechanical properties are studied by dynamic mechanical analysis (DMA), impact test and scanning electron Microscopy (SEM). Although in each case we obtained the intersecting results which are presented in our

papers, the real goal is to fabricate the highly exfoliated nanostructure which is obtained from the first three procedures.

Among these three procedures, it is difficult to decide which one is more effective on the exfoliation process based on the TEM images which shows the small part of the nanostructure. Therefore, the mechanical properties such as modulus, impact test and fracture surface which display the behavior of the whole nanostructure are helpful tools to compare the degree of exfoliation between these cases. As results, the mechanical properties measurements suggested that incorporation of the cationic initiator is the best protocol to achieve the highly exfoliated epoxy/clay nanocomposites.

List of Papers

This thesis consists of the following papers:

I. J.M. Hutchinson, F. Shiravand, Y. Calventus, I. Fraga, "Isothermal and non-isothermal cure of a tri-functional epoxy resin (TGAP): a stochastic TMDSC study", Thermochimica Acta, 529, p: 14-12, 2012.

II. J.M. Hutchinson, F. Shiravand, Y. Calventus, "Intra- and extra-gallery reactions in tri-functional epoxy polymer layered silicate nanocomposites", Journal of Applied Polymer Science, 128(5), pp: 2961-2970, 2013.

III. F. Shiravand, J.M. Hutchinson, Y. Calventus, "Influence of the isothermal cure temperature on the nanostructure and thermal properties of an epoxy layered silicate nanocomposite", Polymer Engineering and Science, 54(1), pp: 51-58, 2014.

IV. J.M. Hutchinson, F. Shiravand, Y. Calventus, X. Fernández-Francos, X. Ramis "Highly exfoliated nanostructure in trifunctional epoxy/clay nanocomposites using boron trifluoride as initiator", Journal of Applied Polymer Science, 131(6), DOI: 10.1002/app.40020, 2014.

V. F. Shiravand, J.M. Hutchinson, Y. Calventus, "Study of the non-isothermal cure kinetics of tri-functional epoxy nanocomposites", to be submitted.

VI. F. Shiravand, J.M. Hutchinson, Y. Calventus, F. Ferrando, "Comparison of the nanostructure and mechanical performance of highly exfoliated epoxy-clay nanocomposites prepared by three different protocols", submitted to Materials, 2013.

VII. J.M. Hutchinson, F. Shiravand, Y. Calventus, F. Ferrando, "Comparative results between three protocols for achieving highly exfoliated epoxy-clay nanocomposites", Polimery, in press, 59(9), 2014.

VIII. J.M. Hutchinson, F. Shiravand, I. Fraga, P. Cortés, Y. Calventus, "Thermal analysis of polymer layered silicate nanocomposites: identification of nanostructure development by DSC", Journal of Thermal Analysis and Calorimetry, DOI: 10.1007/s10973-014-3709-3, 2014.

The content of above papers has been presented at the following conferences:

- J.M. Hutchinson, F. Shiravand, Y. Calventus, I. Fraga "The advantages of TOPEM in studying the cure of trifunctional epoxy resin (TGAP)", European Polymer Federation Conference (EPF), Granada, Spain, 26 June-1 July 2011, p:260, ISBN: 978-84-694-3124-5. (Paper I)

- F. Shiravand, J. M. Hutchinson, Y. Calventus, "A protocol for exfoliation of epoxy-based polymer layered silicate nanocomposites", 4th ECNP Young Researchers Conference, Lyon, France, November 7-10, 2011. (Paper II)

- F. Shiravand, J.M. Hutchinson, Y. Calventus, "Isothermal cure of tri-functional epoxy-clay nanocomposites: effect of cure temperature on the nanostructure and thermal properties", 3rd International Symposium Frontiers in Polymer Science, Sitges, Spain, 21-23 May, 2013. (Paper III)

- F. Shiravand, J.M. Hutchinson, Y. Calventus, "Cationic initiation of homo-polymerisation in the intra-gallery regions of tri-functional epoxy polymer layered silicate nanocomposites", 3rd International Symposium Frontiers in Polymer Science, Sitges, Spain, 21-23 May, 2013. (Paper IV)

- J.M. Hutchinson, F. Shiravand, Y. Calventus, F. Ferrando, "Comparative results between three protocols for achieving highly exfoliated epoxy-clay nanocomposites", Nanocomposites MoDeSt Workshop, Warsaw, Poland, 8-10 September, 2013, p:57-60. ISBN: 978-83-925627-2-6. (Paper VI and VII)

- F. Shiravand, I. Fraga, P. Cortés, Y. Calventus, J.M. Hutchinson, "Thermal analysis of polymer layered silicate nanocomposites: identification of nanostructure development by DSC", 2nd CEEC-TAC Conference (Central and Eastern European Conference on Thermal Analysis and Calorimetry), Vilnius, Lithuania, 27-30 August, 2013, p:100, ISBN: 978-3-940237-33-0. (Paper VIII)

These conference proceedings are not included in the presentation of this thesis.

List of Contents

Introduction

Cured epoxy is known to exhibit excellent properties for engineering applications, such as high stiffness and strength, creep resistance and chemical resistance. However, like most thermosetting plastics, epoxy is intrinsically brittle, which limits its wider application. Consequently, enormous effort has been devoted to improving the fracture toughness of epoxy while still maintaining its desirable properties [1] [2].

One approach to toughening epoxy is to add a second phase of polymeric particles, such as rubbers and thermoplastics as well as inorganic fillers such as silica, talc and microspheres. However, the addition of soft particles often results in a significant loss of stiffness, while the addition of large amounts of thermoplastic or other modifier can cause a significant decrease in some of the other desirable properties, such as glass transition temperature and solvent resistance [1].

Another approach in epoxy toughening is to use fiber as the reinforcement. Fiber reinforced composite materials consist of fibers of high strength and modulus embedded in or bonded to a matrix with a distinct interface between them. In this form, both fiber and matrix retain their physical and chemical properties. They produce a combination of properties that cannot be achieved by either of the components alone [3].

The addition of nano-fillers is a new type of reinforcing method. Nanocomposites represent new kinds of composites that are particle filled polymers for which at least one dimension of the dispersed phase is in the nanometre range [3] [4]. Materials with nanometre scale features often exhibit superior properties as compared to their macro-scale counterparts, such as strength, stiffness, thermal stability, and barrier properties. Another unique benefit of nanocomposites is the lack of trade-offs [2] [4]. For the first time, there is an opportunity to design materials without the trade-offs that are typically found in conventional polymer composites. In general, nanocomposites consist of a nanometre scale phase combined with another phase. Classified by nano-filler dimension, there are a number of types of nanocomposites, such as zero dimensions (nanoparticle), one dimension (nanotube or whisker), two dimensions (clay or layered silicate) and three dimensions (for example; polyhedral oligomeric silsesquioxane (POSS)) [3] [5].

Nanoclay reinforced polymers are just one example of the large variety of new materials with nano-scale fillers and inorganic/organic hybrid materials which are being developed and investigated. Clays have been recognized as potentially useful filler in polymer composites

because of their high aspect ratio and plate-like morphology, as well as their low cost. Considerable research activity has been focused on polymer-clay nanocomposites [3] [6]. It has been demonstrated that nanocomposites consisting of nanometre-sized, exfoliated clay layers have exceptionally high modulus as compared to conventional composites filled with micron-sized fillers of the same composition [3] [7]. Such materials also exhibit other desirable physical properties, such as flame retardance and gas barrier properties [3] [8] [9].

The purpose of this introductory chapter is to provide an overview of epoxy layered silicate nanocomposites which will help the reader to obtain the necessary background for understanding the papers which form the basis of this thesis. Therefore, a brief literature review about epoxy nanocomposites and the possible strategies to facilitate exfoliation of clay in an epoxy matrix is presented. Then, after the brief description of analytical techniques, which are necessary to investigate the thermal behaviour, mechanical properties and exfoliation development, the list of materials which have been used in this thesis are presented.

1-1) Epoxy Nanocomposites

The term “nanocomposites” describes a two-phase material with one of the phases dispersed in the second one at the nanometre level. This term is commonly used in two distinct areas of materials science: ceramics and polymers. Polymer nanocomposites are commonly based on polymer matrices reinforced by nano-fillers such as clay, silica beads and nanotubes [2].

Clays are layered silicates with a layer thickness around 1 nm and the lateral dimensions of the layers around several hundred nanometres. They have been recognized as potential useful fillers in polymer composites because of their high aspect ratio (high aspect ratio means the ratio of largest (L) dimension to smallest dimension (h) must be greater than 300; $L/h>300$) and platy morphology (particle size and shape) and low cost [4] [10]. However, the efficiency of a filler to improve the mechanical and thermal properties of a polymer system is sensitive to its degree of clay intercalation in a polymer matrix. Polymer-clay interactions have been studied for over 20 years.

In the early 1990s, Toyota researchers discovered that treatment of montmorillonite clay with amino acids allowed dispersion of the individual 1 nm thick silicate layers of the clay on a molecular scale in polyamide 6. Their hybrid material showed major improvements in physical and mechanical properties even at very low clay content (1.6 vol %). Since then many researchers have performed investigations in the new field of polymer nanocomposites. A number of excellent illustrations of this can be found in the literature [11] [12] [13] [14] [15]. Polymer-clay nanocomposites can be divided into three general types, as seen in Figure 1: conventional nanocomposites, where the clay acts as a conventional filler; intercalated nanocomposites, consisting of a regular insertion of the polymer in between the clay layers; and exfoliated nanocomposites, where the 1 nm-thick layers are dispersed in the matrix forming a monolithic structure on the micro-scale. The latter morphology leads to dramatic changes in mechanical and physical properties [1].

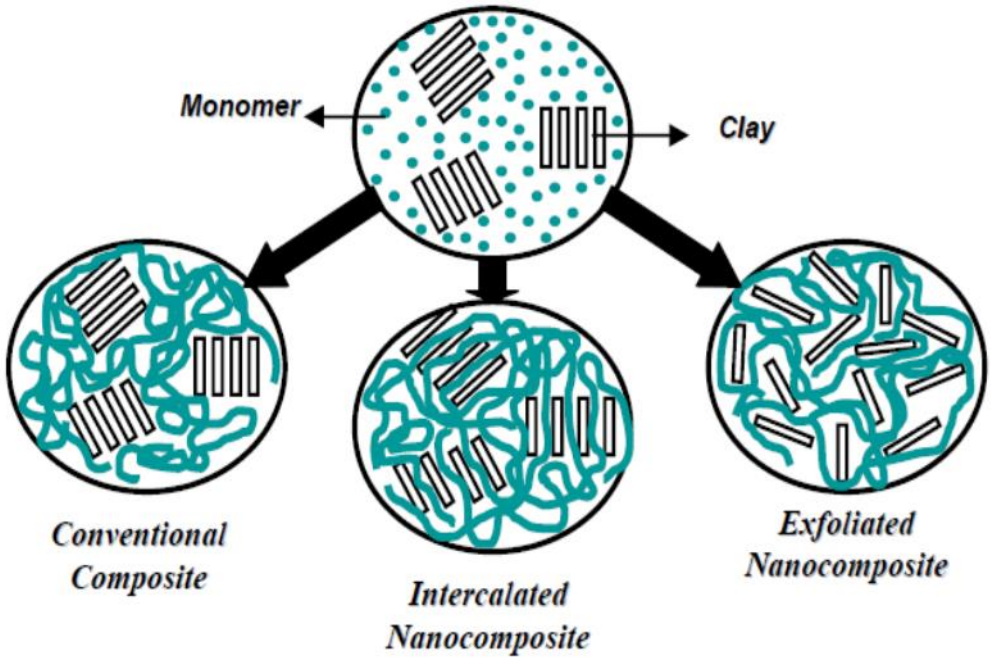

Figure 1: The three structures of polymer-clay composites system

There are mainly three approaches to synthesize polymer-clay nanocomposites: melt intercalation, solution and in situ polymerization, as seen in Figure 2. In our work, the last of these, in situ-polymerization [16] [17] [12] [18] [19] [20] [21] [22] [23] [24], was used to synthesize thermoset-clay nanocomposites in all of the papers (I-VIII) presented in this thesis.

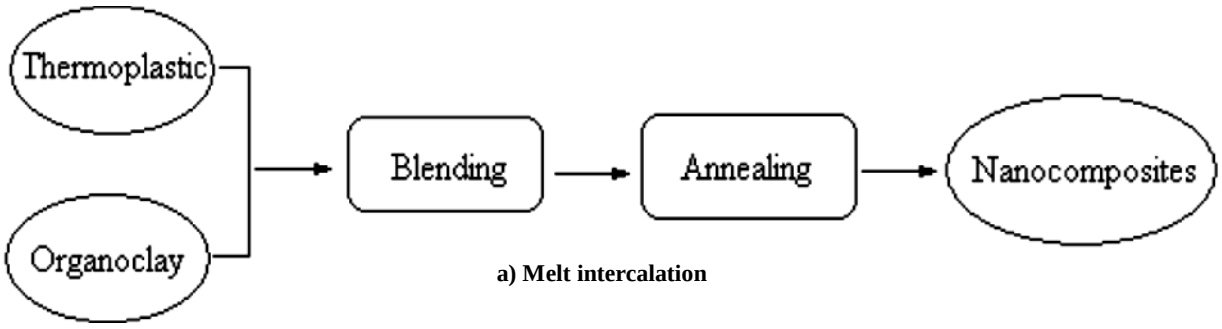

a) Melt intercalation

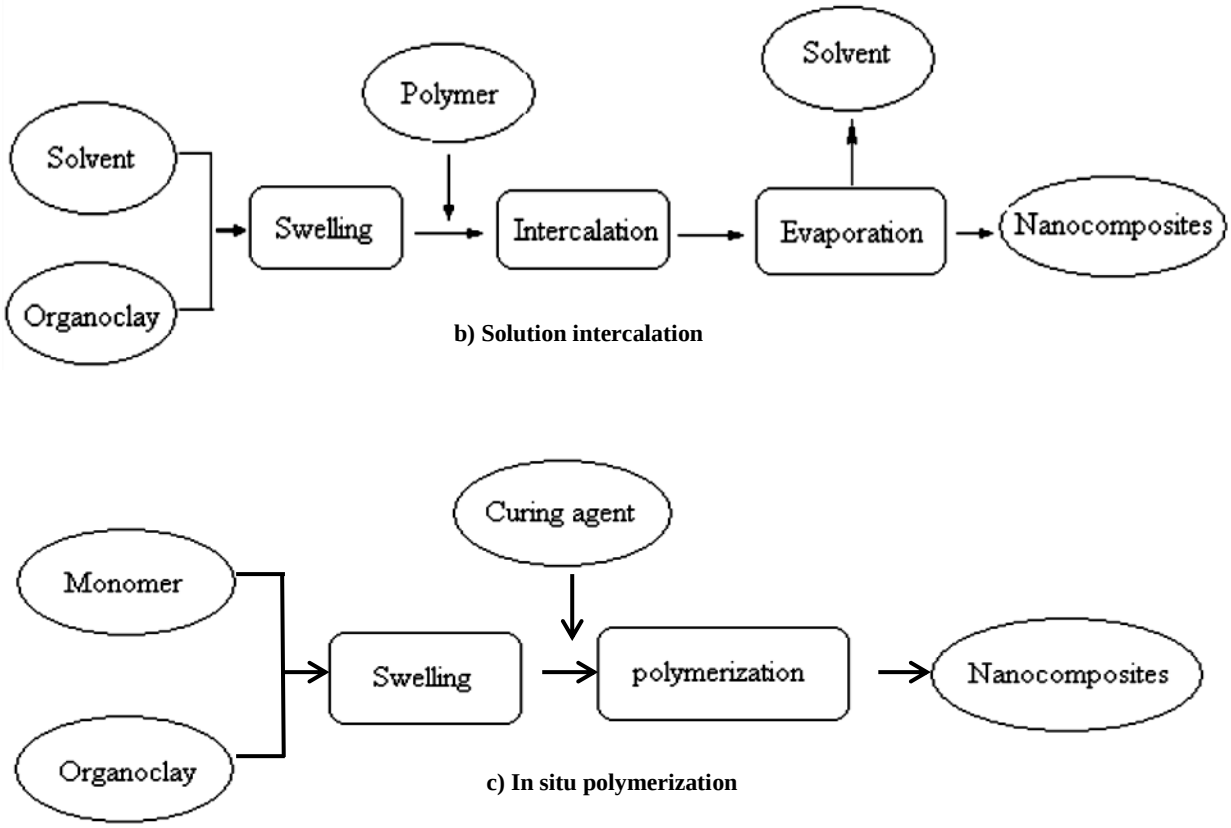

Figure 2: Flowcharts presenting the different steps in preparing polymer layered silicate nanocomposites

The curing process for thermosetting resins involves a series of steps starting from a fluid reactant, proceeding through the gel stage, and finally reaching the cross-linked solid. The reaction mechanism changes from chemical to diffusion control when the material vitrifies from an elastic gel to gelled glass. Due to complexities that might influence the exfoliation of the clay in the thermosetting matrix, considerable investigative work is still required in this area, and especially the question of which stage in the overall process has the greatest effect on exfoliation.

1-1-1) Epoxy Resins

Epoxy resins are thermosetting polymers that are widely used in structural adhesives, surface coatings, engineering composites, and electrical laminates. Most of the composite applications utilize conventional bi-functional epoxy as a matrix; however, many high-performance applications such as aerospace and critical defence applications require the thermally stable high performance epoxy resins. So the multifunctional epoxies, with functionality of three and four epoxy groups, cured with a suitable curing agent, can satisfy

thermo-mechanical properties which are specified for these applications. Tri- and tetra-functional epoxy resins are available commercially [25].

Epoxy resins, before curing, have one or more active epoxide groups at the ends of the molecule and a few repeat units in the middle of the molecule. Their molecular weights can vary greatly. They exist either as liquids with low viscosity or as solids [26]. The chemical structures of selected bi-functional and multifunctional epoxies are shown in Figure 3 and the physicochemical properties of the epoxy resins are given in Table 1 [26] [27]. In the research presented in this thesis, the tri-functional epoxy resin (triglycidyl p-amino phenol; TGAP), with trade name Araldite MY0510 (Huntsman Advanced Materials), is used as the matrix material for the fabrication of polymer layered silicate nanocomposites.

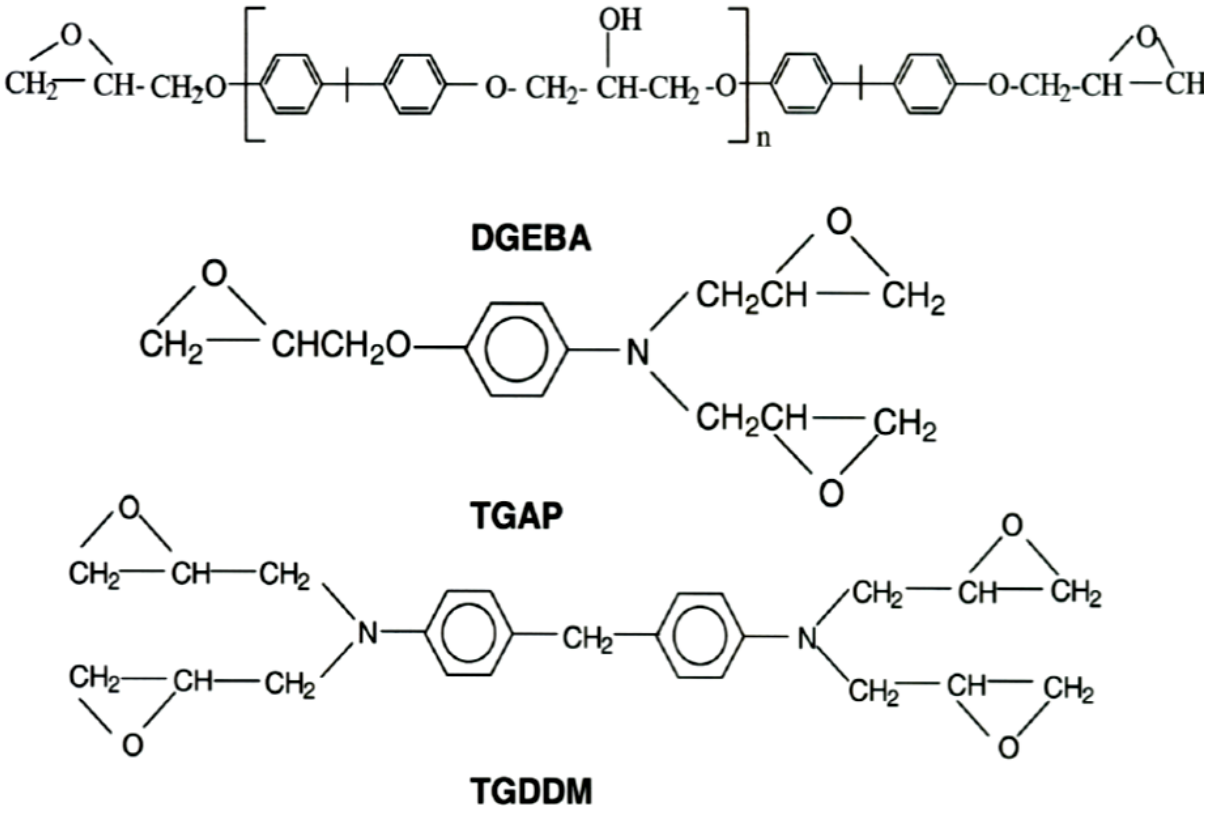

Figure 3: Chemical structures of bi-functional and multifunctional epoxies [28]

Table 1: Physicochemical properties of the resins [30]

Epoxy resin	Viscosity(Pa-s)	Epoxy equivalent (g/eq)	Functionality (eq/mol)
DGEBA	4-6 (DGEBA 332) 11-14 (DGEBA 331)	171-175 (DGEBA 332) 182-192 (DGEBA 331)	2
TGAP	0.55-0.85	95-106	3
TGDDM	94.5	100	4
DGEBA: Diglycidyl ether of bisphenol A TGAP: Triglycidyl p-amino phenol TGDDM: Tetraglycidylether of 4,4′ diaminodiphenyl methane			

1-1-2) Layered Silicates

The generic term "layered silicates" refers not only to the natural clays but also to the synthesized layered silicates such as mica, etc. Both natural clays and synthetic layered clays have been successfully used in the synthesis of polymer nanocomposites. This research is focused on the use of natural clays, such as montmorillonite (MMT), which have been commercially modified to make them organophilic. Montmorillonite with chemical formula $M_x^+ (Al_{4-x}Mg_x)Si_8O_{20}(OH)_4$ [x; degree of isomorphous substitution, between 0.5 and 1.3] is a phyllosilicate $(Si_2O_5)^{-2}$ type of mineral which belongs to the smectite group with a 2:1 layer disposition. Smectites show a feature (platelet morphology) that allows them to intercalate molecules between their layers (see Figure 4). Montmorillonite is nowadays one of the clays most widely used as a nanofiller due to its suitable layer charge density [28] [29] [30].

In this research, the effect of three different layered silicate clays was studied on the epoxy network. These clays include; natural montmorillonite modified by octadecyl ammonium ion, with trade name Nanomer I.30E (Nanocor Inc.), natural montmorillonite modified by a methyl tallow bis-2-hydroxyetyl) quaternary ammonium ion, with trade name Cloisite 30B (Southern Clay Products, Inc.) and organically modified nanodispersible layered silicate based on natural bentonite[a] which is modified by dimethyl-di (hydrogenated tallow) alkyl ammonium salt, with trade name Nanofil SE 3000 (Rockwood Additives, Inc.), as shown in Table 2.

[a] Bentonite and Montmorillonite clays often interchange names and have similar properties. The Montmorillonite name was actually given to smectite clay that was found in the Montmorillon area of France and Bentonite was originally named for Smectite clay found near Fort Benton in Wyoming, USA.

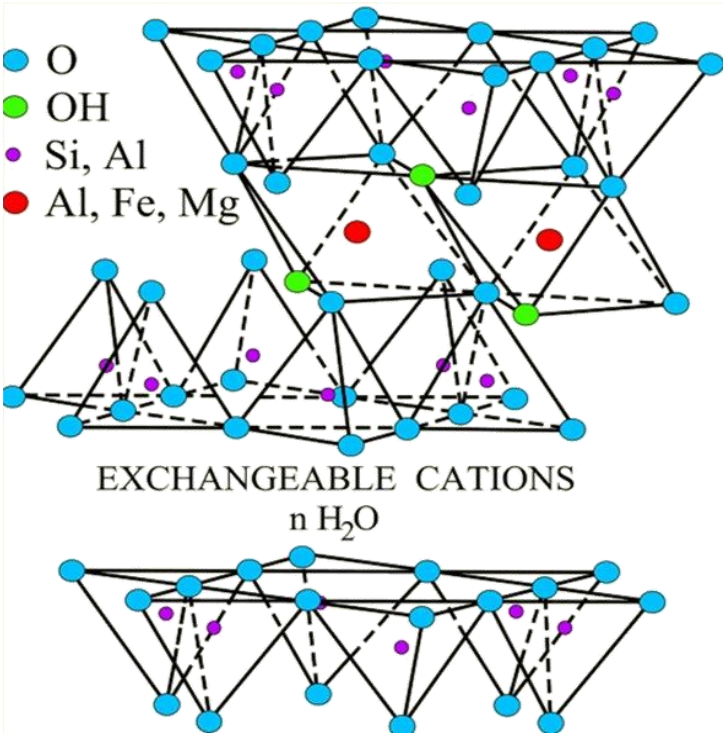

Figure 4: Structure of montmorillonite clay

Table 2: Typical properties of the three different types of layered silicate clay

Clay name	*d*-spacing (nm)[b]	Density (g/cm^3)	Median particle size (μm)
Nanomer I.30E	2.1-2.2	1.9	14-18
Cloisite 30B	1.85	1.7-1.9	13
Nanofil SE3000	3.6	1.8	10

1-1-3) Curing Agents

Epoxy resins can be cured using a range of materials with different types of curing conditions. The choice of curing agents (also called 'hardeners') depends on the curing conditions applicable and the final application of the resin. Amines are widely used as hardeners for epoxy resins. The chemical structures of some commonly used amine curing agents are seen in Figure 5; according to the overview of Mika and Bauer [31], aromatic amine gives better chemical resistance and thermal properties of the resulting network compared with other kinds of amine cured systems, although aromatic amines react slowly with epoxy resin at room temperature and require high temperatures for the curing process. In

[b] These data are obtained from the SAXS (Small Angle X-ray Scattering) pattern.

this study, DDS[c] (4-4 diamino diphenyl sulfone), with trade name Aradur 976-1 (Huntsman Advanced Materials) is used as the curing agent for the tri-functional epoxy layered silicate nanocomposites.

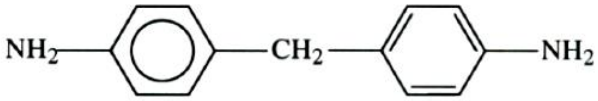

Diamino diphenyl methane (DDM)

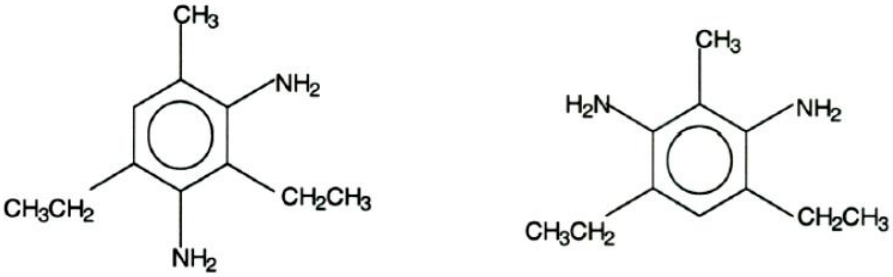

Diethyl toluene diamine (DETDA)

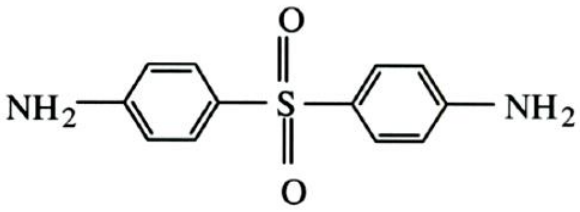

Diamino diphenyl sulfone (DDS)

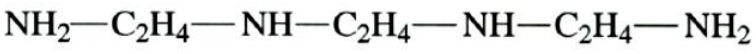

Triethylene tetramine (TETA)

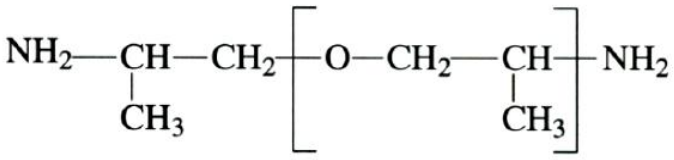

Jeffamine
(Polypropyletheramine)

Figure 5: Chemical structures of commonly used amine curing agents

[c] DDS is a high performance hardener which is used with Araldite epoxy resins and classified as a solid aromatic amine curing agent.

1-2) Parameters Affecting the Exfoliation of Layered Silicate Nanocomposites

As mentioned before, one of the procedures to increase the toughness of epoxy systems is by the addition of layered silicate clay, which can improve the mechanical properties such as elastic modulus and impact strength of the final nanocomposite [32] [33] [34] [35] [36]. The enhancement of the mechanical properties of nanocomposites is dependent on the quality of the clay dispersion in the matrix. An intercalated nanocomposite tends to show a smaller increase in the modulus and impact energy than an exfoliated nanocomposite [37]. However, some studies show a reduction in elastic modulus and tensile strength of polymer clay nanocomposites with clay addition [1] [38].

It is generally accepted that the exfoliated nanocomposites have the greatest potential for property enhancement. When the clay layers are separated completely and uniformly in the polymer matrix, the final nanostructure is considered as fully exfoliated. In practice, a nanostructure can be attributed as a fully exfoliated nanocomposite when the clay layers have a *d*-spacing larger than 8 nm (the limit of detection by Small Angle X-ray Scattering (SAXS)) and the disordered arrangement of the clay layers in the bulk can be detected by Transmission Electron Microscopy (TEM).

Hence, several reports have discussed the mechanism of organoclay exfoliation in epoxy matrix. Lan et al [18] and Park et al [39] both reported that increase in the distance between organoclay platelets requires the driving force of the resin/hardener cure reaction or homopolymerisation reaction to overcome the attractive electrostatic forces between the negative charge of the silicate layers and the counterbalancing cations in the galleries. Chen et al [40] have divided the interlayer expansion mechanism into three stages, the initial interlayer expansion due to resin and hardener monomers intercalating the silicate galleries, second interlayer expansion due to intra-gallery polymerization and the final stage of interlayer expansion is characterized by a decreasing interlayer expansion rate due to restrictions through extra-gallery polymerization (gelation).

It has been pointed out by several researchers [18] [41] [42] [43] [44] that the relative rates of the intra-gallery and extra-gallery reactions play a key role in the synthesis of exfoliated nanocomposites. These workers found that the exfoliation process occurs when the curing rate of the intra-gallery polymerization is faster than the extra-gallery reaction, and also that a faster intra-gallery reaction accelerates the exfoliation process, which allows exfoliation to take place to a great extent in the nanostructure before the system becomes rigid.

It is therefore generally agreed that the intra-gallery reaction must occur before the extra-gallery reaction in order to achieve an exfoliated nanostructure; as a consequence, the cure conditions must be consistent with meeting this requirement. There are some cure conditions which lead to improved degrees of exfoliation in epoxy nanocomposites, but these conditions can be different depending on the nanocomposite system.

The fact that very few workers have reported complete exfoliation (implying in principle that every individual clay layer is distributed homogeneously and in a disordered arrangement throughout the network), and for some of those who have reported complete exfoliation the evidence is not compelling, indicates that this is a difficult issue. Nevertheless, many researchers refer to an "exfoliated structure". The point is that the expression "exfoliated structure" is often used to refer to systems which are highly exfoliated, but not fully exfoliated.

Our research is focused on identifying the procedures which significantly improve the degree of exfoliation. These procedures are based upon the idea of promoting the intra-gallery reaction, and can be listed as follows:

- Clay dispersion: the intra-gallery reaction can only occur if there is resin between the clay galleries; if there are significant agglomerations, then the resin cannot easily penetrate all the clay galleries, and hence the dispersion of the clay in the resin is an essential pre-requisite for good exfoliation.
- Clay type: the charge density of clay layers determines the amount of epoxy monomer that can participate in the intra-gallery reaction.
- Curing agent type: the reactivity of the resin/curing agent system is obviously important in respect of the rate of extra-gallery reaction.
- Cure conditions: it is necessary to find suitable conditions which lead to the reaction in the galleries occurring before the reaction outside the galleries.
- Hyperbranched polymers (HBPs): these provide a possible way, for example, for improving the dispersion of the clay in the resin.
- Pre-conditioning: the idea is to use the catalytic effect of the clay to promote the homopolymerisation of the resin within the galleries.
- Initiator: another idea is to deliberately include an initiator of homopolymerisation within the clay galleries.

As mentioned above, the aim of this research is to synthesize highly exfoliated epoxy nanocomposites by means of these proposed procedures which are explained in more detail in the subsequent sections.

1-2-1) Dispersion of Layered Silicates

The first step in the preparation of the epoxy nanocomposite is to intercalate the organoclay with the epoxy resin before the curing process. This intercalation influences the clay morphology in the nanocomposites. In other words, a good dispersion of the clay in the epoxy matrix helps to improve the exfoliation degree, whereas poorly dispersed clay, in which there are many large clay agglomerations, not only leads to difficulty in epoxy monomer penetration into the clay galleries but also decreases the accessibility of the curing agent to resin. Therefore, the quality of the clay dispersion is considered as an important parameter to enhance the exfoliation process.

The common processes for clay dispersion in the epoxy matrix are the direct mixing method and the solvent mixing method. In both methods, the epoxy and clay can be premixed together by means of different mixing techniques; hand mixing, mechanical stirring, ultrasound sonication [17] [45] [46] and high shear mixing [38] [47] [48] [49]. Ball milling [50] and high pressure mixing [51] [52] are other mixing techniques which have also been applied in the solvent mixing process.

Direct mixing of organoclay and epoxy with mechanical mixing is widely used to disperse nanoclay in epoxy. However, it is not sufficient to produce a high degree of exfoliated nanostructure. Many researchers have reported the effects of mixing techniques on the morphology and properties of the cured nanocomposites, but very few studies can be found which compare directly the effect of different mixing techniques on the quality of clay dispersion in epoxy/clay mixtures. In particular, Messersmith and Giannelis [17] were the first to prepare layered silicate nanocomposites based upon epoxy resin. They found that the modified clay dispersed readily in DGEBA when sonicated for a short period of time and TEM images of the cured nanocomposites showed the clay layers with a *d*-spacing of more than 10 nm. Lam et al. [45] prepared epoxy nanocomposites with 4 wt.% clay content which were subjected to different sonication times (5 to 60 min). They found that 10 min ultrasonication resulted in an optimum mechanical performance for their epoxy nanocomposites. Yasmin et al [38] used a three-roll mill to provide external shearing forces during mixing in order to disperse well the silicate clay layers in the epoxy matrix which leads to an increase in the degree of exfoliation in the cured sample. The TEM images of the

final nanostructure are apparently quite well exfoliated. This technique can be used for fabricating nanocomposites with a high degree of exfoliation. However, it is important to mention that the processing of nanocomposites by shear mixing produces a foamy and viscous solution and makes degassing quite difficult. Vaia et al [53] have suggested that the degree of exfoliation could be improved through the aid of conventional shear devices such as extruders, mixers, ultrasonicators. Finally, Zunjarro et al [46] synthesized epoxy nanocomposites by dispersing the clay in the epoxy matrix through two different mixing techniques: high speed shear mixing and ultrasonication. They found that high speed shear mixing yielded better mechanical properties compared to ultrasonication, even though both methods gave an exfoliated morphology. It can be concluded that sonication and high shear mixing techniques can improve the exfoliation process. This improvement is a direct result of improving the clay dispersion. These methods, especially high shear mixing, help to break down the clay agglomerations to a smaller size and produce a more homogeneous dispersion of the clay in the epoxy resin. Therefore, the epoxy resin has more chance to diffuse into the clay galleries so more intra-gallery reaction can occur, which would lead to an enhancement of the exfoliation process.

The solvent mixing process is another preparation method for clay dispersion in the epoxy matrix. It seems that the clay dispersion after the solvent process is better than after the direct mixing process; however, there is no comprehensive agreement on this. Brown et al [54] studied the use of a low-boiling solvent such as acetone, and reported that the solvent mixing process does not alter the morphology and properties of the final nanocomposite and only enhances the processability due to a reduction in the viscosity of the system. This observation is not in agreement with other researchers, in particular Hutchinson et al [48] [55]. They stated that the dispersion plays an important role in the exfoliation process and better dispersion leads to better exfoliation in the final nanocomposites. They showed by optical microscopy that the quality of clay dispersion was clearly better for the solvent mixing method than the direct mixing method, and that the final nanostructure of nanocomposites fabricated by solvent mixing showed a higher degree of exfoliation than the nanostructure of samples prepared by direct mixing. Chen et al [56] prepared fully exfoliated layered silicate epoxy nanocomposites by the combination of high shear mixing and ultrasonication in the presence of acetone. TEM images showed a dramatic improvement in exfoliation compared to the direct mixing process.

Ngo et al [49] studied the effect of mixing methods, including hand mixing, mechanical mixing, high shear mixing and high pressure mixing, on the epoxy/resin mixture and on the

final nanocomposites. SAXS data showed that the different mixing techniques have no significant influence on the *d*-spacing of the clay layers in the epoxy/clay mixture. The same results are reported by Hutchinson et al [48], who found that the intercalation of the resin into the clay galleries results in a *d*-spacing which is essentially independent of mixing techniques or process. However, the results from SAXS, SEM (scanning electron microscopy) and TEM for the cured nanocomposite [49] indicated that direct mixing process, which was done by high shear mixing at elevated temperature, results in a fine dispersion at the micro-scale which increases the degree of exfoliation in the final nanostructure, compared to the other mixing methods, especially the solvent mixing process, which was done by high pressure mixing technique. This result is not in accord with the results which are presented by Hutchinson et al [48] who showed that the quality of the nanostructure of samples prepared by solvent mixing is better than that of samples prepared by direct mixing.

Therefore, it is difficult to say which mixing process is better. However, many novel ideas have been presented by researchers for the preparation of epoxy nanocomposites based on the solvent mixing of epoxy/clay mixtures. In particular, Lu et al [50] utilized ketone as a solvent and the shearing force of ball milling as a mixing technique to prepare their epoxy nanocomposites. Their TEM images showed that an increase in exfoliation can be achieved by this preparation procedure in comparison to the direct mixing process, either by means of high shear mixing or simply using a magnetic stirrer. Liu et al [51] [52] used a high-pressure mixing method with assistance of acetone solvent to improve the dispersion of clay in epoxy nanocomposites and observed a significant improvement in the fracture toughness and exfoliation relative to the direct mixing process. However, the large amount of solvent required meant that considerable time was required for removing it.

Generally, it can be concluded that the quality of clay dispersion in the epoxy matrix before adding the curing agent in both processes depends on many factors such as mixing technique and mixing time, so that it is hard to decide which process (direct/solvent) is advantageous in respect of the exfoliation process. However, both processes have a positive effect on the morphology of the final nanostructure due to the improvement in the quality of the clay dispersion, which leads to an increase in the degree of exfoliation.

1-2-2) Nature of the Silicate (Clay Type) and the Interlayer Exchange Ion

The impact of the nature of the layered silicate clay on the intercalation/exfoliation process has attracted the interest of many researchers. There are two fundamental aspects of the organoclay that determine the formation of epoxy nanocomposites by in-situ polymerization:

the ability of the interlayer exchanged ion to act as a compatibiliser and render the layered silicate 'epoxyphilic', and the catalyzing effect of the exchanged ion on the polymerization reaction in the galleries [30].

The charge density of the smectite determines the amount of ions in the interlayer galleries that can be exchanged and therefore the amount of epoxy monomer that can be preloaded in the galleries of the modified organoclay. Lan and co-workers [18] investigated the effect of various smectites with cation exchange capacities (CEC) varying from 67 mmol equivalent/100 g (meq/100 g) for hectorite to 200 meq/100 g for vermiculite. It was reported that silicates such as montmorillonite and hectorite ($Na_{0.4}Mg_{2.7}Li_{0.3}Si_4O_{10}(OH)_2$, a clay mineral from altered volcanic tuff ash, with intermediate layer charge densities are found to be well suited for the required layered silicate modification. Generally, layered silicates with a low charge density are more easily accessible for intra-gallery polymerization than high charge density clays with a higher population of gallery onium ions. Thus, the low charge density layered silicates provide higher degrees of layer exfoliation.

Kornmann et al [57] reported similar results for two different montmorillonite clays, with a CEC of 94 and 140 meq/100 g. After modifying the layer surfaces of the clay with an octadecylamine ion, the resulting DGEBA/Jeffamine D-230 nanocomposites were examined by TEM, from which it was found that they displayed layer stacking of 9 nm *d*-spacing for high CEC and 11 nm for the low CEC montmorillonite. The difference in organoclay layer separation was assumed to be due to the population density of alkylamine ions in the galleries and hence the space available for the epoxy resin. It was theorized that the layered silicate with the lower CEC contains fewer alkylamine ions, which leaves more space for the DGEBA molecules and allows homopolymerisation to occur to a larger extent compared to the layered silicate with the higher CEC.

The nature of the interlayer exchanged ion also significantly determines the compatibility of the layered silicate with the epoxy resin, as well as the intra-gallery reaction rate. Pinnavaia and co-workers performed several studies using different types of organically modified layered silicates [18] [58] [59]. It was shown [18], for a series of alkylammonium ion, $CH_3(CH_2)_{n-1}NH_3^+$, exchanged montmorillonites with n = 4, 8, 10, 12, 16 and 18, that the length of the alkylammonium ion greatly affects the clay expansion before cure. Long-chain alkylammonium ions allow epoxy monomers to be accommodated in the gallery by adopting a vertical orientation that optimizes solvation interactions with the alkyl chains. The degree of exfoliation was also found to depend on the amount of intercalated resin in the clay galleries.

In earlier work by Zilg et al [60] it was reported that the alkyl chain length for an organically modified fluorohectorite had to exceed six C-units to give interlayer separations greater than 11 nm, although complete exfoliation was not observed from the TEM images. However, a chain length higher than eight C-units did not further improve the exfoliation process.

Wang and Pinnavaia [61] found, for a series of primary to quaternary octadecyl onium ion modified clays $CH_3\ (CH_2)_{17}NH_{3-n}\ (CH_3)_n^+$ (n=0, 1, 2, 3) as shown in Figure 6, that the primary and secondary ion-modified clays exfoliated in a DGEBA/ Jeffamine D-2000 system based on SAXS data whilst the tertiary and quaternary ion-modified clays remained in an intercalated formation. This effect has been ascribed to the high acidic-catalytic effect of the primary and secondary onium ions of the clay on the intra-gallery reaction.

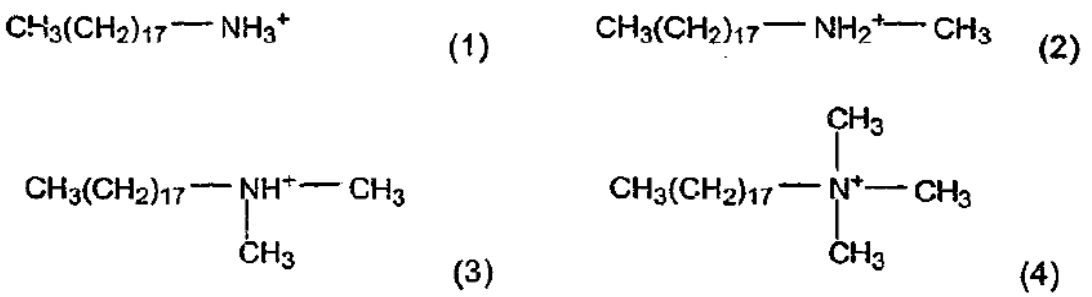

Figure 6: Example of primary (1), secondary (2), tertiary (3) and quaternary (4) octadecyl amine ions

These results are in good agreement with work reported by Zilg et al [22]. In their work, nanocomposite formation based upon various layered silicate modification has shown that ion exchange with protonated primary amines gave larger interlayer distances in the nanocomposite than those based on quaternary amine modification.

Generally, long primary linear chain alkyl ammonium ions such as $CH_3\ (CH_2)_{15}NH_3^+$ have proven to be appropriate substances for the synthesis of exfoliated systems and have been the most widely used in epoxy layered silicate nanocomposite systems to date.

In appendix A, the effects of three different layered silicate clays, Nanomer I.30E, Cloisite 30B and Nanofil SE 3000, on the exfoliation process of epoxy nanocomposites were investigated. As mentioned in section 1-1-2, these clays are modified with different modifiers which include primary, secondary and quaternary ammonium ions for Nanomer I.30E, Nanofil SE 3000 and Cloisite 30B, respectively. Hence, it is expected that the primary and

secondary ion modified clays, Nanomer I.30 and Nanofil SE 3000, should present a good possibility for achieving an exfoliated nanocomposite in contrast to the quaternary ion modified clay, Cloisite 30B which is widely used in the fabrication of epoxy nanocomposites due to improved chemical compatibility (there are 2-hydroxyethyl groups in Cloisite structure) with the relatively polar epoxy resin [49]. The final nanostructure was examined by SAXS for these systems and the SAXS pattern was found to display a small shoulder around 2.53°, which corresponds to about 3.5 nm *d*-spacing, for the Cloisite and Nanofil systems, whilst no scattering peak appeared for the Nanomer system for *d*-spacings between 1.15 nm and 8 nm. These results implied that, for the Nanomer system, the *d*-spacing of layer stacking in the nanostructure is more than 8 nm, which was also confirmed by TEM images. In other words, the onium ion in the Cloisite and Nanofil could not accelerate the intra-gallery reaction before the matrix became rigid and highly cross-linked, whereas the catalytic effect of the primary onium ion of Nanomer on the intra-gallery reaction, which appeared as an initial peak in the DSC scan before the extra-gallery reaction peak, led to an increase in the degree of exfoliation in the Nanomer system.

1-2-3) Curing Agent

The choice of a suitable curing agent is also reported to be a significant factor which determines whether exfoliated or intercalated clay layers are distributed within the cured thermosetting network. Early work by Jiankun et al [62] has shown, for example, that low viscosity curing agents can intercalate more easily into the clay galleries than highly viscous curing agents, thus favouring the interlayer reaction and therefore exfoliation.

Kornmann et al [41] showed that the molecular mobility and reactivity of the curing agent are important factors affecting the balance between intra-gallery and extra-gallery reactions. For the three different curing agents investigated, Jeffamine D-230, 3,3-dimethylmethylenedi(cyclohexylamine) (3DCM) and bisparaamine-cyclohexylmethane (PACM), it was found that the Jeffamine D-230 gave better exfoliation of a DGEBA based nanocomposite than the cycloaliphatic polyamines 3DCM and PACM. In other words, the aliphatic amine curing agent produced an exfoliated morphology for the epoxy nanocomposite compared to the cycloaliphatic amine curing agent, as a consequence of the lower reactivity of the aliphatic amine curing agent.

Messersmith and Giannelis [17] investigated the influence of four different curing agents (nadic methyl anhydride (NMA), benzyldimethylamine (BDMA), boron trifluoride monoethylamine (BTFA) and methylenedianiline (MDA)) on the formation of a DGEBA

based nanocomposite. The *d*-spacing of the clay layers within the cross-linked epoxy matrix was verified by SAXS and showed that cure of the DGEBA with both NMA, anhydride curing agent, and BDMA, aromatic amine curing agent, resulted in exfoliation whereas cure of the DGEBA with MDA did not give exfoliation, while they did not present any data about the cure of DGEBA with BTFA. The aromatic amine and anhydride can therefore be considered as suitable curing agents, yielding an increase in exfoliation for DGEBA based nanocomposites.

Kong et al [63] studied the exfoliation behaviour of DGEBA/clay nanocomposites which were cured with three aromatic diamine curing agents; 1,3-phenylenediamine (PDA), 4,4-methylenedianiline (MDA) and 4,4-diaminodiphenyl sulphone (DDS). Epoxy clay nanocomposites based on DGEBA/PDA and DGEBA/MDA systems produced an intercalated structure due to the high reactivity of the curing agents which induces faster gelation in the extra-gallery region, while DGEBA/DDS system gave an exfoliated structure due to the low reactivity of the curing agent, which thereby slowed down the extra-gallery gelation and provided enough time for intra-gallery polymerization. The TEM pictures showed the exfoliation in the DGEBA/DDS system and intercalation in the DGEBA/MDA system.

In all the papers which are presented in this thesis, DDS, an aromatic diamine, has been used as the curing agent for the TGAP/clay system due to the low reactivity that allows more intra-gallery reaction to occur before the system becomes rigid and highly cross-linked.

1-2-4) Cure Conditions

The curing process includes isothermal or non-isothermal (dynamic) cure schedules, or a combination or sequence of either of these. The effect of the isothermal cure temperature on epoxy nanocomposite formation has been the subject of several studies, typically on DGEBA nanocomposites. Considerably less attention has been paid to the study of the effect of the isothermal and/or non-isothermal cure behaviour on the exfoliation process for epoxy nanocomposites based upon high-functionality epoxy resin.

It was reported [41] [64] that the basal spacing of clay layers in DGEBA-based nanocomposites increased with increment of isothermal cure temperature. During isothermal cure, the molecular mobility and diffusion rate of the resin and hardener into the clay galleries increased with increasing cure temperature, which leads to an improved balance between intra-gallery and extra-gallery reaction rates, thus allowing the clay layers to separate such that no diffraction peaks can be detected by SAXS. As a result, increased

isothermal cure temperatures exfoliated the organoclay in a shorter period of time and increased the basal spacing in the final morphology.

Lan et al [18] explained that too low cure temperatures (75^{o}C) may lead to slow intercalation rates in DGEBA/mPDA(meta-phenylene diamine) nanocomposites, while a high cure temperature (140^{o}C) leads to an increase in the extra-gallery reaction rate. Under these circumstances, the extra-gallery polymerization will be faster than intra-gallery reaction, leading to intercalated rather than exfoliated nanocomposite structures. They also showed that the nanocomposite cured at an intermediate rate (125^{o}C for 4h) did not show any diffraction peaks, which indicated that the nanocomposite was exfoliated. These results are in contrast to those of the previous workers discussed [41] [64]. Kornmann et al [41] cured the DGEBA-based nanocomposites with curing agents other than mPDA, which leads to a change in the kinetics of cure, thus the suitable cure temperature for this system will be different from the system which is studied by Lan et al [18]. On the other hand, Benson Tolle and Anderson [64] studied the same system (mPDA-cured DGEBA nanocomposites) but with different modified layered silicate clays, thus again leading to different kinetics for the intra-gallery reaction, which required a high cure temperature to promote the intra-gallery reaction. Therefore it may be concluded that the selection of the suitable cure temperature which would result in an increase in the rate of the intra-gallery reaction relative to the extra-gallery reaction, and thereby improve the degree of exfoliation, is dependent on both the nature of the curing agent and the layered silicate clay.

Montserrat et al [43] [65] investigated the isothermal and non-isothermal cure reaction kinetics of a nanocomposite system, consisting of DGEBA/modified MMT/ Jeffamine D-230, and examined the effects of different cure schedules on the nanostructure of the cured samples. Based on the SAXS pattern for non-isothermal cure, an exfoliated nanostructure could be obtained when the heating rate is slow (2.5 and 5 K/min), for which there were *d*-spacings greater than 8 nm, but for faster heating rates (15 and 20 K/min), as well as for isothermal cure at 70^{o}C and 100^{o}C, the exfoliation process was accompanied by the occurrence of 1.4 and 1.8 nm *d*-spacings for isothermal and non-isothermal cure, respectively. These values of *d*-spacing were attributed to the clay agglomerations in the final matrix and are less than those of the intercalated clay. It is supposed that the shrinkage of the bulk resin during cure compresses the clay agglomerates. They also related the nanostructure development to the cure reaction kinetics. They reported that the DSC scan of the non-isothermal cure of DGEBA-based nanocomposites showed a peak with a shoulder on the high temperature side of the exotherm. The peak is related to the cross-linking reaction and the

shoulder is attributed to the intra-gallery reaction. In other words, the intra-gallery reaction is happening after the extra-gallery reaction during the non-isothermal cure, so it is not possible for exfoliation to occur before the system becomes rigid. Hence, it was concluded that a highly exfoliated nanostructure cannot be expected for this system, and this was confirmed by TEM studies. It can be concluded that control of the rates of intra- and extra-gallery reaction by means of the cure temperature is an important key to promote the degree of exfoliation.

Becker et al [32] examined the influence of the cure temperature during isothermal cure and resin type (in particular, high functionality epoxy resins) on the morphology of epoxy nanocomposites. These epoxy nanocomposites were based on DGEBA, TGAP and TGDDM which were cured with DETDA. They found that higher cure temperature led to an improvement in the exfoliation process and also that DGEBA nanocomposites cured with DETDA showed a higher degree of exfoliation than the TGAP and TGDDM epoxy resins, which is completely different from the results that are presented in Paper III about TGAP-based nanocomposites. This discrepancy is probably related to the use of different curing agents, leading to different kinetics of reaction within and outside the clay galleries.

The most important aspect in the fabrication of epoxy-clay nanocomposites is that the intra-gallery reaction must occur before the extra-gallery reaction for significant exfoliation to occur. Therefore strategies should be sought which lead to an enhancement of the intra-gallery reaction. The above summary of results published in the literature show that, while in many cases it is beneficial to cure isothermally at high temperatures, this is not always the case. The situation is complicated by a number of factors. First, different combinations of resin and curing agent imply different reactivities, both for the cross-linking reaction as well as for the homopolymerisation reaction within the clay galleries, and they may have different temperature dependences. Second, the preparation of the resin-clay mixture, in respect of the quality of the dispersion of the clay, can also play an important role. For example, improved dispersion of the clay allows easier access of the resin to the clay galleries leading to better exfoliation, whereas the presence of agglomerations will inhibit the separation of the clay layers, resulting in a poorer degree of exfoliation. Thus it is difficult to draw any definitive conclusions from these published results. In order to understand better the process of exfoliation, the work presented in this thesis has concentrated on a single resin-clay system, namely that of TGAP epoxy resin with organically modified MMT, cured with DDS. It transpires that this system offers the potential for high degrees of exfoliation, and hence it has been studied under various curing conditions, as detailed below.

In the isothermal cure of TGAP-based nanocomposites (Paper III), two distinct reactions take place: the first one gives rise to a rapid peak in the DSC trace, taking place within the clay galleries and due to homopolymerisation of the resin intercalated between the clay layers, whereas the second results in a broad bell-shaped peak which is attributed to the bulk cross-linking reaction between the TGAP and DDS, taking place outside the clay galleries. This is significantly different from the DGEBA/Jeffamine system, because already the intra-gallery reaction in the TGAP system is both separate from and occurs before the cross-linking reaction, which is an essential requirement for exfoliation. Furthermore, increasing the cure temperature increases significantly the contribution of the intra-gallery reaction, corresponding to the first peak, which implies that a greater degree of exfoliation would be expected in the final nanostructure when this system is cured at high temperatures. This expectation is confirmed by TEM images, which show that the most significant increase in the degree of exfoliation is obtained for the TGAP-based nanocomposites when they are cured at the highest cure temperature, namely 180^{o}C. These TGAP-based nanocomposites have greater degrees of exfoliation, as identified by TEM, in comparison with earlier studies of DGEBA-based nanocomposites [43] [65] [66], which can be attributed directly to the fact that the intra-gallery reaction occurs before the extra-gallery reaction in the former system, which is crucial in respect of obtaining exfoliated nanocomposites.

In the non-isothermal cure of TGAP-based nanocomposites (Paper V), the DSC cure curve appears as a composite peak which can be deconvoluted into three separate peaks. These are tentatively assigned as follows: (i) a combination of the cross-linking reaction of the TGAP with the DDS and an intra-gallery homopolymerisation reaction; (ii) an extra-gallery homopolymerisation reaction, catalyzed by the MMT; and (iii) another extra-gallery homopolymerisation reaction, catalyzed by the tertiary amines. Hence, for non-isothermal cure, the intra-gallery reaction occurs simultaneously with the cross-linking reaction, whereas for isothermal cure, the intra-gallery reaction occurs before the cross-linking reaction. This difference between the response of the curing system to these different cure schedules is associated with differences in the cure kinetics. Therefore, a high degree of exfoliation cannot be anticipated for the non-isothermally cured TGAP system. This hypothesis is supported by TEM images which show that the nanostructure of non-isothermally cured TGAP nanocomposites is not exfoliated to the same extent as is that of the same nanocomposite system cured isothermally.

1-2-5) Hyperbranched Polymers

An alternative solution for increasing the degree of exfoliation which has relatively recently been reported in the literature [67] [68] [69] [70] is the use of dendritic polymers, or more generally hyperbranched polymers (HBPs) as shown in Figure 7 [71]. These polymers have highly branched structures with numerous reactive groups. Both dendrimers and hyperbranched polymers are prepared based on polymerization of AB_x (x >2) monomers [71] [72]. It is difficult to obtain a large quantity of dendrimer as the production procedure is both costly and time consuming, therefore hyperbranched polymers are considered as a promising candidate for use in industrial fields such as nanocomposites because of the ease of the preparation relative to the dendrimers and are suitable for mass production [71] [72]. Due to the unique properties of the hyperbranched polymers, they have been rather widely studied for their use in a variety of fields such as a base material for coating resins [71], as powder coatings [73], as additives for thermosets in which the reaction kinetics is modified by the presence of a hydroxyl terminated HBP, for example to increase toughness [74] [75] [76] [77] [78] [79] [80], as cross-linking agents, where the HBP reacts with an epoxy monomer and is incorporated into the network structure [81] [82] [83], and to increase the toughness of epoxy polymer layered silicate (PLS) nanocomposites by using an epoxy-functionalized HBP to enhance the exfoliation of the clay layers [69] [84]. They can also act as membrane materials for gas and solution separation [85] and find use in biological applications [86].

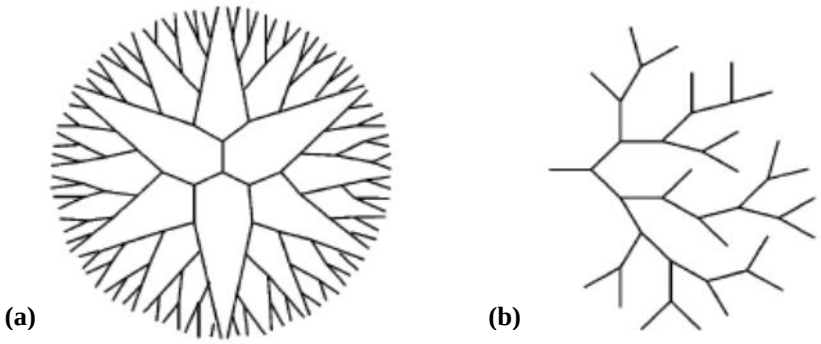

Figure 7: Schematic structure of a dendrimer (a) and a hyperbranched polymer (b) [71]

To date, several research studies have investigated the effect of hyperbranched polymers on the morphology of nanocomposites. In respect of the exfoliation process, these studies can be classified in three categories. The first category is concerned with the quality of clay intercalation in HBP/clay blending, which could result in an improvement in the degree of

exfoliation. In particular, Plummer et al [67] reported that hydrophilic end group hyperbranched polymers (OH terminated) help to achieve clay intercalation with larger *d*-spacings than for the equivalent linear polymer. Although, as these authors pointed out, the dispersion of this intercalated clay in the organic matrix without re-aggregation of the clay layers is a practical issue, they were successful in maintaining the exfoliated state of the clay without agglomeration for their system.

The second category to be considered concerns the effect of the hyperbranched polymer structure on the basal spacing of the clay layers. There are some results presented in the literature that are interesting in this respect, and in particular the work of Singh and Balazs [87]. These authors used self-consistent field theory to predict the effects of polymer architecture on the quality of clay dispersion in the polymer matrix, as well as the possibilities in respect of either intercalation (increase of the layer spacing) or exfoliation (layers dispersed throughout the polymer matrix). The architectures used are: linear; comb (3-arm), and star (4-, 6- and 10-arm). In systems with a favourable polymer-surfactant interaction parameter, the free energy decreases with increasing layer separation, but there is a local minimum in the free energy at small layer separations for the linear, comb and 4-arm star architectures, implying intercalation. In contrast, the 6-arm and 10-arm star architectures do not show any local minimum, implying the possibility of exfoliation for these architectures. They also showed that in situations in which the polymer-surfactant interaction is energetically unfavourable the 10-arm star architecture presents an intercalated structure in contrast to phase-separation which occurs for the other architectures. This is of relevance to the dispersion. These simulations clearly predict that the choice of HBP or dendritic polymer to be used has an important effect on both the possibility of exfoliation and the quality of clay dispersion in these nanocomposites.

The third category is related to the effect of the incorporation of a hyperbranched polymer on the morphology of epoxy nanocomposites. Fu et al [88] investigated the effects of incorporating an epoxy terminated HBP into DGEBA epoxy resin containing Al_2O_3 nanoparticles. They obtained a good dispersion of nanoparticles in the epoxy matrix as a consequence of the incorporation of HBP, which led to an improvement in the toughness. Li et al [89] reported the effect of a new type of hyperbranched polyester with a flexible ethoxylated bisphenol-A structure and terminal hydroxyl groups when it is incorporated into an epoxy-novolac silica filled system. They found that the addition of the HBP improved the mechanical properties relative to the neat epoxy system. Ratna et al [69] investigated the effect of an epoxy terminated HBP on the cure kinetics and morphology development in PLS

nanocomposites based upon DGEBA epoxy resins. The TEM images of DGEBA/clay/HBP system showed that, despite the lack of any scattering peak in XRD, there existed distinct regions of clay tactoids, and therefore the final nanocomposite had an intercalated nanostructure. More recently, Hutchinson et al [90] [91] studied the cure kinetics and corresponding nanostructure of DGEBA/clay nanocomposites which were cured by an amine terminated hyperbranched polymer (Lupasol), and compared this with the same epoxy/clay system cured with diamine (Jeffamine). The Jeffamine cured system showed a shoulder on the high temperature flank of the non-isothermal cure curve, which indicated that the intra-gallery reaction was occurring after the cross-linking reaction [43] and the final nanostructure was not exfoliated. However, these authors found a symmetric curing peak for the Lupasol cured system, which implied the intra-gallery reaction was now occurring at least concurrently with the cross-linking reaction of the DGEBA and Lupasol. Consequently, partial exfoliation can be expected for the final nanostructure of the cured nanocomposite since the intra-gallery reaction is able to take place to some extent before the system become rigid. The SAXS pattern did indeed show that there was no diffraction peak in the low angle range, and the TEM images showed significantly less clay layer stacking compared with the same DGEBA-based nanocomposites which had been cured with Jeffamine. A significant improvement in the degree of exfoliation was therefore achieved for this system.

In summary, it appears that the incorporation of an HBP can improve the exfoliation in DGEBA-based nanocomposite systems. In this respect, it is of interest to investigate whether an improvement in the degree of exfoliation can be achieved also with the incorporation of a hyperbranched polymer in this tri-functional epoxy-based nanocomposite system. These studies have been made, and in appendix B and appendix C the effects of an amine-terminated HBP and an OH terminated hyperbranched polymer, respectively, on the cure kinetics and resulting nanostructure of tri-functional epoxy-clay nanocomposites are reported.

Appendix B reports on the investigation of the cure behaviour of TGAP-based nanocomposites using Lupasol (amine terminated hyperbranched polymer) as the curing agent. In the non-isothermal scan of the TGAP/Lupasol system without clay, two separate peaks appear. The first peak, which occurs at a relatively low temperature such as 90^{o}C, is ascribed to the cross-linking reaction between Lupasol and TGAP, while the second peak, which appears at high temperature, just more than 250^{o}C, is related to the TGAP homopolymerisation, which is initiated by the tertiary amines in the Lupasol structure. This means that the homopolymerisation reaction in this system does not occur until high temperature. The addition of clay to this TGAP/Lupasol system provides another mechanism

for the homopolymerisation reaction to occur, namely that which is catalyzed by the onium ion of the MMT. It is assumed that the kinetics of the intra-gallery reaction in the TGAP/MMT/Lupasol system is the same as the TGAP/MMT/DDS system, since the same epoxy matrix and clay are used. It was shown in our paper III, however, that the intra-gallery homopolymerisation reaction in the TGAP/MMT/DDS system takes place at high temperature, for example at 150^{o}C. Therefore, for isothermal cure of the TGAP/MMT/Lupasol/MMT system, the cross-linking reaction will always occur before the intra-gallery reaction, whatever the isothermal cure temperature, as a consequence of the low curing temperature of the Lupasol-epoxy reaction, whereas for isothermal cure of the TGAP/MMT/DDS system, the intra-gallery reaction occurs before the cross-linking reaction. This effect of the HBP Lupasol is in direct contrast to the DGEBA/MMT/Lupasol system, for which the Luapsol advances the intra-gallery reaction relative to the cross-linking reaction, allowing some exfoliation to occur [90] [91]. As a result, it is expected that the final nanostructure of the TGAP/MMT/Lupasol system will not be well exfoliated; this is confirmed by TEM images of the cured nanocomposites showing many large clay agglomerations, which consist of numerous clay layers with only a small *d*-spacing, and stacked in an ordered arrangement, implying that the final nanostructure is poorly exfoliated.

In appendix C, the effects of the addition of Hybrane (an OH terminated hyperbranched polymer) on TGAP-based nanocomposites are studied. The results show that the incorporation of Hybrane in the TGAP/Nanomer I.30E/DDS system leads to an acceleration of the cross-linking reaction and a retardation of the intra-gallery reaction. The magnitude of the intra-gallery reaction is dependent on the cure temperature and on the Hybrane content, but the fact that this HBP retards the intra-gallery reaction implies that this system will not show exfoliation to the same extent as for the sample without any hyperbranched polymer. This is confirmed by TEM, for which the images show a small *d*-spacing in the clay stacks, which are located within large agglomerations; this is indicative of a poor quality of exfoliation in this nanostructure.

It can be concluded that from the results presented in Appendices B and C that the desired improvement in exfoliation cannot be achieved in these TGAP-based nanocomposites by the incorporation of either Lupasol as a curing agent or Hybrane as a modifier when DDS is used as the curing agent. This demonstrates again that the exfoliation process is dependent on the kinetics associated with the type of epoxy resin and, in the present case, the hyperbranched polymer, which determine the relative rates of the intra- and extra-gallery reactions.

1-2-6) Other Strategies

A number of other strategies to improve the exfoliation process in epoxy nanocomposites have been discussed in the literature. Chin et al [92] investigated the influence of the stoichiometric resin/hardener ratio on exfoliation of mPDA/DGEBA octadecylammonium montmorillonite. They found that exfoliated/intercalated nanocomposites are formed when the DGEBA epoxy with octadecyl ammonium modified MMT is cured with less than the stoichiometric amount of meta-phenylene diamine (mPDA) or with self-polymerisation without any curing agent (as earlier reported by Lan et al [59]). On the other hand, an intercalated nanostructure is formed when it is cured with a higher concentration of mPDA. Extra-gallery cross linking dominates in the case of higher concentrations of curing agent, resulting in intercalated nanocomposites. It is, however, noted that curing with very little curing agent does not lead to a useful nanocomposite, but to a homopolymerised structure with no mechanical integrity.

Wang et al [93] reported a new method, based on what these authors call the "slurry-compounding" approach, for preparing highly exfoliated epoxy/clay nanocomposites. In this approach the clay is dispersed well in the water, and this dispersion state is retained when it is transferred to the epoxy matrix. They used clay which is not organically modified, and it is first dispersed in water; then acetone is added, the precipitate is taken and washed in acetone several times, and then it is added to more acetone to form what they call a slurry. The epoxy resin is then added and the acetone is removed under vacuum. This procedure is similar to that used by Wang et al [37] but apparently without the coupling agent. The TEM images of the nanocomposite which was prepared by this approach showed that the clay layers were dispersed uniformly throughout the epoxy resin matrix and had been exfoliated, whereas the TEM pictures of another sample, which was prepared without using this slurry method, exhibited large clay aggregates with a narrow *d*-spacing, indicating an ordered arrangement. According to these authors, this approach leads to a better clay exfoliation and excellent thermal mechanical properties of the nanocomposites. However, the situation is not so clear when their X-ray diffraction and TEM results are examined in detail. For samples containing 1.0%, 2.5% and 3.5% clay content, there is a scattering peak at about 6º, which corresponds to about 1.4 nm *d*-spacing, whereas the authors claim this peak is almost invisible for those samples with less than 3.5% clay. In addition, the TEM images for a sample with 2.5% clay content supposedly shows exfoliation into single layers in the cured matrix; however, the TEM images shown have scale bars of 200 or 500 nm, about 200 or 500 times larger than the thickness of the individual clay layers, which is about 1 nm, such that single clay layers

would not be visible at this magnification. The interpretation that this represents a highly exfoliated nanostructure, as the title of the paper suggests, should therefore be treated with caution.

Another possibility for developing an exfoliated nanostructure is the so-called "pre-conditioning" procedure, which was first suggested by Benson Tolle and Anderson [94]. These authors found that the storage of the epoxy-silicate mixture at room temperature for periods of time from a few hours to a number of weeks before curing led to a remarkable improvement in the degree of exfoliation, which was identified by SAXS and TEM images Furthermore, they postulated that the exfoliation mechanism during the pre-conditioning procedure was related to some epoxy reaction, but they did not identify any specific reaction. The procedure of pre-conditioning was investigated in more detail by Pustkova et al [55], who reported that the epoxy reaction which occurred during the pre-conditioning procedure was a homopolymerisation reaction. In order to arrive at this conclusion about homopolymerisation, these authors measured the epoxy equivalent (EE) and the glass transition temperature (T_g) of the pre-conditioned mixtures as a function of pre-conditioning time. These mixtures are stored at different temperature such as RT, 60^{o}C, 80^{o}C and 100^{o}C. It was observed that both T_g and EE increased with the pre-conditioning time, the increase being more rapid the higher is the temperature. The value of EE changed linearly with T_g, and at a rate that depended on the pre-conditioning temperature. It was argued that two different homopolymerisation mechanisms are occurring: one is the activated monomer (AM) mechanism, which dominates at high temperature, while the other is the activated chain end (ACE) mechanism, which dominates at low temperature, the latter being the mechanism that most significantly enhances the exfoliation process. It was also shown that the pre-conditioning procedure leads to a remarkable improvement in the quality of the clay dispersion in the resin/clay mixture. Although TEM images showed that the final nanostructure remains intercalated, the increase in *d*-spacing of the clay layers (from about 3.5 nm in the freshly intercalated resin) can be observed.

It can be concluded from these results that pre-conditioning could promote exfoliation by advancing the intra-gallery reaction in the bi-functional epoxy resin. As an extension of these ideas, it is clearly interesting to investigate the effect of pre-conditioning of the tri-functional epoxy-based nanocomposite system on its ability to exfoliate. This was investigated in paper II, in which the isothermal cure of pre-conditioned TGAP/clay mixtures, to which the curing agent DDS was subsequently added, was monitored by DSC. These results show that the intra-gallery reaction, which for samples that have not been pre-conditioned is seen in the

DSC trace as a sharp peak in the very early stages of the cure reaction, completely disappears for pre-conditioned samples, with only the extra-gallery reaction now taking place and seen as the usual broad bell-shaped peak. In other words, homopolymerisation of the TGAP epoxy resin within the clay galleries is occurring during the pre-conditioning procedure before adding the curing agent. Hence, the pre-conditioning process allows a greater extent of intra-gallery reaction to take place before curing process, and therefore pre-conditioning is an effective means for enhancing the intra-gallery reaction, which can lead to an increase in the degree of exfoliation.

The pre-conditioning at low temperatures, which is preferred to high temperatures in respect of exfoliation, requires long storage times, and is therefore somewhat impractical. The use of an initiator is one way of avoiding this practical difficulty, whereby a suitable initiator could promote the epoxy homopolymerisation reaction within the clay galleries. This idea is presented in Paper IV. The suggested initiator is BF_3·MEA (boron trifluoride monoethyl amine) which is known to be an effective initiator for epoxy self-polymerisation. In particular, Li et al [95] reported that the cationic self-polymerisation of DGEBA epoxy resin by the addition of BF_3·MEA occurred at about 120^{o}C and, more recently, Bounds et al [96] found that the BF_3-amine acted as a Lewis acid in epoxy systems and initiated the homopolymerisation reaction. Hence, paper IV presents a novel method for the fabrication of highly exfoliated epoxy/clay nanocomposites, which involves the incorporation of this initiator of cationic homopolymerisation, BF_3·MEA, into the clay galleries before the intercalation of the tri-functional epoxy resin TGAP into the clay. The isothermal DSC scan of this system shows that the intra-gallery reaction occurs at relatively low temperatures, such as 100ºC in the presence of BF_3·MEA, which is in good agreement with temperature of self-polymerisation that was found by Li et al [95]. According to the isothermal cure of the TGAP/MMT/DDS system, the cross-linking reaction between the DDS and TGAP takes place in a temperature range between 120^{o}C and 180^{o}C, for example. Thus the system with BF_3 can be cured in two stages: first at low temperature, allowing the intra-gallery reaction to occur, and then subsequently at higher temperature to complete the curing reaction with DDS. This procedure allows the intra-gallery reaction to occur to a greater extent before the extra-gallery cross-linking reaction, which facilitates the exfoliation of the clay layers during the curing process, and hence leads to a significant increase in the exfoliation degree. The final nanostructure is examined by SAXS. No diffraction peak can be observed in the low angle range, which indicates that the final nanostructure may be exfoliated. However, there is a small peak at 6.6°, corresponding to a *d*-spacing of 1.3 nm; this *d*-spacing is the same as

that of the clay layers when BF_3·MEA is intercalated into the clay galleries, before the addition of the epoxy resin. This implies that some clay layer stacking remains with a very small *d*-spacing within the clay agglomerations, which is observed by TEM. Furthermore, by comparing the TEM images of the samples with and without BF_3 initiator, it can be found that the number and average size of agglomerations which are dispersed throughout the bulk of the sample are decreased significantly with the incorporation of the BF_3·MEA.

1-3) Characterization Techniques for Polymer Layered Silicate Nanocomposites

In this research, the following characterization techniques are utilized for studying the thermal behaviour, degree of intercalation/exfoliation and mechanical properties of the final nanocomposites.

1-3-1) Thermal Characterization

The thermal analytical techniques such as differential scanning calorimetry (DSC or TOPEM) are valuable tools which allow us to monitor and analyze the many reactions that are taking place; some occur within the clay galleries (intra-gallery reaction) and some outside the galleries (extra-gallery reaction) during the curing process of nanocomposites. As an illustration of the usefulness of these techniques, we can consider the need for the intra-gallery reaction to occur before the extra-gallery cross-linking reaction in order to achieve an exfoliated nanostructure. In this respect, it is clear that the cure kinetics is very important because it has a significant influence on the final nanostructure. Paper VIII shows that the DSC is able to identify these two different reactions, intra- and extra-gallery, and whether they occur simultaneously or sequentially during the curing process, and compares the cure behaviour of three different systems as follows: the TGAP/clay/diamine system, the DGEBA/clay/diamine system and the DGEBA/clay/HBP system. The results show that the DSC cure kinetics can be correlated directly with the nanostructure of the cured nanocomposites: for example, the TGAP/clay/diamine system displays the greatest degree of exfoliation as seen from TEM micrographs, which correlates with the appearance in the DSC traces of the intra-gallery reaction before the extra-gallery curing reaction. This same paper also shows how DSC can be used to assess the cure conditions, such as the isothermal cure temperature, for optimizing their nanostructure by controlling the relative rates of the intra- and extra-gallery reactions.

Furthermore, thermal analysis techniques can be used to determine the change in the thermal properties such as the glass transition temperature (T_g) and the thermal stability of the cured nanocomposites, which result from the presence of clay, and thus enables these observations to be related to the nanostructure. For example, thermogravimetric analysis (TGA) determines the thermal stability of materials by monitoring the weight change during heating in a controlled way and in a controlled environment.

Differential Scanning Calorimetry (DSC) and TOPEM®

Differential Scanning Calorimetry experiments were carried out using a conventional calorimeter, DSC821e (Mettler-Toledo), and a stochastic temperature modulated DSC technique, TOPEM® (DSC823e, Mettler-Toledo), both being equipped with STARe software and intra-cooling. Small sample quantities (6-10 mg for DSC and 10-15 mg for TOPEM®) were placed in sealed aluminium pans and the experiments were performed under a flow of dry nitrogen gas at 50 mL/min. The heat of reaction was determined by carrying the reaction isothermally to completion at the different selected cure temperatures or non-isothermally at various heating rates. The first scans of both DSC and TOPEM® for each isothermal cure temperature provided the curve of heat flow versus cure time, from which the isothermal (partial) heat of cure was obtained, and allow us to study the cure kinetics. The TOPEM® experiments additionally gave the frequency independent specific heat capacity, c_{p0}, as a function of cure time, from which the vitrification time, t_v, at each isothermal cure temperature was determined as the time at which the sigmoidal decrease in c_{p0} occurred.

After the isothermal cure was completed, the sample was cooled rapidly either in the DSC to 50ºC or in TOPEM® to 100ºC. It was then heated at a rate of 10 K/min from 50ºC to 300ºC in the DSC in order to determine the residual heat of reaction *(*ΔH_{res}) and in order to determine the glass transition temperature of the partially cured sample, and at 2 K/min from 100ºC to 290ºC in TOPEM® in order to determine the glass transition temperature of the fully cured sample [97]. The sum of the isothermal heat of cure and the residual heat was taken to represent the total heat of the reaction (ΔH_{tot}). The degree of cure conversion, α, after isothermal scan, is calculated (expressed as a percentage) based on ΔH_{tot} and ΔH_{res}:

$$\alpha_c = (1 - \frac{\Delta H_{res}}{\Delta H_{tot}}) \times 100 \quad (1)$$

After the non-isothermal cure was completed, the sample was cooled rapidly in the DSC to 50ºC. It was then heated at a rate of 10 K/min from 50ºC to 300ºC in the DSC in order to determine the glass transition temperature of the fully cured sample.

Furthermore, the DSC was used to measure the T_g of the unreacted resin and the T_g of TGAP/clay mixtures during the pre-conditioning procedure. The samples were heated from -70°C to 25°C with a heating rate of 10K/min and T_g was determined from the step change in the heat flow versus temperature graph.

Thermogravimetric Analysis (TGA)

The purpose of TGA is to investigate degradation by measuring the changes in the weight of a material as a function of temperature; hence TGA/DSC1 (Mettler-Toledo, TG50-M3) was used to determine how the thermal properties such as degradation temperature and thermal stability differ between the neat resin and the cured nanocomposites, and to identify the effects of the different preparation methods of the nanocomposites. In addition to weight changes, the combined thermogravimetry and differential scanning calorimetry afforded by this equipment, TGA/DSC1, also allows the simultaneous measurement of the energy released or absorbed as a consequence of chemical reactions taking place during the heating process. Small sample quantities (5-10 mg) were placed in sealed alumina pans and the experiments were performed under a flow of dry nitrogen gas (200 mL/min) by heating the sample from 40°C to 600°C with a heating rate of 10 K/min.

1-3-2) Structural Characterization

The following structural characterization techniques are used in this thesis to describe the quality of clay layer dispersion and the morphology of the nanocomposites:

- Optical microscopy (OM)
- Small angle X-ray scattering (SAXS)
- Transmission electron microscopy (TEM)
- Scanning electron microscopy (SEM)

OM is used to examine the clay dispersion in the epoxy resin before the cure and to examine the effect of pre-conditioning on the clay dispersion and on the size of the clay agglomerations. The dispersion of the clay in the resin is of great importance in the overall process of clay exfoliation; for example, if there are many large clay agglomerations, it is not possible for the resin to penetrate easily to the clay galleries, and hence exfoliation does not occur.

SAXS and TEM are used in conjunction as complementary tools to analyse the nanostructure of the nanocomposites, in particular to determine whether they are intercalated or exfoliated, and to examine the degree of exfoliation if it occurs. The former technique is

used in order to measure the *d*-spacing of clay layers in the modified clay, in the epoxy/clay mixtures before curing, as well as in the cured nanocomposites. If the cured nanocomposite is not exfoliated, or is only partially exfoliated, the existence of regularly stacked clay layers will be apparent as scattering peaks in SAXS, at measured scattering angles from which the *d*-spacing can be calculated. As far as exfoliated nanostructures are concerned, no more scattering peaks are visible at low angles in SAXS, either because of too large a spacing between the layers, in the case of ordered exfoliated structures (the limit of detection using the instrument in question is about 8 nm) or because the clay layers do not present any ordering. The latter technique, TEM, provides the most direct way for examining the states of clay exfoliation in cured nanocomposites, and is a necessary confirmation of the SAXS data in the case where no scattering peaks are seen, which could result from an ordered stacking with a *d*-spacing beyond the limit of detection. However, TEM examines only a very small area of the nanostructure, and in any sample it is possible to choose a region for TEM study which shows highly exfoliated clay layers even though the overall nanostructure is not at all exfoliated. Thus the technique of TEM relies very much on the integrity of the author to show what is truly representative of the overall nanostructure. In this thesis, the TEM micrographs are always representative of the overall nanostructure except where specific regions are selected deliberately to show how the nanostructure may not be uniform.

Accordingly, TEM can only investigate a very small part of the nanostructure at any time. This difficulty associated with TEM can be obviated by making measurement on bulk samples, for example impact tests, which can then be complemented by the examination of the fracture surfaces by SEM. The resolution of SEM is not the same as the TEM, so it is not possible to identify the individual clay layers, but SEM is a useful tool for understanding how the clay affects the fracture behaviour of the cured nanocomposites. The features of the fracture surface of nanocomposites seen in SEM are dependent on the exfoliation degree: the relatively smooth fracture surface of a typical brittle fracture, such as appears in the fracture of the unreinforced epoxy resin, for example, is converted into a much rougher surface for the nanocomposites. The extent of the roughness, and of the striations which appear, is related to the deviation of the crack from its planar path. This in turn depends on the distribution of the clay platelets, which acts as the origin of microcracks as well as deflecting the crack from its path, thus increasing the facture surface area and hence the toughness. Furthermore, SEM possibly can be used to see clay agglomerations in cured nanocomposites, although they are often difficult to distinguish.

Optical Microscopy (OM)

To examine the size and the quality of the dispersion of the clay agglomerates in the epoxy/clay mixtures before adding the curing agent, a Leica DME polarising transmission optical microscope was used.

Small Angle X-ray Scattering (SAXS)

Small angle X-ray scattering (SAXS) was used to determine the basal spacing of clay in the cured nanocomposites. This indicates, for example, whether or not they might be exfoliated. The presence of a scattering peak means that the nanocomposite is not exfoliated. The Bragg Law is used to calculate the *d*-spacing as follows:

$$n\times\lambda=2\times d\times \sin\theta \qquad (2)$$

where *d* is the spacing between layers, λ is the wavelength of the X-rays at the incident angle θ [The incident angle is θ, not 2θ; as the sample is tilted relative to the incident X-rays, the scattered signal is tilted through twice the angle], and the values of *n* indicate the order of the scattering peaks. As an example, the *d*-spacing of the clay gallery is around 2.1 nm for the organically modified clay, for which a diffraction peak (*n*=1) appears around $2\theta=4.3^{o}$ in the intensity versus 2θ curve for copper Kα radiation, which has a wavelength of 0.1542 nm. However, there is a limitation for the diffraction angle because of an abrupt increase in the intensity at lower angles as a consequence of the radiation that passes directly through the collimating slits of the instrument. This makes it difficult to detect layer spacings greater than about 8 nm. Hence the minimum angle used is usually around $2\theta=1.2^{o}$ which corresponds to about 8 nm *d*-spacing based on the Bragg Law.

SAXS measurements were made using a Bruker model D8 Advanced diffractometer with Bragg-Brentano geometry in reflection mode. The SAXS scans were taken in a range of $2\theta = 1.2^{o}$ to 8^{o} with Ni-filtered copper Kα radiation of wavelength 0.1542 nm under vacuum at room temperature. The power settings were 50 kV and 40 mA. For all the samples, the scans were made with steps in 2θ of 0.02^{o} and with a time of 10 s for each step. The intercalation of the epoxy resin into the clay galleries was determined for the resin/clay mixtures in the form of viscous liquids; the sample was spread in a thin layer on the sample holder, and the viscosity is such that no significant settling of the clay layers will take place during the scan. For the cured nanocomposites the scattering diagrams were obtained for samples in the form of powder after ball-milling (Retsch model MM 400) the bulk samples using 20 mm diameter steel balls and a frequency of 20 Hz for a period of 4 minutes. The powder samples were packed into the appropriate sample holder to form a sintered disc.

Transmission Electron Microscopy (TEM)

TEM is a necessary complement to X-ray scattering in order to confirm whether those SAXS results, which indicate no scattering peaks, truly correspond to exfoliated clay or if the silicate platelets are simply highly intercalated, with a *d*-spacing greater than that detectable by SAXS (~8 nm, $2\theta=1.2^{o}$), but still retain some level of ordered parallel stacking arrangement. The TEM observations were carried out with a Jeol Jem-2010 HRTEM electron microscope with a resolution of 0.18 nm at an acceleration voltage of 200 kV.

Samples for transmission electron microscopy were cast into a flat embedding mould (Pelco), made of silicone rubber and with overall dimensions 105×70×7 mm deep. This mould contained 24 numbered tapered troughs, 6×13×3 mm deep, designed such that the sample is easily accommodated into the ultramicrotome holder. These samples, which are prepared by casting the nanocomposite into the specific mould described earlier, were cut with a Leica EM UC7 ultramicrotome using a diamond knife (Diatome), to give a thickness of approximately 50 nm. The ultrathin sections were left floating on water and were picked up and mounted on a 400 mesh carbon coated grid.

Scanning Electron Microscopy (SEM)

In the SEM analysis the sample studied must be conductive. Accordingly, if the sample is not conductive, as is the case for these nanocomposites, it must be covered with a thin layer of conductive material. Therefore, before the SEM studies, the fracture surfaces were sputtered with a thin layer of gold under vacuum, the layer thickness being around 10-15 nm, by means of a Baltec DSC005 sputter coater. The SEM observations were then carried out with a Jeol 5610 scanning electron microscope with an accelerating voltage of 15 kV and a spot size of 20, using secondary electron imaging.

1-3-3) Mechanical Characterization

The mechanical characterization technique used here was dynamic mechanical analysis (DMA), which measures the stiffness of the nanocomposite or, more precisely, the dynamic modulus of the material. The modulus should increase with clay content, as the clay has a greater modulus than the resin. However, the modulus is very often found to decrease rather than increase as the clay content increases. The decrease in the modulus with increase in the clay loading is attributed to a change in the morphology of the nanocomposite from an exfoliated/intercalated to an intercalated nanostructure as the clay content increases. It means

that this change in the morphology leads to increase the number of the clay agglomerations (clay clusters) in the structure of the nanocomposites and also, the effective properties of the clay clusters (for example, E=102.8 GPa [98]) are always less than the individual clay platelets (for example, E=170 GPa [99]). Hence, the clay clustering has an influence on the moduli of the nanocomposites.

The modulus is just one example of the bulk properties of the material which has been studied, and which is not dependent on any localised region of the microstructure or nanostructure. However, it is not, perhaps, the most important, because the stiffness of epoxy resins is not usually considered as their major drawback. Hence, other mechanical properties, such as strength, elongation at break and impact energy, are often considered to be more important. The impact test measures the energy absorbed by the material when it is subjected to impact. An exfoliated nanostructure is expected to have a higher impact strength because the nanoclay platelets, when separated and distributed homogeneously in the epoxy matrix, would be very effective in deflecting the propagation of microcracks into tortuous paths, which would lead to an increase in the values of impact energy for the nanocomposite by virtue of a significantly larger energy associated with the creation of new surface area. This would be evident as a much rougher fracture surface when viewed by SEM.

Dynamic Mechanical Analysis (DMA)

The ability of a material to store energy is generally expressed as the dynamic storage modulus, represented as Young's modulus, E'. In contrast the loss modulus, E'', describes the ability of the material to dissipate energy; the ratio of E'' to E' is defined as the loss tangent or loss factor, tan δ. All these dynamic mechanical properties of the samples can be measured as a function of temperature and frequency, which is the function of the DMA861e (Mettler-Toledo). These properties can be measured in any mode such as shear, tension, three point bending, single or dual cantilever, and compression.

In general, the storage modulus of the material decreases with increasing temperature. These stepwise changes in E' are caused by relaxation transitions such as the glass transition, or by melting and crystallization. The observed peaks in the loss modulus and loss tangent curves correspond to step changes in the storage modulus. The relaxation processes such as the glass transition temperature are frequency dependent and the temperature at which they occur increases with increasing frequency. In this respect, the main interest of this thesis is the measurement of the glass transition temperature of the fully cured epoxy nanocomposites as a function of their preparation procedure and shear modulus. Such measurement can only be

performed in the shear mode. Hence, the shear clamp (shear mode) based on the small clamping assembly (SCA) was used for analyzing the mechanical properties. In general, the shear modulus (G') is 2 or 3 times less than Young's modulus (E') and they are related by the following equation:

$$E'=2G'(1+\mu) \quad (3)$$

where μ is Poisson's ratio which lies in the range of 0 to 0.5; an average value for cured epoxy resin is 0.33 [100].

All samples for DMA experiments were used in the form of discs with average dimensions of 6 mm diameter and 2 mm thickness, which were machined from the cylindrical moulded samples. This mould consisted of a cylindrical block with four cylindrical cavities, approximately 10 mm diameter and 11 mm in depth, with a slight taper to facilitate the removal of the cured samples.

In this research, DMA measurements were made over a range of frequencies (0.1, 0.3, 1, 3, 10, 30,100 and 300 Hz) and at 2°C/min heating rate over the temperature range from 50ºC to 285°C. The displacement and force amplitude for DMA experiments are selected as 10 μm and 0.1 N, respectively.

Impact Test

The impact tests were performed at room temperature using a Zwick Izod impact tester 5110 according to ASTM D4508-05 (2008) on rectangular specimens, machined to 25×12×2.5 mm (length×width×thickness), with a pendulum of kinetic energy 0.545 J. At least eight specimens were tested for each composition. Test specimens were prepared by casting nanocomposites in a mould which consisted of a rectangular block with nine separate rectangular cavities. The block was clamped to a rigid rectangular base-plate that could be removed in order to extract the cured samples. The cured samples could be removed from the mould easily. The impact strength (Is) can be determined from the energy absorbed by the material upon fracture as:

$$Is = \frac{(I - I_o)}{s} \quad (4)$$

where I and I_o are the energy loss of the pendulum with and without sample, respectively, and s is the cross-sectional area of the sample.

1-4) Materials

The list of the materials which has been used in the experiments described in this thesis is as follows:

- Epoxy Resin: tri-glycidyl para-amino phenol (TGAP), with trade name Araldite MY0510 (Huntsman Advanced Materials) with an epoxy equivalent between 95-106 g/eq and a glass transition temperature of -40°C, was used as the matrix material.
- Curing Agent: 4,4-diamino diphenylsulphone (DDS), with trade name Aradur 976-1 (Huntsman Advanced Materials) was used throughout as the curing agent.
- Layered Silicate Clay: this acts as rigid phase to improve the toughness of the TGAP composite. Three different organically modified layered silicate clays were chosen for this study, as follows:
    - Montmorillonite, with trade name Nanomer I.30E (Nanocor), which consists of 70-75 wt% montmorillonite and 25-30 wt.% octadecylamine, with a cation exchange capacity (CEC) of 92 meq/100 g.
    - Natural montmorillonite modified with a quaternary ammonium salt, with trade name Cloisite 30B (Southern Clay Products, Inc.), with CEC of 90 meq/100 g.
    - Organically modified nanodispersible layered silicate based on natural bentonite, with trade name Nanofil SE 3000 (Rockwood Additives, Inc).
- Initiator: boron trifluoride monoethylamine complex, BF_3·MEA, (Sigma-Aldrich), was used as the cationic initiator for the homopolymerisation reaction.
- Hyperbranched Polymers: two different types of hyperbranched polymer, NH terminated and OH terminated, were chosen for study, as follows:
    - NH terminated hyperbranched polyethylenimine, with trade name Lupasol PR 8515 (BASF), which has a glass transition temperature of -54°C, and was used as the curing agent, the stoichiometric conditions being determined assuming 37.2 g/eq for Lupasol [82] (see Figure 8).

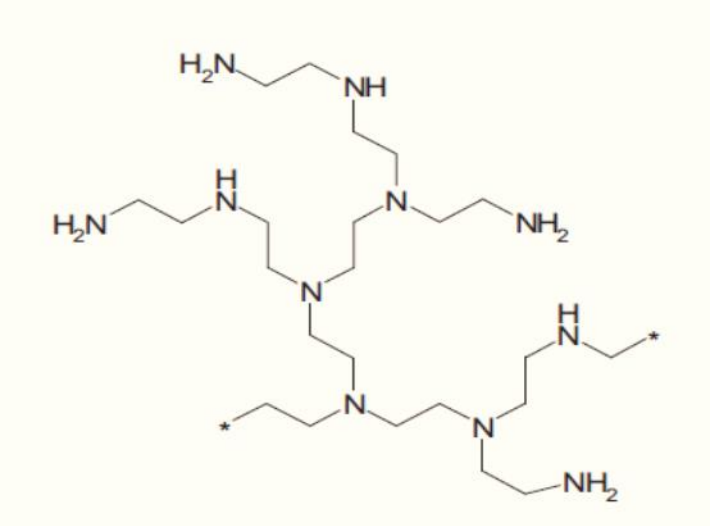

Primary amine	Secondary amine	Tertiary amine	Lupasol: $(C\text{-}C\text{-}NH)_n$
$R\text{-}NH_2$	2R-NH	3R-N	Ratio 1:0.92:0.7

Figure 8: The chemical structure of Lupasol PR 8515

- OH terminated hyperbranched polyesteramide, with trade name Hybrane H 1500 (DSM, Inc), was used as a modifier for promoting the exfoliation in epoxy nanocomposites (see Figure 9).

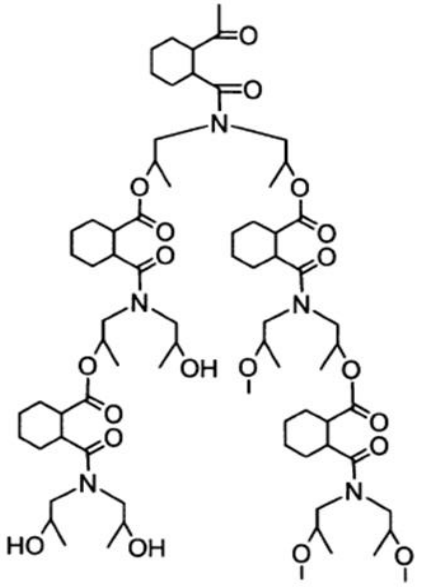

Figure 9: The chemical structure of Hybrane H 1500

1-5) Scope of Work

This thesis is focused on the processing of nanocomposites based on TGAP/MMT with DDS as curing agent to improve the thermal and mechanical properties of polymer layered silicate (PLS) nanocomposites through an optimization of their nanostructure; hence, the following are the objectives of this research:

- To study, by means of differential scanning calorimetry (DSC) or a new modulated DSC technique (TOPEM), the thermal behaviour and kinetic parameters of TGAP/DDS when cured isothermally or dynamically. This serves as a reference for comparison when the nanoclay is added to the mixture. The results of this study are presented in **Paper I**.

- To study the effects of pre-conditioning on the kinetics of cure, thermal properties, degradation and nanostructure of cured nanocomposites. For this purpose, mixtures of TGAP/MMT have been pre-conditioned, at selected temperatures and for selected times, and then cured isothermally with DDS. The resulting nanostructure is characterized by SAXS and TEM. The results are presented in **Paper II**.

- To prepare mixtures of TGAP/MMT without pre-conditioning for cure isothermally and non-isothermally with DDS and to determine the kinetic parameters and thermal properties such as the final glass transition temperature (T_g) and the degradation behaviour, and to characterize the nanostructure of the cured nanocomposite by SAXS and TEM. The results of these isothermal and non-isothermal cure studies are presented in **Paper III** and **Paper V**, respectively.

- To enhance the intra-gallery homopolymerisation rate in comparison with the extra-gallery rate by the use of a cationic initiator such as BF_3·MEA, which is added to the TGAP/MMT/DDS mixture, to examine by thermal analysis the thermal properties and degradation of the cured nanocomposites, and to characterize the final nanostructure by SAXS and TEM. The results of this study are presented in **Paper IV**.

- To determine and compare the dynamic mechanical behaviour and the impact energy, and to examine the fracture surfaces, for nanocomposites which have been cured according to selected schedules corresponding to those used for the nanostructural characterization. These comparative mechanical performances are presented in **Paper VI and Paper VII**.

- To study the effects of different clays such as Cloisite 30B and Nanofil SE3000 on the cure kinetics, thermal properties and degradation of TGAP nanocomposites when cured with DDS; the preparation of pre-conditioned TGAP/Cloisite 30B or TGAP/Nanofil SE3000 mixtures for comparing the pre-conditioning behaviours of TGAP/MMT mixtures; subsequently the final structure of the nanocomposites was characterized by SAXS and TEM. These results are given in **Appendix A**.

- To prepare and characterize a new generation of epoxy nanocomposites, based on TGAP/MMT with the incorporation of hyperbranched polymers (HBPs) such as Lupasol PR8515 and Hybrane H 1500. The nanocomposite is cured isothermally or non-isothermally, the thermal properties, degradation behaviour and cure kinetics are studied by calorimetry, and then the final nanostructure is assessed by SAXS and TEM. **Appendix B** describes the results corresponding to the incorporation of Lupasol into the epoxy/clay mixture and **Appendix** C shows the results for the incorporation of Hybrane.

1-6) Future Work

Toughening of epoxy composites by the addition of a rigid phase such as layered silicate clay has attracted the attention of many researchers in recent years. This includes the toughening of tri-functional epoxy composites, which are used in high performance applications such as in the aerospace industry. Since the toughness in these systems depends on the optimization of the nanostructure, most of these studies have been devoted to finding procedures for increasing the degree of exfoliation in the cured nanocomposite.

The thesis presented here is focused on producing highly exfoliated TGAP based nanocomposites by means of different procedures such as pre-conditioning, selection of the appropriate cure conditions, incorporation of hyperbranched polymers, modifying the clay type, and using an initiator of epoxy homopolymerisation. The final results show that the pre-conditioning procedure, the selection of the isothermal cure conditions, and the use of an initiator all lead to a significant enhancement of the degree of exfoliation.

However, there are other possibilities for promoting the exfoliation process, including the following suggestions:

- Use liquid curing agents such as liquid aromatic amine, DETDA (diethyl-toluenediamine), and liquid ethylene amine, TETA (triethyenetetr amine), and to study the kinetic reaction, clay dispersion and final nanostructure of the TGAP nanocomposite. The advantage of these curing agents over DDS is that they are liquid and offer better processability.
- Use an epoxy terminated hyperbranched polymer such as Boltorn E1 or Boltorn E2 as an alternative toughener for TGAP based nanocomposites. It is expected that the cured nanocomposite would show a two phase morphology, which would lead to an improvement in the toughness.

Finally, the mechanical properties of the cured nanocomposite, prepared according to the suggestions above, should be compared with the corresponding nanostructures, in order to define which is the most effective in the process of exfoliation.

References

[1] M. Alexandre, P. Dubois, "Polymer-layerd silicate nanocomposites: preparation, properties and uses of a new class of materials", *Materials Science and Engineering,* vol. 28, no. 1-2, pp. 1-63, 2000.

[2] N. Karak, "Polymer (epoxy) clay nanocomposites", *Journal of Polymer Materials,* vol. 23, no. 1, pp. 1-20, 2006.

[3] F. Hussain, M. Hojjati, M. Okamoto, R.E. Gorga, "Polymer-matrix nanocomposites, processing, manufacturing and application: an overview", *Journal of Composite Materials,* vol. 40, no. 17, pp. 1511-1575, 2006.

[4] W.Gacitua, A. Ballerini, J. Zhang, "Polymer nanocomposites: synthetic and natural fillers a review", *Maderas. Ciencia y Tecnologia*, vol. 7, no. 3, pp. 159-178, 2005.

[5] H.Y. Liu, G.T. Wang, Y.W. Mai, Y. Zeng, "On fracture toughness of nano-particle modified epoxy", *Composites: Part B,* vol. 42, no. 8, pp. 2170-2175, 2011.

[6] O. Becker, G.P. Simon, K. Dusek, "Epoxy layered silicate nanocomposites", *Inorganic Polymeric Nanocomposites and Membranes in Advances in Polymer Science series*, vol. 179, Springer Berlin Heidelberg, 2005, pp. 29-82.

[7] P.C. Lebaron, Z. Wang, T.J. Pinnavaia, "Polymer-layered silicate nanocomposites: an overview", *Applied Clay Science,* vol. 15, no. 1-2, pp. 11-29, 1999.

[8] T.J. Pinnavaia, G.W. Beal, *Polymer-clay nanocomposites*, Wiley, New York, 2000.

[9] D. Porter, E. Metcalfe, M.J.K. Thomas, "Nanocomposite Fire Retardants-A Review", *Fire and Materials,* vol. 24, no. 1, pp. 45-52, 2000.

[10] H.M. Cordeiro, "Nanocomposite for food packaging application", *Food Research International,* vol. 42, no. 9, pp. 1240-1253, 2009.

[11] N. Hasegawa, A. Tsukigase, A. Usuki, "Silicate layer dispersion in copolymer/clay nanocomposites", *Applied Polymer Science,* vol. 98, no. 4, pp. 1554-1557, 2005.

[12] T. Lan, T.J. Pinnavaia, "Clay-reinforced epoxy nanocomposites", *Chemistry of Materials,* vol. 6, no. 12, pp. 2216-2219, 1994.

[13] T. Lan, Z. Wang, H. Shi, T.J. Pinnavaia, "Clay-epoxy nanocomposites:relationships between reinforcement properties and the extent of clay layer exfoliation", *Polymeric Materials Science and Engineering Proceeding,* vol. 73, pp. 296-297, 1995.

[14] A.A. Azeez, K.Y. Rhee, S.J. Park, D. Hui, "Epoxy clay nanocomposites: processing,

properties and applications: A review", *Composites: Part B,* vol. 45, no. 1, p. 308–320, 2013.

[15] S.S. Ray, M. Okamoto, "Polymer/layered silicate nanocomposites: a review from preparation to processing", *Progress in Polymer Science,* vol. 28, no. 11, pp. 1539-1641, 2003.

[16] H.L. Tyan, K.H. Wei, T.E. Hsieh, "Effect of montmorillonite on thermal and moisture absorption properties of polyimide ofdifferent chemical structures", *Journal of Applied Polymer Science,* vol. 81, no. 7, pp. 1742-1741, 2001.

[17] P.B. Messersmith, E.P. Giannelis, "Synthesis and characterization of layered silicate-epoxy nanocomposites", *Chemistry of Materials,* vol. 6, no. 10, pp. 1719-1725, 1994.

[18] T. Lan, P.D. Kaviratna, T.J. Pinnavaia, "Mechanism of clay tactoid exfoliation in epoxy-clay nanocomposites", *Chemistry of Materials,* vol. 7, no. 11, pp. 2144-2150, 1995.

[19] T.J. Pinnavaia, T. Lan, Z. Wang, H. shi, P.D. Kaviratna, "Nanotechnology Molecularly Designed Materials", American Chemical Society, Washington DC, 1996.

[20] Z. Wang, T. Lan, T.J. Pinnavaia, "Hybrid organic-inorganic nanocomposites formed from an epoxy polymer and a layered silicic acid", *Chemistry of Materials,* vol. 8, no. 9, pp. 2200-2204, 1996.

[21] J. Massam, T.J. Pinnavaia, "Clay nanolayer reinforcement of a glassy epoxy polymer", *Materials Research Society Proceedings,* vol. 520, no. 1, pp. 223-232, 1998.

[22] C. Zilg, R. Mülhaupt, J. Finter, "Morphology and toughness/stiffness balance of nanocomposites based upon anhydride-cured epoxy resins and layered silicates", *Macromolecular Chemistry and Physics,* vol. 200, no. 3, pp. 661-670, 1999.

[23] A. Lee, J.D. Lichtenhan, "Thermal and viscoelastic property of epoxy–clay and hybrid inorganic-organic epoxy nanocomposites", *Journal of Applied Polymer Science,* vol. 73, no. 10, pp. 1993-2001, 1999.

[24] T.J. Pinnavaia, S. Xue, "Porous synthetic smectic clay for the reinforcement of epoxy polymers", *Microporous and Mesoporous Materials,* vol. 107, no. 1-2, pp. 134-140, 2008.

[25] D. Ratna, "Epoxy Composites: Impact Resistance and Flame Retardancy", *Rapra Review Report: report 158,* vol. 16, no. 5, pp. 1-28, 2005.

[26] Y. Tanaka, "Chapter 2: synthesis and characteristics of epoxides", *Epoxy resins: chemistry and technology*, Marcel Dekker Inc., New York, 1988, pp. 9-284.

[27] D. Ratna, "Chapter 3: epoxy resin", *Handbook of thermost resin*, Smithers Rapra Publishing, Shropshire, UK, 2009, pp. 155-174.

[28] M.M. Shen, M.G. Lu, Y.L. Chen, C.Y. Ha, "Effects of modifiers in organoclays on the curing reaction of liquid-crystalline epoxy resin", *Journal of Applied Polymer Science,* vol. 96, no. 4, pp. 1329-1334, 2005.

[29] T.J. Pinnavaia, "Intercalated clay catalysts", *Science,* vol. 220, no. 4595, pp. 365-371, 1983.

[30] Z. Wang, J. Massam, T.J. Pinnavaia, "Chapter 7: Epoxy-clay nanocomposites", in *Polymer-Clay Nanocomposites*, Wiley, New York, 2000, pp. 127-149.

[31] T.F. Mika, R.S. Bauer, "Chapter 4: curing agents and modifiers", *Epoxy Resins: Chemistry and Technology*, Marcel Dekker Inc., New York, 1988, pp. 465-550.

[32] O. Becker, Y-B. Cheng, R. J. Varley, G.P. Simon, "Layered silicate nanocomposites based on various high-functionality epoxy resins: The influence of cure temperature on morphology, mechanical properties, and free volume", *Macromolecules,* vol. 36, no. 5, pp. 1616-1625, 2003.

[33] K. Zhang, L. Wang, F. Wang, G. Wang, Z. Li , "Preparation and characterization of modified-clay-reinforced and toughened epoxy-resin nanocomposites", *Journal of Applied Polymer Science,* vol. 91, no. 4, p. 2649–2652, 2004.

[34] S. Ingram, I. Rhoney, J.J. Liggat, N.E. Hudson, R.A. Pethrick, "Some factors influencing exfoliation and physical property enhancement in nanoclay epoxy resins based on diglycidyl ethers of bisphenol A and F", *Journal of Applied Polymer Science,* vol. 106, no. 1, pp. 5-19, 2007.

[35] F. Hussain, J. Chen, M. Hojjati, "Epoxy-silicate nanocomposites: cure monitoring and characterization", *Materials Science Engineering: Part A,* Vols. 445-446, no. 3, pp. 467-476, 2007.

[36] T. Liu, W.C. Tjiu, Y. Tong, C. He, S.S. Goh, T.S. Chung, "Morphology and fracture behavior of intercalated epoxy/clay nanocomposites", *Journal of Applied Polymer Science*, vol. 94, no. 3, p. 1236–1244, 2004.

[37] K. Wang, L. Chen, J. Wu, M. L. Toh, C. He, A. F. Yee, "Epoxy nanocomposites with

highly exfoliated clay: mechanical properties and fracture mechanisms", *Macromolecules*, vol. 38, no. 3, pp. 788-800, 2005.

[38] A. Yasmin, J.L. Abot, I.M. Daniel, "Processing of clay/epoxy nanocomposites by shear mixing", *Scripta Materialia*, vol. 49, no. 1, pp. 81-86, 2003.

[39] J.H. Park, S.C. Jana , "Mechanism of exfoliation of nanoclay particles in epoxy-clay nanocomposites", *Macromolecules*, vol. 36, no. 8, pp. 2758-2768, 2003.

[40] J.S. Chen, M.D. Poliks, C.K. Ober, Y. Zhang, U. Wiesner, E. Giannelis, "Study of the interlayer expansion mechanism and thermal-mechanical properties of surface-initiated epoxy nanocomposites", *Polymer*, vol. 43, no. 18, pp. 4895-4904, 2002.

[41] X. Kornmann, H. Lindberg, L.A. Berglund, "Synthesis of epoxy-clay nanocomposites. Influence of the nature of the curing agent on structure", *Polymer*, vol. 42, no. 10, pp. 4493-4499, 2001.

[42] Q. Wang, C. Song, W. Lin, "Study of the exfoliation process of epoxy-clay nanocomposites by different curing agents", *Journal of Applied Polymer Science*, vol. 90, no. 2, pp. 511-517, 2003.

[43] S. Montserrat, F. Roman, J.M. Hutchinson, L. Campos, "Analysis of the cure of epoxy based layered silicate nanocomposites: reaction kinetics and nanostructure development", *Journal of Applied Polymer Science*, vol. 108, no. 2, p. 923–938, 2008.

[44] C. Chen, D. Curliss, "Preparation, characterization, and nanostructural evolution of epoxy nanocomposites", *Journal of Applied Polymer Science*, vol. 90, no. 8, pp. 2276-2287, 2003.

[45] C. Lam, K. Lau, H. Cheung, H. Ling , "Effect of ultrasound sonication in nanoclay clusters of nanoclay/epoxy composites", *Materials Letters*, vol. 59, no. 11, pp. 1369-1372, 2005.

[46] S.C. Zunjarrao, R. Sriraman, R.P. Singh, "Effect of processing parameters and clay volume fraction on the mechanical properties of epoxy-clay nanocomposites", *Journal of Materials Science*, vol. 41, no. 8, pp. 2219-2228, 2006.

[47] R. Velumurugan, T.P. Mohan , "Room temperature processing of epoxy-clay nano composites", *Journal of Materials Science*, vol. 39, no. 24, pp. 7333-7339, 2004.

[48] J.M. Hutchinson, S. Montserrat, F. Roman, P. Cortes, L. Campos, "Intercalation of epoxy resin in organically modified montmorillonite", *Journal of Applied Polymer*

Science, vol. 102, no. 4, pp. 3751-3763, 2006.

[49] T.D. Ngo, M.T. Ton-That, S.V. Hoa, K.C. Cole, "Preparation and properties of epoxy nanocomposites. I. The effect of premixing on dispersion of organoclay", *Polymer Engineering and Science,* vol. 49, no. 4, pp. 666-672, 2009.

[50] H.J. Lu, G.Z. Liang, X.Y. Ma, B.Y. Zhang, X.B. Chen, "Epoxy/clay nanocomposites: further exfoliation of newly modified clay induced by shearing force of ball milling", *Polymer International,* vol. 53, no. 10, pp. 1545-1543, 2004.

[51] W. Liu, S.V. Hoa, M. Pugh, "Organoclay-modified high performance epoxy nanocomposites", *Composites Science and Technology,* vol. 65, no. 2, pp. 307-316, 2005.

[52] W. Liu, S.V. Hoa, M. Pugh, "Fracture toughness and water uptake of high performance epoxy/nanoclay nanocomposites", *Composites Science and Technology,* vol. 65, no. 15-16, pp. 2364-2373, 2005.

[53] R.A. Vaia, K. D. Jandt, E.J. Kramer, E.P. Giannelis, "Microstructural evolution of melt intercalated polymer-organically modified layered silicates nanocomposites", *Chemistry of Materials,* vol. 8, no. 11, pp. 2628-2635, 1996.

[54] J.M. Brown, D. Curliss, R.A. Vaia, "Thermoset-layered silicate nanocomposites, quaternary ammonium montmorillonite with primary diamine cured epoxies", *Chemistry of Materials,* vol. 12, no. 11, pp. 3376-3384, 2000.

[55] P. Pustkova, J.M. Hutchinson, F. Roman, S. Montserrat, "Homopolymerisation effects in polymer layered silicate nanocomposites based upon epoxy resin: implications for exfoliation", *Journal of Applied Polymer Science,* vol. 114, no. 2, pp. 1040-1047, 2009.

[56] C. Chen, T.B. Tolle, "Fully exfoliated layered silicate epoxy nanocomposites", *Journal of Polymer Science: Part B: Polymer Physics,* vol. 42, no. 21, p. 3981–3986, 2004.

[57] X. Kornmann, H. Lindberg, L.A. Berglund, "Synthesis of epoxy–clay nanocomposites: influence of the nature of the clay on structure", *Polymer,* vol. 42, no. 4, pp. 1303-1310, 2001.

[58] H. Shi, T. Lan, T.J. Pinnavaia, "Interfacial effects on the reinforcement properties of polymer-organoclay nanocomposites", *Chemistry of Materials,* vol. 8, no. 8, pp. 1584-1587, 1996.

[59] T. Lan, P.D. Kaviratna, T.J. Pinnavaia, "Epoxy self-polymerization in smectite clays",

Journal of Physics and Chemistry of Solids, vol. 57, no. 6-8, p. 1005–1010, 1996.

[60] C. Zilg, R. Thomann, J. Finter, R. Mülhaupt, "The influence of silicate modification and compatibilizers on mechanical properties and morphology of anhydride-cured epoxy nanocomposites", *Macromolecular Material and Engineering,* Vols. 280-281, no. 1, pp. 41-46, 2000.

[61] Z. Wang, T.J. Pinnavaia, "Hybrid organic-inorganic nanocomposites: exfoliation of magadiite nanolayers in an elastomeric epoxy polymer", *Chemistry of Materials,* vol. 10, no. 7, pp. 1820-1826, 1998.

[62] L. Jiankun, K. Yucai, Q. Zongneng, Y. Xiao-Su, "Study on intercalation and exfoliation behavior of organoclays in epoxy resin", *Journal of Polymer Science Part B: Polymer Physics,* vol. 39, no. 1, pp. 115-120, 2001.

[63] D. Kong, C.E. Park, "Real time exfoliation behavior of clay layers in epoxy-clay nanocomposites", *Chemistry of Materials,* vol. 15, no. 2, pp. 419-424, 2003.

[64] T. Benson Tolle, D.P. Anderson, "Morphology development in layered silicate thermoset nanocomposites", *Composites Science and Technology,* vol. 62, no. 7-8, pp. 1033-1041, 2002.

[65] F. Román, S. Montserrat, J.M. Hutchinson, "On the effect of montmorillonite in the curing reaction of epoxy nanocomposites", *Journal of Thermal Analysis and Calorimetry,* vol. 87, no. 1, pp. 113-118, 2007.

[66] F. Roman, Y. Calventus, P. Colomer, J.M. Hutchinson, "Identification of nanostructural development in epoxy polymer layered silicate nanocomposites from the interpretation of differential scanning calorimetry and dielectric spectroscopy", *Thermochimica Acta,* vol. 541, p. 76–85, 2012.

[67] C.J.G. Plummer, L. Garamszegi, Y. Leterrier, M. Rodlert, J.A.E. Manson, "Hyperbranched polymer layered silicate nanocomposites", *Chemistry of Materials,* vol. 14, no. 2, pp. 486-488, 2002.

[68] A. Amin, M. Samy, "Preparation and Characterization of Some Hyperbranched Polyesteramides/Montmorillonite Nanocomposites"," *International Journal of Polymer Science,* DOI:10.1155/2013/528468, 2013.

[69] D. Ratna, O. Becker, R. Krishnamurthy, G.P. Simon, R.J. Varley, "Nanocomposites based on a combination of epoxy resin, hyperbranched epoxy and a layered silicate", *Polymer,* vol. 44, no. 24, pp. 7449-7457, 2003.

[70] M. Rodlert, C.J.G. Plummer, L. Garamszegi, Y. Leterrier, H.J.M. Grünbauer, J.A.E. Manson, "Hyperbranched polymer/montmorillonite clay nanocomposites", *Polymer*, vol. 45, no. 3, p. 949–960, 2004.

[71] C. Gao, D. Yan, "Hyperbranched polymers: from synthesis to applications", *Progress in Polymer Science*, vol. 29, no. 3, pp. 183-275, 2004.

[72] M. Jikei, M. A. Kakimoto, "Hyperbranched polymers:a promising new class of materials", *Progress in Polymer Science*, vol. 26, no. 8, pp. 1233-1285, 2001.

[73] M. Johansson, E. Malmström, A. Jansson, A. Hult A, "Novel concept for low temperature curing powder coatings based on hyperbranched polyesters", *Journal of Coatings Technology*, vol. 72, no. 906, pp. 49-54, 2000.

[74] J.H. Oh, J.S. Jang, S.H. Lee, "Curing behaviour of tetrafunctional epoxy resin/hyperbranched polymer system", *Polymer*, vol. 42, no. 20, pp. 8339-8347, 2001.

[75] D. Ratna, G.P. Simon, "Thermal and mechanical properties of a hydroxyl-functional dendritic hyperbranched polymer and trifunctional epoxy resin blends", *Polymer Engineering and Science*, vol. 41, no. 10, pp. 1815-1821, 2001.

[76] D. Ratna, G.P. Simon, "Thermomechanical properties and morphology of blends of a hydroxy-functionalized hyperbranched polymer and epoxy resin", *Polymer*, vol. 42, no. 21, pp. 8833-8839, 2001.

[77] M. Frigione, E. Calo, "Influence of an hyperbranched aliphatic polyster on the cure kinetic of a trifunctional epoxy resin", *Journal of Applied Polymer Science*, vol. 107, no. 3, pp. 1744-1758, 2008.

[78] X. Fernandez-Francos, A. Rybak, R. Sekula, X. Ramis, F. Ferrando, L. Okrasa, A. Serra, "Modification of epoxy–anhydride thermosets with a hyperbranched poly(ester amide). II. thermal, dynamic mechanical and dielectric properties and thermal reworkability", *Journal of Applied Polymer Science*, vol. 128, no. 6, pp. 4001- 4013, 2013.

[79] X. Fernandez-Francos, A. Rybak, R. Sekula, X. Ramis, A. Serra, "Modification of epoxy–anhydride thermosets using a hyperbranched poly(ester-amide): I. kinetic study", *Polymer International*, vol. 61, no. 12, pp. 1710-1725, 2012.

[80] J. Zhang, Q. Guo, B. Fox, "Thermal and mechanical properties of a dendritic hydroxyl-functional hyperbranched polymer and tetrafunctional epoxy resin blends", *Journal of Polymer Science: Part B: Polymer Physics*, vol. 48, no. 4, pp. 417-424, 2010.

[81] D. Ranta, R. Varley, G.P. Simon, "Toughening of trifunctional epoxy using an epoxy functionalized hyperbranched polymer", *Journal of Applied Polymer Science,* vol. 89, no. 9, pp. 2339-2345, 2003.

[82] D. Santiago, X. Fernandez-Francos, X. Ramis, J.M. Salla, M. Sangermano, "Comparative curing kinetics and thermal-mechanical properties of DGEBA thermosets cured with a hyperbranched poly(ethylenimine) and an aliphatic triamine", *Thermochimica Acta,* vol. 526, pp. 9-21, 2011.

[83] M.M. Eissa, M.S.A. Youssef, A.M. Ramadan, A. Amin, "Poly(ester-amine) hyperbranched polymer as toughening and co-curing agent for epoxy/clay Nanocomposites", *Polymer Engineering and Science,* vol. 53, no. 5, pp. 1011-1020, 2013.

[84] D. Foix, M.T. Rodríguez, F. Ferrando, X. Ramis, A. Serra, "Combined use of sepiolite and a hyperbranched polyester in the modification of epoxy/anhydride coatings: A study of the curing process and the final properties", *Progress in Organic Coatings,* vol. 75, no. 4, pp. 364-372, 2012.

[85] J. Fang, H. Kita, K. Okamoto , "Gas permeation properties of hyperbranched polyimide membranes", *Journal of Membrane Science,* vol. 182, no. 1-2, pp. 245-256, 2001.

[86] C.C. Lee, J.A. Mackey, J.M.J. Frechet, F.C. Szoka, "Designing dendrimers for biological applications", *Nature Biotechnology,* vol. 23, no. 12, pp. 1517-1526, 2005.

[87] C. Singh, A.C. Balazs, "Effect of polymer architecture on the miscibility of polymer/clay mixtures", *Polymer International,* vol. 49, no. 5, pp. 469-471, 2000.

[88] J.F. Fu, L.Y Si, Q.D. Zhong, Y. Chen, L.Y. Chen, "Thermally conductive and electrically insulative nanocomposites based on hyperbranched epoxy and nano-Al2O3 particles modified epoxy resin", *Polymers for Advanced Technologies,* vol. 22, no. 6, pp. 1032-1041, 2011.

[89] T. Li, H.J. Qin, Y. Liu, X.H. Zhong, Y.F. Yu, A. Serra, "Hyperbranched polyester as additives in filled and unfilled epoxy-novolac systems", *Polymer,* vol. 53, no. 25, pp. 5864-5872, 2012.

[90] J.M. Hutchinson, F. Shiravand, I. Fraga, P. Cortés, Y. Calventus, "Thermal analysis of polymer layered silicate nanocomposites: identification of nanostructure development by DSC", *Journal of Thermal Analysis and Calorimetry*, DOI: 10.1007/s10973-014-3709-3, 2014.

[91] P. Cortés, I. Fraga, Y. Calventus, F. Román, J.M. Hutchinson, F. Ferrando, "A new epoxy-based layered silicate nanocomposite using a Hyperbranched Polymer: study of the curing reaction and nanostructure development", *Materials,* vol. 7, pp. 1830-1849, 2014.

[92] I-J. Chin, T. Thurn-Albrecht, H-C. Kim, T.P. Russell, J. Wang, "On exfoliation of montmorillonite in epoxy", *Polymer,* vol. 42, no. 13, pp. 5947-5952, 2001.

[93] K. Wang, L. Wang, J. Wu, L. Chen, C. He, "Preparation of highly exfoliated epoxy/clay nanocomposites by 'slurry compounding: process and mechanisms", *Langmuir,* vol. 21, no. 8, pp. 3613-3618, 2005.

[94] T. Benson Tolle, D. P. Anderson, "The role of preconditioning on morphology development in layered silicate thermoset nanocomposites", *Journal of Applied Polymer Science,* vol. 91, no. 1, pp. 89-100, 2004.

[95] Y.S. Li, M.S. Li, F.C. Chang, "Kinetics and curing mechanism of epoxy and boron trifluoride monoethyl amine complex system", *Journal of Polymer Science: Part A: Polymer Chemistry,* vol. 37, no. 18, p. 3614–3624, 1999.

[96] C.O. Bounds, R. Goetter, J.A. Pojman, M. Vandersall, "Preparation and application of microparticles prepared via the primary amine-catalyzed michael addition of a trithiol to a triacrylate", *Journal of Polymer Science: Part A: Polymer Chemistry,* vol. 50, no. 3, pp. 409-422, 2012.

[97] J.M. Hutchinson, F. Shiravand, Y. Calventus, I. Fraga, "Isothermal and non-isothermal cure of a tri-functional epoxy resin (TGAP): a stochastic TMDSC study", *Thermochimica Acta,* vol. 529, pp. 14-21, 2012.

[98] O. Shishkina, L. Gorbatikh, S.V. Lomov, I. Verpoest, "Modeling of elastic properties of the cell wall material in nanoclay-reinforced foams", *19th International Conference on Composite Materials (ICCM-19),* Montreal, Canada, 2013.

[99] K. Anoukou, F. Zairi, M. Nait-Abdelaziz, A. Zaoui, T. Messager, J.M. Gloaguen, "On the overall elastic moduli of polymer-clay nanocomposite materials using a self-consistent approach. Part II: Experimental verification", *Composites Science and Technology,* vol. 71, no. 2, pp. 206-215, 2011.

[100] A. Mouloud, R. Cherif, S. Fellahi, Y. Grohens, I. Pillin, "Study of morphological and mechanical performance of amine-cured glassy epoxy–clay nanocomposites", *Journal of Applied Polymer Science,* vol. 124, no. 6, pp. 4729-4739, 2012.

Paper I

Isothermal and non-isothermal cure of a tri-functional epoxy resin (TGAP): A stochastic TMDSC study

J.M. Hutchinson, F. Shiravand, Y. Calventus, I. Fraga

Thermochimica Acta

529, pp: 14-21, 2012

Paper II

Intra- and extra-gallery reactions in tri-functional epoxy polymer layered silicate nanocomposites

J.M. Hutchinson, F. Shiravand, Y. Calventus

Journal of Applied Polymer Science

128(5), pp: 2961-2970, 2013

Paper III

Influence of the isothermal cure temperature on the nanostructure and thermal properties of an epoxy layered silicate nanocomposite

F. Shiravand, J.M. Hutchinson, Y. Calventus

Polymer Engineering and Science

54(1), pp: 51-58, 2014

Paper IV

Highly exfoliated nanostructure in trifunctional epoxy/clay nanocomposites using boron trifluoride as initiator

J.M. Hutchinson, F. Shiravand, Y. Calventus, X. Fernández-Francos, X. Ramis

Journal of Applied Polymer Science

131(6), 2014

DOI: 10.1002/app.40020

Paper V

Study of the non-isothermal cure kinetics of tri-functional epoxy nanocomposites

F. Shiravand, J.M. Hutchinson, Y. Calventus,

To be submitted (2014)

Study of the Non-Isothermal Cure Kinetics of Tri-functional Epoxy-Clay Nanocomposites

Fatemeh Shiravand, John M Hutchinson,* Yolanda Calventus

Centre for Research in NanoEngineering, and Departament de Màquines i Motors Tèrmics, ETSEIAT, Universitat Politècnica de Catalunya, 08222 Terrassa, Barcelona, Spain

hutchinson@mmt.upc.edu

Abstract

The non-isothermal cure kinetic of the polymer silicate layered nanocomposite based on the tri-functional epoxy resin was investigated by calorimetric technique (DSC). The dynamic cure reaction consists of four reactions; cross-linking reaction, intra-gallery reaction which occurs concurrently with cross-linking reaction and two extra-gallery homopolymerization reactions which catalysed by MMT or tertiary amine. The final nanostructure displays the similar quality of exfoliation which is observed for the isothermal cured sample. This implies that the intra-gallery reaction is not inhibited by the extra cross-linked regions.

Keywords: non-isothermal cure; nanocomposites; intra-gallery reaction, cross-linking reaction, homopolymerization, exfoliation.

Introduction

Polymer layered silicate (PLS) nanocomposites based on thermosetting polymers, such as epoxy resin, are interesting as a new class of material. In comparison with the unreinforced epoxy resin, these nanocomposites can exhibit significant improvements in mechanical properties, such as an increase in the modulus, tensile strength and impact strength, and in thermal properties such as flame retardance. As a consequence of the enhancement in these properties, they can find increased use in a wide range of industrial areas, from adhesives to coatings, and from microelectronic applications to high performance aerospace composite systems [1-7].

The procedure for the fabrication of epoxy-clay nanocomposites is based on in-situ polymerisation. Although this procedure is apparently simple, involving the mixing of the resin, clay and curing agent and effecting a suitable cure schedule, it transpires that the nanostructure and properties of the cured nanocomposite are very much dependent on the detailed conditions of the whole fabrication procedure, which includes, for example, the method of mixing the components as well as the curing process itself [4, 6]. The curing process, which may involve isothermal or non-isothermal (dynamic) cure schedules, or a combination or sequence of either of these, may be monitored and characterised by thermal analysis techniques, from which a number of kinetic parameters may be obtained. These parameters and other details of the cure process can be related to the nanostructure development, and hence thermal analysis is a useful tool in the study of these PLS nanocomposites [8-20].

Most of the studies of the cure reaction of epoxy PLS nanocomposites have concentrated on the isothermal or non-isothermal cure of bi-functional epoxy resin systems, typically diglycidyl ether of bisphenol-A (DGEBA); for example, only reference 13 of those cited immediately above (references 8 to 20) does not use DGEBA. Considerably less attention has been paid to the isothermal and/or non-isothermal cure behaviour of PLS nanocomposites based upon high-functionality epoxy resins, though there are exceptions, such as the study of tri- and tetra-functional epoxy resin systems [21] and our own earlier investigations of a tri-functional epoxy resin nanocomposite system based upon tri-glycidyl p-amino phenol (TGAP) [22, 23]. Strangely, Becker et al [21] found that the DGEBA resin resulted in better exfoliation than for the resins of

higher functionality, which is exactly contrary to our own experience. We found that, in the isothermal cure of TGAP-based nanocomposites, two distinct reactions occurred: the first of these reactions was very rapid and could be associated with the homopolymerisation reaction of the resin within the clay galleries, while the second reaction represented the cross-linking reaction of the TGAP with the curing agent, diaminodiphenyl sulphone (DDS) [22]. These TGAP systems resulted in significantly better exfoliation of the cured nanocomposite, as observed by both small angle X-ray scattering (SAXS) and transmission electron microscopy (TEM), in comparison with earlier studies of DGEBA-based nanocomposites [16-18, 20]. We attributed this to the beneficial occurrence, in the TGAP system, of the intra-gallery reaction before the bulk cross-linking reaction, whereas the homopolymerisation reaction in the DGEBA system does not occur until after the major part of the bulk cross-linking reaction has occurred, which inhibits any further separation of the clay layers from taking place.

This earlier work was related to the isothermal cure behaviour of TGAP/hardener/clay systems. Not only were the kinetic parameters and activation energy determined for each of these two reactions, intra- and extra-gallery, but also the effect of the cure temperature on the thermal properties and final nanostructure was studied [23]. It transpires that the first reaction, which takes place within the clay galleries and promotes the exfoliation of the clay, is enhanced at higher cure temperature, and hence higher isothermal cure temperatures give rise to increased exfoliation in the cured nanocomposite. This result is in agreement with the observations of Becker et al [21], who concluded that higher cure temperatures were found to improve clay delamination, as well as increasing the toughness and modulus in the case of both DGEBA- and TGAP-based materials. In order to further clarify the process of exfoliation in these TGAP-based systems, the goal of the present paper is to investigate the non-isothermal (dynamic) cure behaviour of the same system for comparison with the isothermal cure behaviour, to obtain the kinetic parameters and activation energy, and to analyse the quality of the final nanostructure.

Materials and Methods

The epoxy resin (TGAP), with trade name Araldite MY0510 (Huntsman Advanced Materials)

and an epoxy equivalent between 95-106 g/eq, the curing agent, 4,4-diamino diphenyl sulphone (DDS), with trade name Aradur 976-1 (Aldrich), and the organically modified montmorillonite (MMT), with trade name Nanomer I.30E (Nanocor Inc.), were used without further purification. First, TGAP and MMT were mixed mechanically in various proportions of MMT: 0, 2, 5 and 10 wt%. The curing agent, DDS, was added to the resin-clay mixture in a proportion of 52 wt%, which corresponds to a slight excess of epoxy, as is recommended by the manufacturer. The mixture was then degassed under vacuum at room temperature.

Small sample quantities (6-10 mg) were taken from this preparation and placed in sealed aluminium pans, ready for the curing experiments that were carried out using a conventional differential scanning calorimeter, DSC821e (Mettler-Toledo). This instrument is equipped with a robot for sample placement in the furnace, with intra-cooling for sub-ambient temperatures, and with STAR^e software for data evaluation. The DSC was calibrated with indium for both heat flow and temperature, and the experiments were performed under a flow of dry nitrogen gas at 50 mL/min.

All the samples were cured non-isothermally from 0ºC to 290ºC at different heating rates, β: 2, 5 and 10ºC/min. The glass transition temperature, T_g, of the fully cured nanocomposite was determined from a second non-isothermal scan, from 50ºC to 300ºC at 10ºC/min heating rate. It is worth pointing out that the T_g of the non-isothermally cured nanocomposites is significantly lower than that for the isothermally cured nanocomposites, as a consequence of the difference in network structure. Therefore, whereas the determination of the T_g of the isothermally cured nanocomposites required the use of a temperature modulated technique, TOPEM [24], the T_g of the non-isothermally cured samples can be measured in the conventional way from the step change in the heat flow during the second scan in the DSC.

The final nanostructure was observed for bulk samples which had been cured in an air-circulating oven in which the temperature was increased linearly with time at a rate of 10ºC/min. The nanostructural characterisation was made by small angle X-Ray scattering (SAXS) and by transmission electron microscopy (TEM). X-ray diagrams were obtained using a Bruker D8 Advanced diffractometer, measurements being taken in a range of 2θ from 1° to 8° with copper

*K*α radiation (λ=0.1542 nm); for this, powder samples were obtained by ball-milling (Retsch model MM 400) the bulk samples using 20 mm diameter steel balls and a frequency of 20 Hz for a period of 4 minutes. The TEM studies were carried out on a high resolution microscope (Jeol-2010) at 200 kV accelerating voltage with high resolution imaging and with 0.23 nm point resolution; for this, sections of approximately 50 nm thickness were cut from the bulk sample by ultra-microtomy.

Kinetic analysis

The kinetic model for the time dependence of the degree of cure, α, for a non-isothermal curing process with a constant heating rate can be described by the following equation:

$$\mathrm{d}\alpha/\mathrm{d}t = k\,T\,f(\alpha) \tag{1}$$

where $k(T)$ is the rate constant, which depends on the temperature, T, and $f(\alpha)$ is a function of the kinetic model. The rate constant $k(T)$ can be further expressed by the Arrhenius equation:

$$k\,(T) = A\,\exp(-E/RT) \tag{2}$$

where E is the activation energy, A is the pre-exponential factor, and R is the universal gas constant. In this paper, the autocatalytic model in which the initial cure rate is zero, known as the Sesták-Berggren equation, is chosen for the $f(\alpha)$ function, as follows:

$$f(\alpha) = \alpha^{m}(1-\alpha)^{n} \tag{3}$$

where m and n are the reaction orders.

In the DSC experiments, the heat flow, ϕ, that is measured and which results from the curing reaction is assumed to be proportional to the rate of cure:

$$\phi = (d\alpha / dt)\, \Delta H_{tot} \quad (4)$$

where ΔH_{tot} is the total heat of cure of the reaction, obtained from the total area under the non-isothermal cure curve.

The usual approach in the kinetic analysis is to determine the activation energy by a direct method, and subsequently to determine ln(A) and the kinetic parameters of the function $f(\alpha)$. There has been considerable discussion in the literature about the numerous methods for the evaluation of the kinetic parameters, and in particular of the activation energy [25]. For example, Starink [26] gives an extensive comparison of methods for the analysis of constant heating rate experiments, and concludes that so-called "Type B" methods, such as those due to Ozawa [27] and Vyazovkin [28, 29], in which some approximations of the temperature integral are made, are often to be preferred to those methods (Type A), such as the Friedman isoconversional method, which make no such approximations, in particular as a consequence of uncertainty in the application of a baseline to the experimental data. Accordingly, here we adopt the most commonly used Type B method, the Kissinger method [30, 31], for the determination of the activation energy. This method is based upon the determination, as a function of the heating rate β, of the temperature, T_p, at which the heat flow passes through a maximum. The approximation made here is that the degree of conversion is a constant value at this peak, independent of the heating rate, and leads to a linear relationship between $\log(\beta/T_p^2)$ and the reciprocal of T_p, from which the activation energy, E, is obtained.

Once the activation energy has been determined, the other kinetic parameters can be obtained from the DSC curves by the method suggested by Málek [32], which involves the calculation of two functions, $y(\alpha)$ and $z(\alpha)$, defined as follows for non-isothermal cure:

$$y(\alpha) = \phi \exp x = \Delta H_{tot}\, A\, f(\alpha) \quad (5)$$

$$z(\alpha) = \phi T^2 = C f(\alpha)\, g(\alpha) \quad (6)$$

where $x = E/RT$ is a dimensionless quantity, $C = \Delta H_{tot}\beta /RT$, and $g(\alpha) = \int d\alpha /f(\alpha)$ between the limits of 0 and α. The functions $y(\alpha)$ and $z(\alpha)$ are invariant with respect to the heating rate and are sensitive to small changes in the kinetic model $g(\alpha)$. In practice, the $y(\alpha)$ and $z(\alpha)$ functions are normalised between 0 and 1 for convenience.

Results and Discussion

DSC study of the TGAP/DDS system

As a starting point and reference with which to compare the dynamic cure behaviour of the TGAP clay nanocomposite, we begin by describing the cure kinetics of the system without clay, namely the TGAP/DDS system. In the isothermal cure of TGAP/DDS studied earlier [24], a single exothermic peak appears, as shown in Figure 1, which is related to the cross-linking reaction of TGAP/DDS. In contrast, during a dynamic scan of the same system, as shown in Figure 2, the cure curve exhibits both a peak and a shoulder, which shift to higher temperature for faster heating rates. It is clear that the non-isothermal cure process consists of two overlapping reactions: the first is the main reaction, and is attributed to the cross-linking reaction between the TGAP and DDS; the second, which appears as a shoulder on the high temperature flank of the main peak, could be attributed to a number of different reactions, and is discussed further after examining the total heat of reaction.

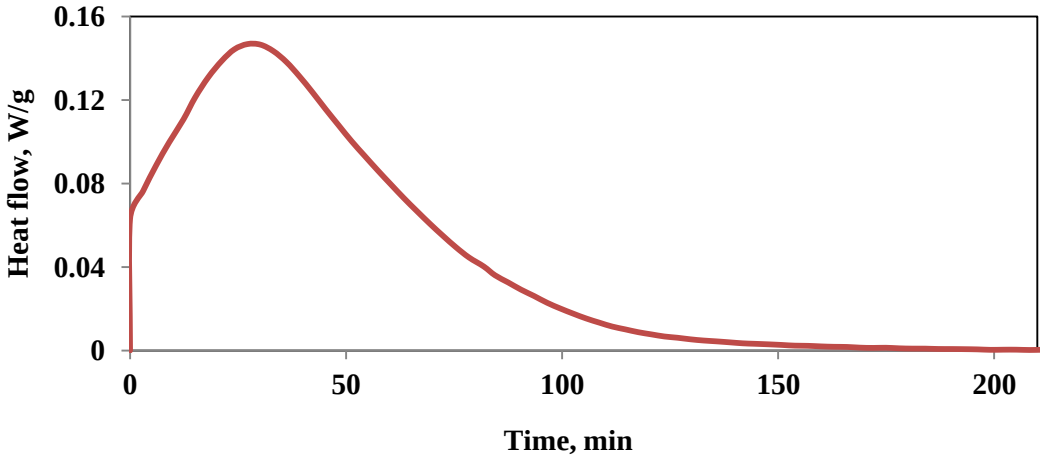

Figure 1. Isothermal DSC curve for TGAP/DDS system at 150ºC.

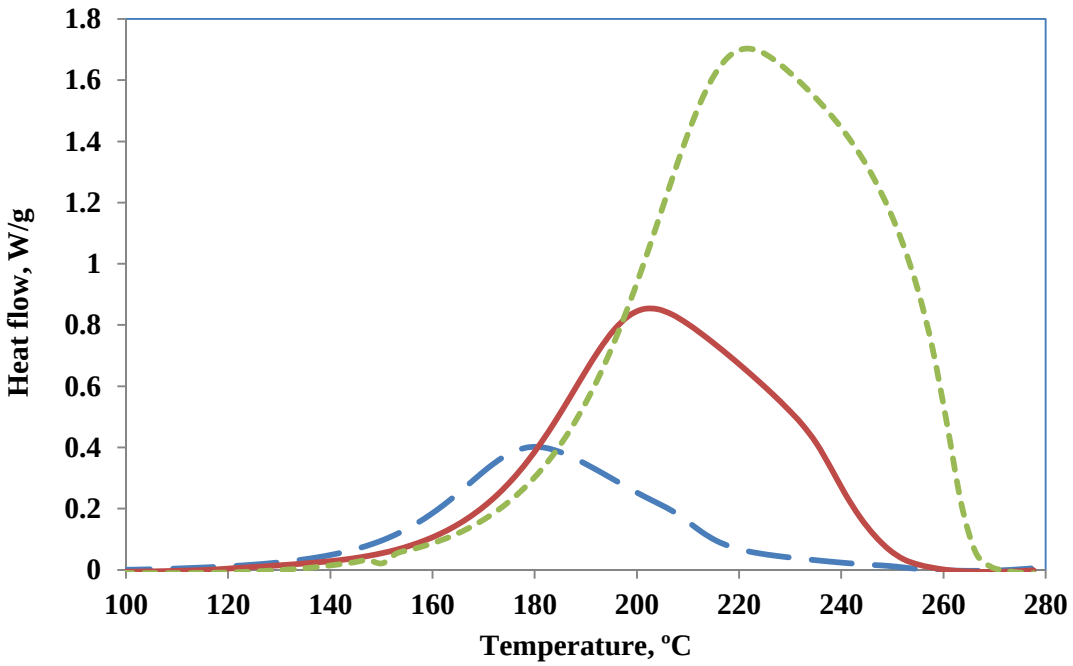

Figure 2. Non-isothermal DSC cure curve for TGAP/DDS system from 0-280ºC with different heating rates as indicated: long dash, 2ºC/min; full line, 5ºC/min; short dash, 10ºC/min.

The total heat of the reaction, represented by the area under both the first and second peaks, and determined as the average from the non-isothermal scans at the three different heating rates, is found to be 98.5 kJ/ee. This result lies between the range of values 94.6 kJ/ee to 96.8 kJ/ee, obtained from the results of Frigione and Calò [33] for non-isothermal cure of the same TGAP epoxy with diamino diethyltoluene as curing agent at heating rates from 5 to 15ºC/min, and the value of 110.5 kJ/ee quoted by Varley et al [34] for the non-isothermal cure of TGAP with DDS. There are several reasons why there appears to be a range of values for the heat of reaction of TGAP. Frigione and Calò [33] use an epoxy equivalent of 101 g/ee, from the manufacturer's literature, and a stoichiometric ratio of epoxy:amine, whereas Varley et al [34] determine the epoxy equivalent by titration as 106 g/ee and use a molar ratio epoxy:amine of 1:0.9, implying a slight excess of epoxy. Whereas previously we determined the epoxy equivalent by titration as 95 g/ee [24], which is at the lower end of the range of values 95 to 106 g/ee given in the manufacturer's literature, in the present work we found that some homopolymerisation of the epoxy resin had taken place, presumably initiated by the N in the TGAP chemical structure, resulting in a slight increase in the glass transition temperature of the resin. Accordingly, for the

determination of the heat of reaction in units of kJ/ee we also use the value of 106 g/ee together with the molar ratio of 1:0.9 for the epoxy:amine mixture.

We discuss now the composite peak that appears in the non-isothermal scan of TGAP/DDS, which can be deconvoluted into two separate exothermic peaks by means of the PeakFit program (PF version v4, Jandel Scientific software). Similar observations were made by Frigione and Calò [33], who found a pronounced shoulder in the last part of the dynamic exotherm peak, which they attributed to "diffusional processes taking place at higher conversions", and which they were unable to fit using an autocatalytic model based upon the equation [35, 36]:

$$d\alpha/dt = (k_1 + k_2\alpha^m)(1 - \alpha)^n \qquad (7)$$

where k_1 and k_2 represent the temperature dependent rate coefficients for the reaction catalysed by proton donors initially present in the system and those that are produced during cure, respectively. Here, the fit obtained using the asymmetric double sigmoidal function (ADL) shows quite good agreement with the experimental data, a typical example being shown in Figure 3 for a heating rate of 10ºC/min. It is noticeable, however, that the abrupt decrease in the experimentally measured heat flow at the end of the reaction, at temperatures higher than about 260ºC, is not well modelled by the PeakFit programme, even though the fit using the ADL function shown here was better than that obtained using any of the other available functions.

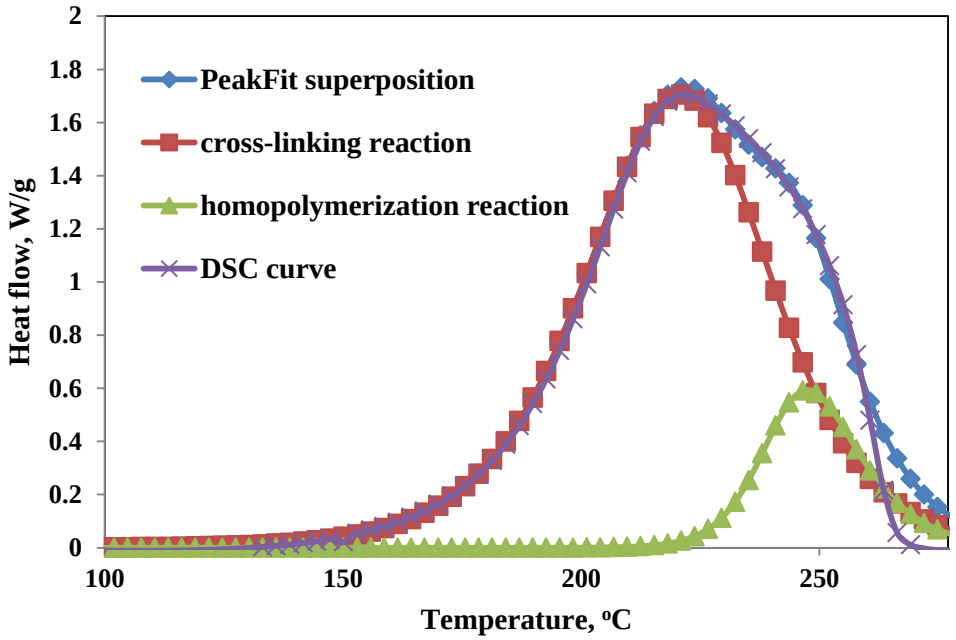

Figure 3. Deconvoluted peaks for non-isothermal cure of TGAP/DDS system at 10ºC/min: crosses, original DSC curve; square, first reaction, cross-linking; triangles, second reaction, homopolymerisation; rhombus, PeakFit superposition.

We now consider the following possibilities for the appearance of such a composite peak.

(a) The first peak is due to the reaction of the epoxy groups with primary amines, whereas the second is due to reactions with secondary amines. The argument here would be that the reactivity of primary and secondary amines is significantly different. It should be noted that DDS, particularly in respect of the secondary amines, is less reactive than other aromatic amines.

(b) For some reason the TGAP/DDS cross-linking reaction during non-isothermal cure results in a topological network structure which inhibits, at some degree of cure, the further reaction of the TGAP with the DDS. For this reason, higher temperatures are required in order to provide sufficient mobility to the reacting species, whereupon a further reaction occurs. This argument is similar to that put forward by Frigione and Calò [33], which was based upon the need for diffusional processes to take place at higher temperatures.

(c) The cure process begins with the reaction of epoxy groups with primary amines. This reaction produces secondary amines which themselves react with the epoxy to produce tertiary amines, which in turn act as an initiator of epoxy homopolymerisation. These tertiary amines act in conjunction with the nitrogen of the TGAP and the alcohol groups formed by the reaction of the TGAP with the DDS to provide a strong driving force for homopolymerisation. Possibly in combination also with topological constraints, as proposed in (b) above, this would promote epoxy homopolymerisation as the preferred reaction mechanism.

In order to distinguish between these various possibilities, some further information is required, which is afforded by the determination of the glass transition temperature of the fully cured system, $T_{g\infty}$. The $T_{g\infty}$ for the non-isothermally cured sample of TGAP/DDS can be determined from a second DSC scan, and the results are presented in Figure 4. As is often observed, the glass transition temperature of the sample that has been cured non-isothermally is lower than that of a sample cured isothermally, which was determined in earlier work by means of the temperature modulated DSC technique TOPEM to be around 256ºC [24]. Here, though, the $T_{g\infty}$ of the non-isothermally cured system is very much lower, and decreases with increasing heating to reach a value as low as 206ºC at 10ºC/min heating rate. This observation needs to be consistent with the possible explanation for the presence of a composite reaction curve, as shown in Figures 2 and 3, as discussed immediately above.

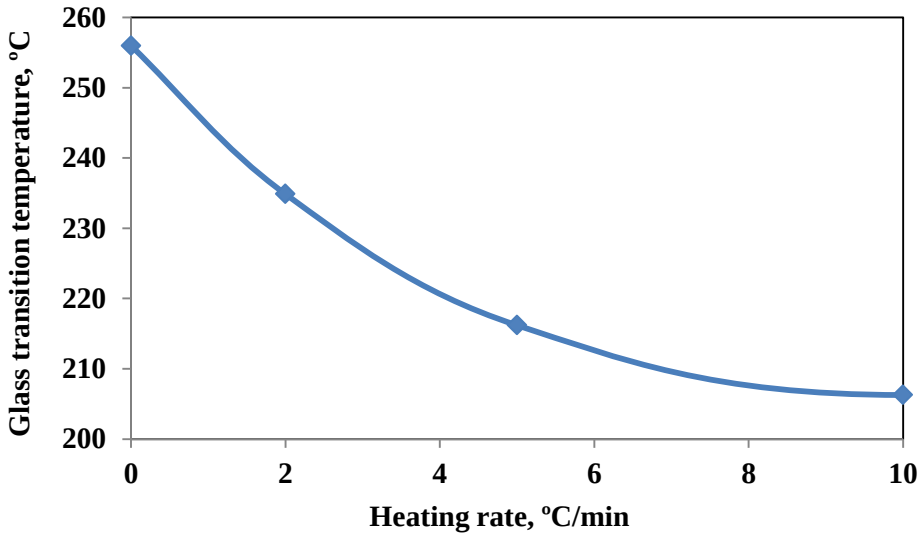

Figure 4. Glass transition temperature of the non-isothermally cured TGAP/DDS system as a function of the heating rate.

Possibility (a) does not present any obvious reason for why the $T_{g\infty}$ should decrease with increasing heating rate, as primary and secondary amines would be expected to lead to similar network structures in the cured system. Nor does possibility (b) explain this observation if the effect of the topological restraint is simply to delay the secondary amine reaction. On the other hand, possibility (c) implies that the network structure would indeed be different, as more homopolymerisation would occur the higher is the heating rate. The asymmetric shape of the second deconvoluted peak in Figure 3 might result from the gradually increasing contribution from the homopolymerisation reaction as the tertiary amines are progressively created. Since homopolymerisation is associated with a reduced cross-link density, and hence with a reduction in $T_{g\infty}$, we believe that the second peak in the composite non-isothermal curing reaction occurs as a consequence of homopolymerisation.

We now examine the corresponding behaviour of the same system in which clay is now incorporated.

DSC study of the TGAP/DDS/MMT system

A typical isothermal cure curve, obtained by DSC, for the TGAP/DDS/MMT system is shown in Figure 5, for the particular case of cure at 165ºC. As can be seen, there are clearly two exothermic peaks, distinctly different from the single exothermic reaction seen for isothermal cure of the system without clay shown in Figure 1; the first rapid peak is attributed to the TGAP homopolymerisation within the clay galleries (intra-gallery reaction), while the main broad peak is related to the cross-linking reaction between TGAP and DDS in the bulk of the sample (extra-gallery reaction). The justification for assigning the first peak to a homopolymerisation reaction catalysed by the organically modified clay has been given earlier [22, 23]. One might therefore anticipate, for the non-isothermal cure of the TGAP/DDS/MMT system, more complex reaction kinetics than has been shown above for the TGAP/DDS system without clay, where the TGAP/DDS reaction is accompanied by an epoxy homopolymerisation reaction catalysed by the tertiary amines. This is indeed found to be the case.

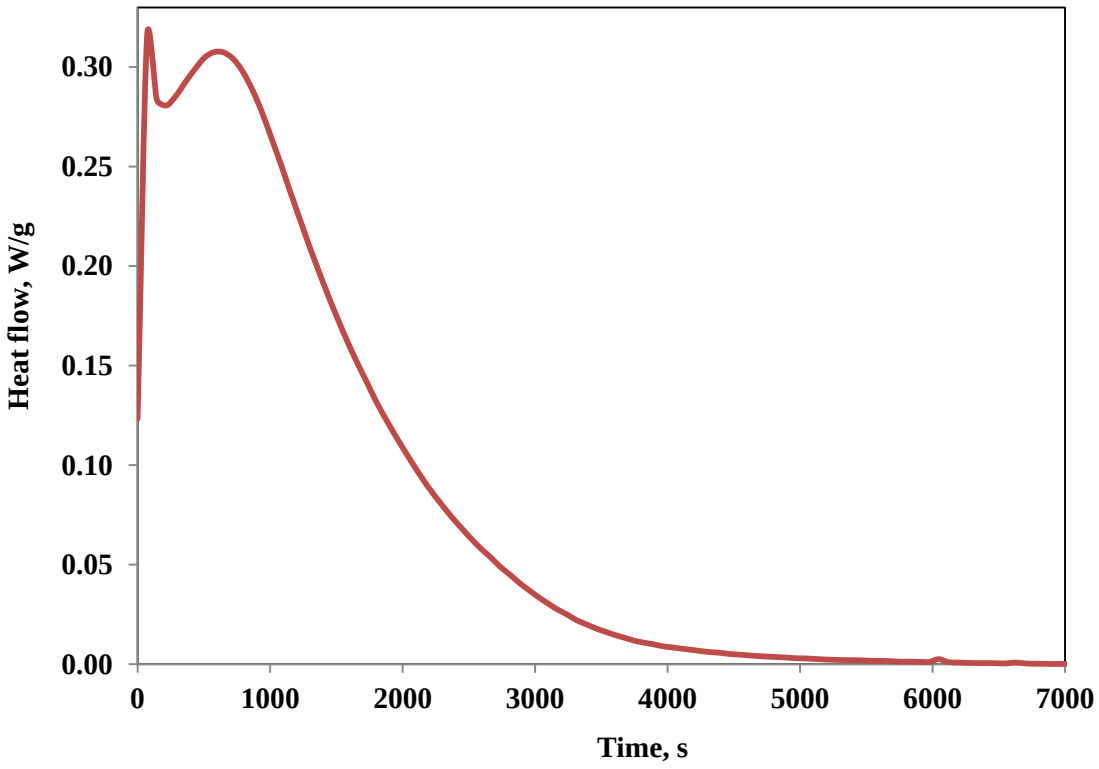

Figure 5. Isothermal DSC scan of the TGAP/DDS/MMT(5 wt%) system at 165ºC.

A typical non-isothermal cure curve for the TGAP/DDS/MMT system is shown in Figure 6. The appearance of these curves is very similar to that of the non-isothermal cure curves for the system without clay shown in Figures 2 and 3, and when they are deconvoluted by the same PeakFit program software, there appear three distinctly separate peaks, as shown in Figure 7 for the particular case of the heating rate of 10ºC/min.

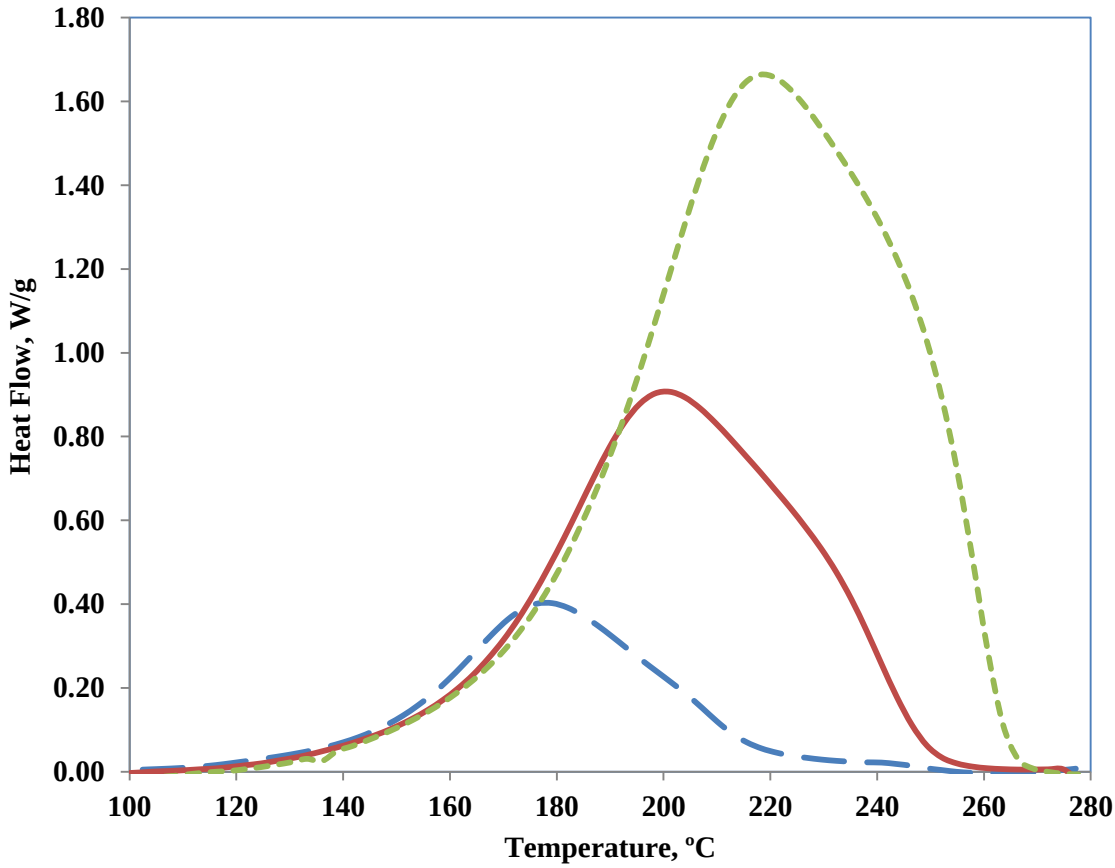

Figure 6. Non-isothermal DSC cure curve for TGAP/DDS/MMT(5 wt%) system from 0ºC to 280ºC for different heating rates: long dash, 2ºC/min; full line, 5ºC/min; short dash, 10ºC/min.

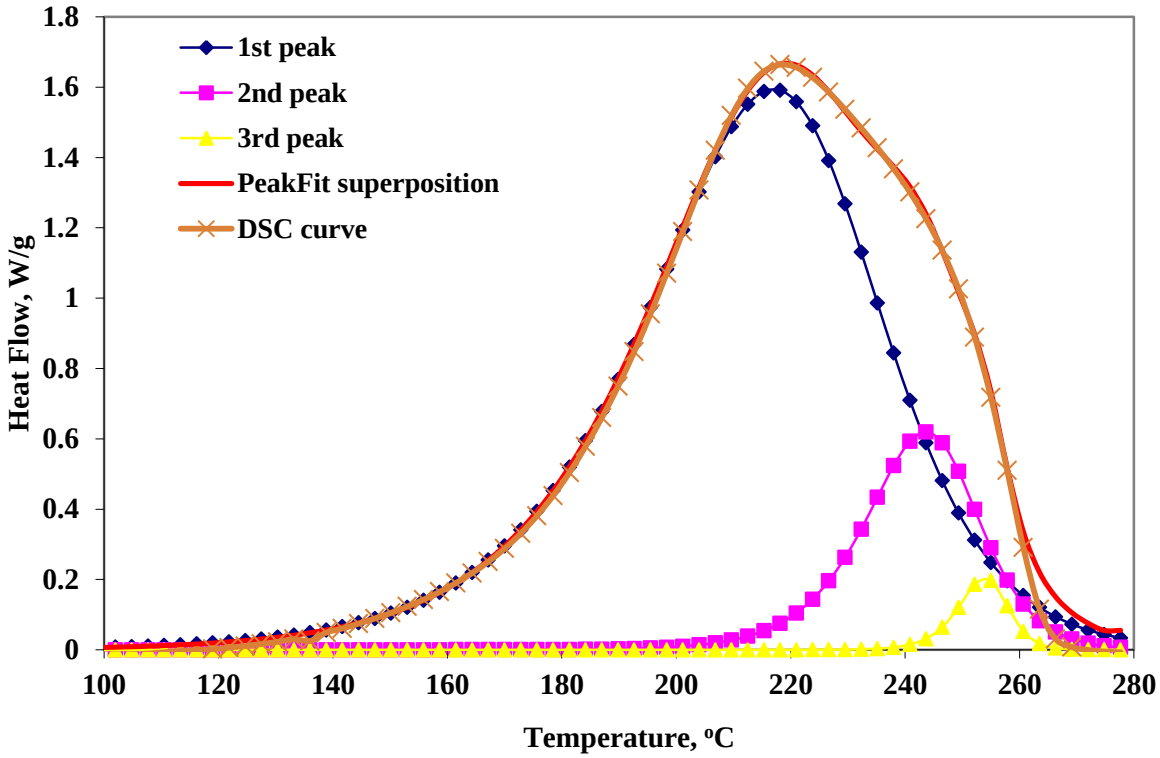

Figure 7. Deconvolution, using PeakFit program, of non-isothermal DSC scans (indicated by crosses) of TGAP/MMT/DDS system with 5 wt% MMT at 10ºC/min heating rate, into three peaks: 1st peak, rhombus; 2nd peak, squares; 3rd peak, triangles. The full line shows the overall fit.

The assignment of the reactions associated with each of these peaks is now considered. In order to distinguish between them, the heat of reaction is determined for each deconvoluted peak, denominated 1st, 2nd and 3rd peak in order of increasing temperature. The average values, ΔH_{av}, are determined from the cure curves for the three different heating rates used, for which no significant dependence of heat of reaction on heating rate was observed. The results are presented in Table 1 as a function of the MMT content, where the heats of reaction are given in units of kJ/ee calculated using an epoxy equivalent of 106 g/eq. Each of the three peaks is now considered in turn.

Table 1. Average heat of reaction, ΔH_{av} (kJ/ee), for the total reaction and for each peak after deconvolution of the non-isothermal cure curve for the TGAP/DDS/MMT system.

MMT content, wt%	**0**	**2**	**5**	**10**
ΔH_{av} (1st peak)	74.0	88.5	80.0	71.0
ΔH_{av} (2nd peak)	___	6.2	14.0	19.0
ΔH_{av} (3rd peak)	24.5	7.3	7.6	8.5
ΔH_{av} (total heat)	98.5	102.0	101.6	98.5

The 1st peak is clearly the most intense and occurs at the lowest temperature, with a maximum at just less than 220ºC for the heating rate of 10ºC/min, for example, and is attributed principally to the cross-linking reaction of the TGAP and the DDS. This can be justified by comparison with the system without clay, for which the 1st peak occurred also at about 220ºC for the same heating rate of 10ºC/min, the slight reduction in the peak temperature for the system with clay being attributed to the catalytic effect of the organically modified MMT, observed earlier in epoxy-clay nanocomposites based upon DGEBA epoxy resin [16, 17]. However, the isothermal cure for the TGAP/DDS/MMT system showed that there is a very rapid intra-gallery homopolymerisation reaction that occurs before the cross-linking reaction (see Figure 5). Furthermore, comparison of the heats of reaction given in Table 1 shows that the introduction of a small amount of clay (less than or equal to 5 wt%) into the system considerably increases the heat of reaction of this 1st peak. We believe, therefore, that this first peak includes both the cross-linking reaction and the intra-gallery homopolymerisation reaction.

It is interesting to examine further the effect of clay content on the heat of reaction of the 1st peak. The heat of reaction first increases, from 74.0 to 88.5 kJ/ee for a clay content of 2 wt%, and thereafter decreases with increasing clay content. Such a reduction in the heat of reaction with increasing clay content (here from 2 to 10 wt%) has been observed in much of our earlier work on epoxy/clay systems [16, 17, 20, 37], and can be attributed either to the effect of the stoichiometry of the reaction or to the fact that the heat of reaction for homopolymerisation is

smaller than that for the epoxy-amine reaction [17, 38, 39]. The initial increase in the heat of reaction for the clay content of 2 wt% may be explained on the basis of stoichiometry, as follows. During the non-isothermal cure, the cross-linking reaction of the 1st peak is accompanied by a homopolymerisation reaction, which consumes epoxy groups without any reaction with the DDS. For 0 wt% clay in the system TGAP/DDS, there is a slight excess of epoxy, and hence the cross-linking reaction occurs in conditions that are not stoichiometric, for which reason the heat of reaction will be smaller than it would be in stoichiometric conditions. As the clay content is increased, the contribution of the homopolymerisation reaction increases, and consequently the cross-linking reaction associated with the 1st peak will move first into stoichiometric conditions, with a concomitant increase in the heat of reaction, and then into conditions of excess DDS, which would result in a decrease of the heat of reaction with increasing clay content. We believe that the results presented in Table 1 indicate that stoichiometric conditions for the cross-linking reaction occur when the clay content is between 0 and 5 wt%, possibly close to 2 wt%.

In addition to this effect, it must also be borne in mind that the heat of reaction for homopolymerisation is smaller than that for the epoxy-amine reaction [17, 38, 39]. As a consequence, there is a significant reduction in the heat of reaction as the clay content is increased beyond 2 wt%, and in fact to such an extent that for 10 wt% MMT the heat of reaction is even less than that for the system without clay. This result may also be taken to indicate that the amount of intra-gallery homopolymerisation that takes place is greatest for the highest clay loading; this observation will be considered later when the nanostructure of these nanocomposites is discussed.

Considering now the 2nd peak, Table 1 shows that the heat of reaction for this peak increases systematically with clay content. This is further illustrated in Figure 8, where it can be confirmed that the heat of reaction is essentially independent of heating rate. The presence of MMT therefore clearly enhances this 2nd reaction. Examination of Figure 7 shows that the 2nd reaction begins at about the temperature of the maximum of the 1st peak, and since the intra-gallery reaction has therefore already largely occurred simultaneously with the cross-linking reaction in the 1st peak, we attribute the 2nd peak to an extra-gallery epoxy homopolymerisation reaction

catalysed by the organically modified MMT.

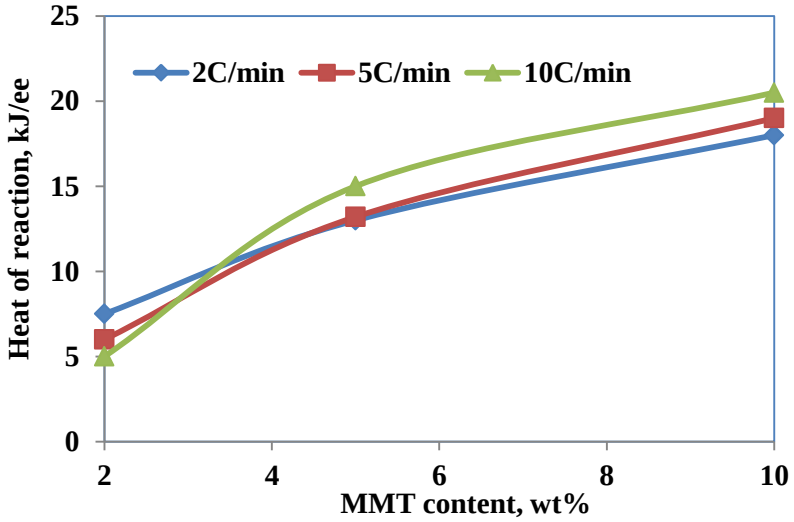

Figure 8. Dependence on MMT content of the heat of reaction corresponding to the 2nd peak for different heating rates: 2 ºC/min, rhombus; 5ºC/min, squares; 10ºC/min, triangles.

The 3rd peak shows a dramatic decrease in the heat of reaction simply as a result of the presence of clay, with no significant or systematic dependence on the clay content. This peak is assigned to the extra-gallery epoxy homopolymerisation reaction, initiated by tertiary amines. The strong reduction in the heat of reaction corresponding to this peak when the clay is added may be attributed mainly to the epoxy homopolymerisation that is now taking place within the clay galleries, leaving fewer epoxy groups to react in the extra-gallery regions.

Kinetic analysis of the TGAP/DDS/MMT system

The separation of the composite peak into the three peaks corresponding to the reactions discussed above allows also the determination of, amongst other things, their individual activation energies. By applying the Kissinger method, the activation energy for each of these reactions has been found, and the results are given in Table 2.

Table 2. Kinetic parameters for non-isothermal cure of the TGAP/DDS/MMT system

MMT content	0 wt%	2 wt%	5 wt%	10 wt%
1st peak: cross-linking + intra-gallery homopolymerization				
***E* (kJ/mol)**	74	77	72	80
***A* (s^{-1})**	4.0×10^5	1.7×10^6	6.4×10^5	4.4×10^6
m	0.5	0.4	0.5	0.2
n	1.6	1.6	1.5	1.7
m+n	2.1	2.0	2.0	1.9
2nd peak: extra-gallery homopolymerization, catalyzed by MMT				
***E* (kJ/mol)**	-	93	79	62
3rd peak: extra-gallery homopolymerization, catalyzed by tertiary amine				
***E* (kJ/mol)**	82	106	97	97

As shown in Table 2, The activation energy of the 1st peak for the TGAP/DDS system, corresponding to the cross-linking reaction, is about 74 kJ/mol. This value is completely different from the values of activation energy reported by another authors, in particular, Varley et al [34], who found the activation energy of TGAP/DDS system to be 50.9 kJ/mol by employing the Kissinger method. This difference in values is caused by the difficulty in determination of the peak temperature at higher heating rate such as 20 and 30°C/min which influences on calculation of the activation energy and leads to obtain a lower value for activation energy. This interoperation will be explained in more details now. As shown earlier, the non-isothermal cure curve is combination of peak as the cross-linking reaction and shoulder as homopolymerization reaction. By increasing the heating rate, the peak and the shoulder shift along the temperature axes up to overlap each other thus, the shoulder cannot easily be detected at higher heating rate and leads to error in distinguishing the peak temperature. In our study, if the peak temperatures are determined from the non-isothermal composite curve (the curve which has not deconvoluted into two peaks) for calculation of the activation energy by applying the Kissinger method, the activation energy will be 53.54 kJ/mol, which compares well with value of Varley et al and it is less than the calculated value in the Table 2.

For the other peaks, we note the following characteristics. The activation energies for both the 2nd and 3rd peaks are significantly higher than that for the 1st peak, which is consistent with their assignation as homopolymerisation reactions. The 3rd peak in particular has a very high activation energy, which would be anticipated for a thermally catalysed homopolymerisation reaction. For the 2nd peak, attributed here to an extra-gallery homopolymerisation reaction catalysed by the onium ion of the organically modified MMT, the activation energy is somewhat lower than that for the 3rd peak, and there is a noticeable decrease in the activation energy with increasing MMT content, consistent with a catalytic effect of the MMT, as has been noted before [22, 23].

After determining the activation energies, the kinetic exponents *m* and *n* (equation 3) for the 1st peak, which is a combination of the cross-linking reaction and the intra-gallery homopolymerisation reaction, can be evaluated by Malek's method [32] using the TAS software. The average values for these parameters are included in Table 2. Typically, *m* must be less than 1 and the sum of the reaction orders ($m+n$) should be around 2 or 3, conditions which are met by these results. It is interesting, however, to compare these values with those found for the isothermal cure of both the same TGAP/DDS/MMT system and the TGAP/DDS system without any clay [23]. For the former system, containing 5 wt% MMT, for which the cross-linking reaction could be deconvoluted from the rapid intra-gallery homopolymerisation reaction, there was some variation of the values of the parameters *m* and *n* depending on the isothermal cure temperature, the average values being $m = 0.6 \pm 0.2$ and $n = 2.1 \pm 0.4$, while for the latter system, without clay, the values were $m = 0.8$ and $n = 2.6$ approximately. The isothermal cure of the TGAP/DDS system is therefore seen to be highly autocatalytic, which can be understood in terms of the production of secondary amines by the reaction of the epoxy with primary amines. In the TGAP/DDS/MMT system, on the other hand, the isothermal cross-linking reaction appears to be less autocatalytic, which we might infer to be an effect of the presence of the clay. For the non-isothermal cure of this TGAP/DDS/MMT system, for which the results are presented in Table 2, the further reduction in the values of *m* and *n* for the 1st reaction, which is attributed to the combination of the cross-linking reaction in the presence of clay and the intra-gallery homopolymerisation reaction, is consistent with this scenario.

Nanostructural analysis

An exfoliated nanostructure can be achieved by promoting the intra-gallery homopolymerisation reaction such that it occurs before the extra-gallery cross-linking reaction. This was shown clearly in earlier work with this same TGAP/DDS/MMT system [22, 23], where the intra-gallery reaction at least partially preceded the cross-linking reaction. In contrast, for PLS nanocomposites based upon DGEBA epoxy, the occurrence of the intra-gallery homopolymerisation reaction after the cross-linking reaction results in a very poorly exfoliated nanocomposite [17]. During the non-isothermal cure of the system studied here, a composite peak appears for which the 1st peak represents the contribution from the combination of the TGAP-amine cross-linking reaction and the intra-gallery homopolymerisation reaction catalysed by the onium ion of the modified MMT, both reactions occurring simultaneously. As this composite peak cannot be deconvoluted into the separate contributions of cross-linking and homopolymerisation, it is not clear from the reaction kinetics how the nanostructure will develop.

Accordingly, nanostructural characterisation is required in order to identify whether or not a high degree of exfoliation is obtained for this system when it is cured non-isothermally. We recall that, from a consideration of the effect of the clay content on the heat of reaction for the 1st peak, shown in Table 1, it was concluded that the greatest amount of intra-gallery reaction occurs for the sample containing 10 wt% MMT. Consequently, we examine by SAXS and TEM the nanostructure of non-isothermally cured samples containing 10 wt% MMT. The SAXS diffractogram is shown in Figure 9, where it can be seen that, after the initial rapid fall corresponding to the background scattering, there are no scattering peaks evident within the range of angles covered here, implying that there is no regular layer stacking with a *d*-spacing less than about 8 nm. The sample would therefore appear to be exfoliated, but this conclusion must be corroborated by TEM observations.

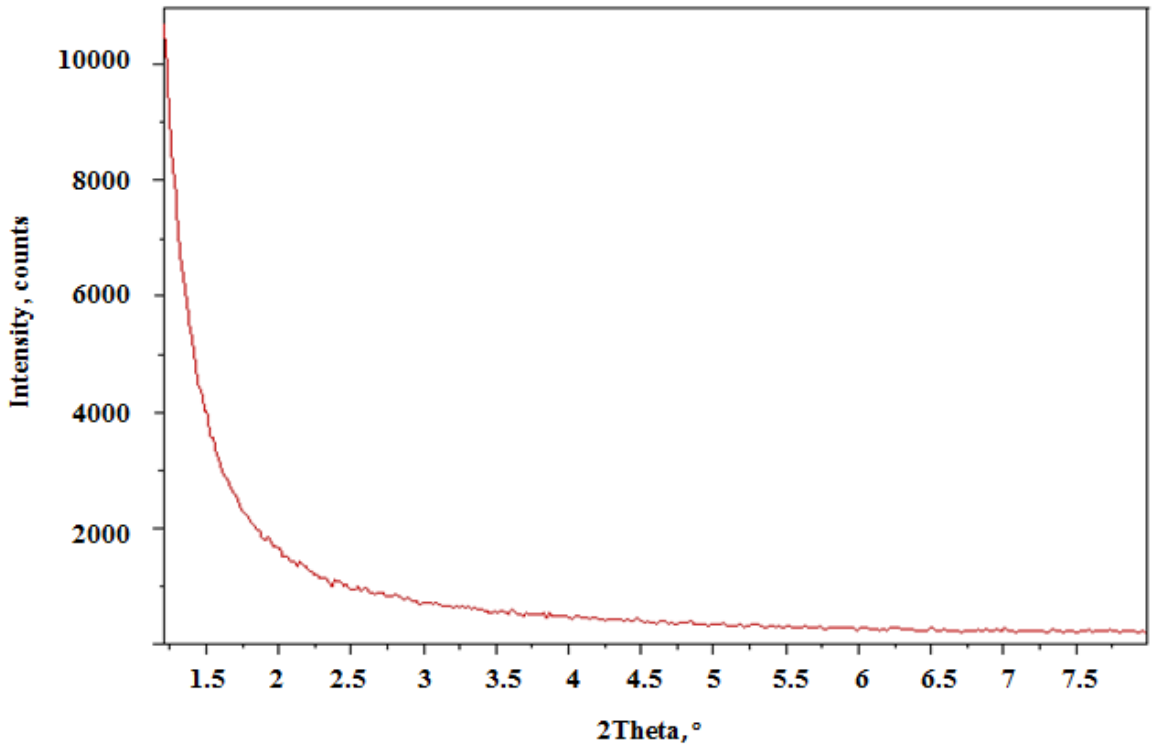

Figure 9. SAXS diffractogram for the TGAP/DDS/MMT (10 wt %) sample cured non-isothermally at 10ºC/min.

The TEM micrographs are shown in Figure 10, at various magnifications. In Figure 10a, at the lowest magnification, for which a portion of the sample is framed by a single grid of the support, a number of clay agglomerations can be seen, the largest being between 5 and 10 μm in size. At higher magnification (Figure 10b), a typical agglomeration is seen to be composed of "islands" of relatively tightly bound clay layers surrounded by the epoxy matrix, presumably containing well distributed and exfoliated clay layers. Any one of these "islands", at even higher magnification, such as that shown in Figure 10c, can be seen to consist of a number of clay layers separated by distances of, typically, between 10 and 20 nm, which represents a significant degree of exfoliation. Nevertheless, there are regions in which some clay layers retain their original layer stacking, albeit with an increased layer separation. Figure 10d shows one such region, where many clay layers can be seen in register, with a spacing of only 4 to 5 nm between them; this region clearly does not represent a well exfoliated nanostructure. Nevertheless, the

overall nanostructure evident from these TEM micrographs is similar to that observed for the isothermal cure of the same nanocomposite system [23]. We infer from this that the combination of the cross-linking reaction and the intra-gallery homopolymerisation reaction which constitutes the 1st peak in the non-isothermal cure of the TGAP/DDS/MMT system retains the relationship between these two reactions that was evident in the isothermal cure, namely that the intra-gallery reaction is not inhibited by the cross-linking reaction in the extra-gallery regions.

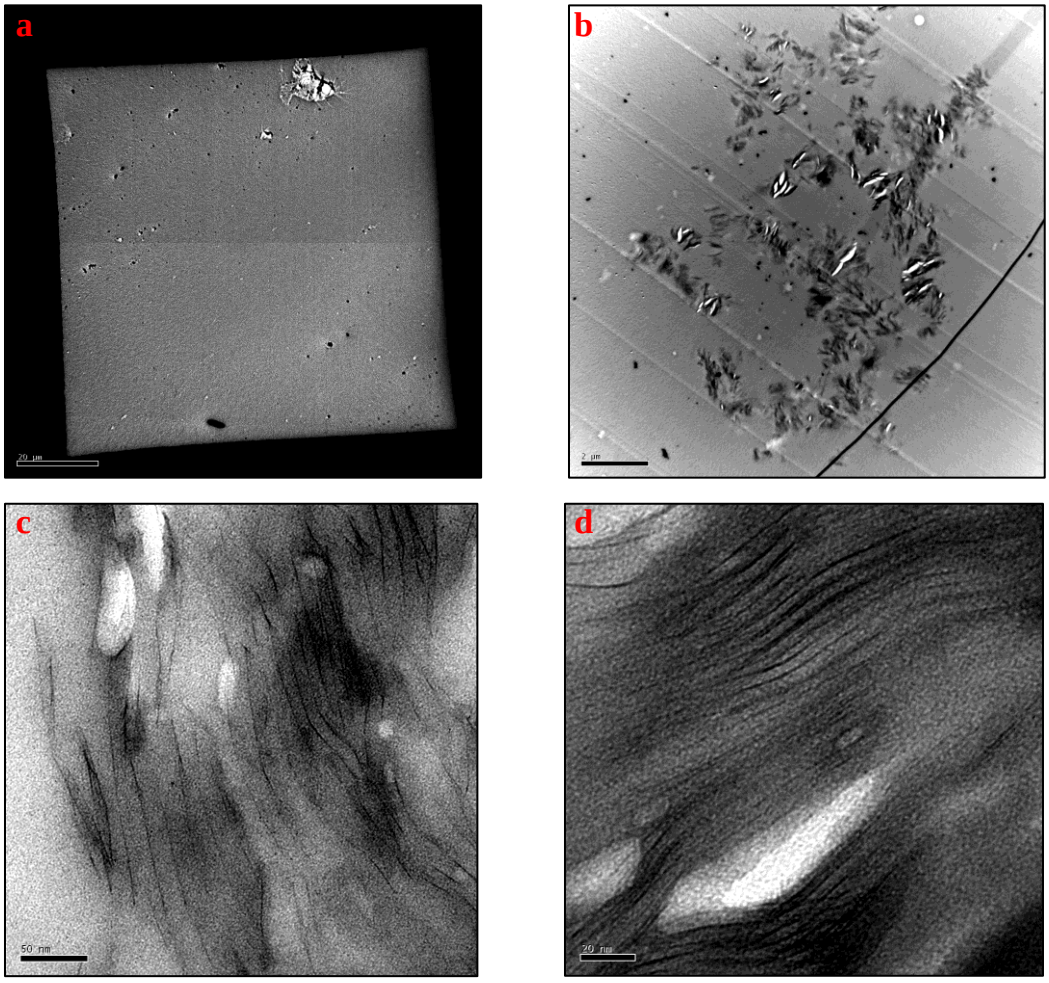

Figure 10. TEM images for the TGAP/DDS/MMT (10 wt%) system cured non-isothermally at 10ºC/min. The scale bars are: (a) 20 μm; (b) 2 μm; (c) 50 nm; (d) 20 nm.

Conclusions

In non-isothermal cure of TGAP/MMT/DDS system, the composite curve can be deconvoluted into three separate peaks corresponding to three different reactions, in contrast to isothermal cure for which there are only two contributions. These three peaks are cross-linking and intra-gallery reaction which is hidden beneath the exothermic curve of cross-linking reaction, extra-gallery homopolymerization which is catalysed by MMT and another extra-gallery reaction which is catalysed by the tertiary amine. But the important distinction is that the intra-gallery reaction now occurs, for non-isothermal cure, concurrently with the crosslinking reaction, in contrast to isothermal cure that the cross-linking reaction occurs after the intra-gallery reaction. This has been related to differences in the kinetics in isothermal and non-isothermal cure. Furthermore, the quality of the final nanocomposite is examined with SAXS and TEM. Although no scattering peak can be detected in the SAXS graph, the TEM images show the clay agglomerations which consist of a number clay layers with the *d*-spacing around 10 and 20 nm. Hence, the final nanostructure is presented the good quality of exfoliation as same as the sample which is cured isothermally, which implies that the intra-gallery reaction is not inhibited by rigid extra-gallery regions.

Acknowledgements

The authors are grateful to Huntsman Corporation for the epoxy resin and curing agent and Nanocor Inc. for the organically modified clay. This work was supported financially by MINECO Project MAT2011-27039-C03. F.S. is grateful for a grant from the Agència de Gestió d'Ajuts Universitaris i de Recerca (AGAUR), FI-DGR 2011

References

1. P. C. LeBaron, Z. Wang, T. J. Pinnavaia, "Polymer-layered silicate nanocomposites: an overview", *Applied Clay Science*, **15** (1999) 11-29.

2. M. Alexandre, P. Dubois, "Polymer-layered silicate nanocomposites: preparation, properties and uses of a new class of materials", *Mater. Sci. Eng.*, **28** (2000) 1-63.

3. S. S. Ray, M. Okamoto, "Polymer/layered silicate nanocomposites: a review from preparation to processing", *Prog. Polym. Sci.*, **28** (2003) 1539-1641.

4. O. Becker, G. P. Simon, "Epoxy layered silicate nanocomposites", *Adv. Polym. Sci.*, **179** (2005) 29-82.

5. N. Karak, "Polymer (epoxy) clay nanocomposites", *J. Polym. Mater.*, **23** (2006) 1-20.

6. F. Hussain, M. Hojjati, M. Okamoto, R. E. Gorga, "Review article: Polymer-matrix nanocomposites, processing, manufacturing, and application: An overview", *J. Comp. Mater.*, **40** (2006) 1511-1575.

7. S. Pavlidou, C. D. Papaspyrides, "A review on polymer–layered silicate nanocomposites", *Prog. Polym. Sci.*, vol. **33** (2008) 1119-1198.

8. M. S. Wang, T. J. Pinnavaia, "Clay-polymer nanocomposites formed from acidic derivatives of montmorillonite and an epoxy resin", *Chem. Mater.*, **6** (1994) 468-474.

9. P. Butzloff, N. A. D'Souza, T. D. Golden, D. Garrett, "Epoxy + montmorillonite nanocomposite: Effect of composition on reaction kinetics", *Polym. Eng. Sci.*, **41** (2001) 1794-1802.

10. X. Kornmann, H. Lindberg, L.A. Berglund, "Synthesis of epoxy-clay nanocomposites. Influence of the nature of the curing agent on structure", *Polymer* **42** (2001) 4493-4499.

11. W. Xu, S. Bao, S. Shen, W. Wang, G. Hang, P. He, "Differential scanning calorimetry study On the curing behaviour of epoxy resin/diethylenetriamine/organic montmorillonite nanocomposite", *J. Polym. Sci., Part B, Polym. Phys.*, **41** (2003) 378-386.

12. O. Becker, G. P. Simon, R. J. Varley, P. J. Halley, “Layered silicate nanocomposites based on various high-functionality epoxy resins: the influence of an organoclay on resin cure”, *Polym. Eng. Sci.*, **43** (2003) 850-862.

13. C. Chen, D. Curliss, “Preparation, characterization, and nanostructural evolution of epoxy nanocomposites”, *J. Appl. Polym. Sci.*, **90** (2003) 2276-2287.

14. M. T. Ton-That, T. D. Ngo, P. Ding, G. Fang, K. C. Cole, S. V. Hoa, “Epoxy nanocomposites: analysis and kinetics of cure”, *Polym. Eng. Sci.*, **44** (2004) 1132-1141.

15. M. Ivankovic, I. Brnardic, H. Ivankovic, H. J. Mencer, “DSC study of the cure kinetics during nanocomposite formation: Epoxy/poly(oxypropylene) diamine/organically modified montmorillonite system”, *J. Appl. Polym. Sci.*, **99** (2006) 550-557.

16. F. Román, S. Montserrat, J. M. Hutchinson, “On the effect of montmorillonite in the curing reaction of epoxy nanocomposites”, *J. Therm. Anal. Calorim.*, **87** (2007) 113-118.

17. S. Montserrat, F. Román, J. M. Hutchinson, and L. Campos, “Analysis of the cure of epoxy based layered silicate nanocomposites: Reaction kinetics and nanostructure development”, *J. Appl. Polym. Sci.*, **108** (2008) 923-938.

18. P. Pustkova, J. M. Hutchinson, F. Román, S. Montserrat “Homopolymerization effects in polymer layered silicate nanocomposites based upon epoxy resin: Implications for exfoliation”, *J. Appl. Polym. Sci.*, **114** (2009) 1040-1047.

19. Y. Xu, H. Peng, X. Wang, S. Su, “Comparative study of different polymerically-modified clays on curing reaction and thermal properties of epoxy resin”, *Thermochim. Acta*, **516** (2011) 13-18.

20. F. Román, Y. Calventus, P. Colomer, J. M. Hutchinson, “Identification of nanostructural

development in epoxy polymer layered silicate nanocomposites from the interpretation of differential scanning calorimetry and dielectric spectroscopy", *Thermochim. Acta*, **541** (2012) 76-85.

21. O. Becker, Y-B. Cheng, R. J. Varley, G. P. Simon, "Layered silicate nanocomposites based on various high-functionality epoxy resins: The influence of cure temperature on morphology, mechanical properties, and free volume", *Macromolecules,* **36** (2003) 1616-1625.

22. J. M. Hutchinson, F. Shiravand, Y. Calventus, "Intra- and extra-gallery reactions in tri-functional epoxy polymer layered silicate nanocomposites", *J. Appl. Polym. Sci.*, **128** (2013) 2961-2970.

23. F. Shiravand, J. M. Hutchinson, Y. Calventus, "The influence of the isothermal cure temperature on the nanostructure and thermal properties of an epoxy layered silicate nanocomposite", *Polym. Eng. Sci.*, **54 (**2014) 51-58.

24. J. M. Hutchinson, F. Shiravand, Y. Calventus, I. Fraga, "Isothermal and non-isothermal cure of a tri-functional epoxy resin (TGAP): a stochastic TMDSC study", *Thermochim. Acta*, **529** (2012) 14-21.

25. S. Vyazovkin, A. K. Burnham, J. M. Criado, L. A. Pérez-Maqueda, C. Popescu, N. Sbirrazzuoli, "ICTAC Kinetics Committee recommendations for performing kinetic computations on thermal analysis data", *Thermochim. Acta*, **520** (2011) 1-19.

26. M. J. Starink, "The determination of activation energy from linear heating rate experiments: a comparison of the accuracy of isoconversion methods", *Thermochim. Acta*, **404** (2003) 163-176.

27. T. Ozawa, "A new method of analyzing thermogravimetric data", *Bull. Chem. Soc. Japan*, **38** (1965) 1881-1886.

28. S. Vyazovkin, "Evaluation of activation energy of thermally stimulated solid-state reactions

under arbitrary variation of temperature", *J. Comput. Chem.*, **18** (1997) 393-402.

29. S. Vyazovkin, "Modification of the integral isoconversional method to account for variation in the activation energy", *J. Comput. Chem.*, **22** (2001) 178-183.

30. H. E. Kissinger, "Variation of peak temperature with heating rate in differential thermal analysis", *J. Res. Nat. Bur. Std.*, **57** (1956) 217-221.

31. H. E. Kissinger, "Reaction kinetics in differential thermal analysis", *Anal. Chem.*, **29** (1957) 1702-1706.

32. J. Málek, "The kinetic analysis of non-isothermal data", *Thermochim. Acta*, **200** (1992) 257-269.

33. M. Frigione, E. Calò, "Influence of an hyperbranched aliphatic polyester on the cure kinetic of a trifunctional epoxy resin," *J. Appl. Polym. Sci.*, **107** (2008) 1744-1758.

34. R. J. Varley, J. H. Hodgkin, D. G Hawthorne, G. P. Simon, "Toughening of a trifunctional epoxy system. II. Thermal characterization of epoxy/amine cure", *J. Appl. Polym. Sci.*, **60** (1996) 2251-2263.

35. I. T. Smith, "The mechanism of the crosslinking of epoxide resins by amines", *Polymer*, **2** (1961) 95-108.

36. M. E. Ryan, A. Dutta, "Kinetics of epoxy cure: rapid technique for kinetic parameter estimation", *Polymer*, **20** (1979) 203-206.

37. J. M. Hutchinson, S. Montserrat, F. Román, "Nanostructure development and cure kinetics in epoxy-based PLS nanocomposites", *J. Nanostruct. Polym. Nanocomp.*, **4** (2008) 13-20.

38. C. H. Klute, W. Viehmann, "Heat of polymerization of phenyl glycidyl ether and of an epoxy

resin", *J. Appl. Polym. Sci.*, **5** (1961) 86-95.

39. I. E. Dell'Erba, R. J. J. Williams, "Homopolymerization of epoxy monomers initiated by 4-(dimethylamino)pyridine", *Polym. Eng. Sci.*, **46 (**2006) 351-359.

Paper VI

Comparison of the nanostructure and mechanical performance of highly exfoliated epoxy-clay nanocomposites prepared by three different protocols

F. Shiravand, J.M. Hutchinson, Y. Calventus, F. Ferrando

Submitted to Materials, 2013

Comparison of the nanostructure and mechanical performance of highly exfoliated epoxy-clay nanocomposites prepared by three different protocols

Fatemeh Shiravand,[1] John M Hutchinson,[1]* Yolanda Calventus,[1] Francesc Ferrando[2]

[1]Centre for NanoEngineering, and Departament de Màquines i Motors Tèrmics, ETSEIAT, Universitat Politècnica de Catalunya, 08222 Terrassa, Barcelona, Spain

[2]Department of Mechanical Engineering, Universitat Rovira i Virgili, C/ Països Catalans 26, 43007 Tarragona, Spain

hutchinson@mmt.upc.edu

Abstract

Three different protocols for the preparation of polymer layered silicate nanocomposites based upon a tri-functional epoxy resin, triglycidyl *para*-amino phenol (TGAP), have been compared in respect of the cure kinetics, the nanostructure and their mechanical properties. The three preparation procedures involve 2 wt% and 5 wt% of organically modified montmorillonite (MMT), and are: isothermal cure at selected temperatures; pre-conditioning of the resin-clay mixture before isothermal cure; incorporation of an initiator of cationic homopolymerisation, a boron tri-fluoride methyl amine complex, BF_3·MEA, within the clay galleries. It was found that features of the cure kinetics and of the nanostructure correlate with the measured impact strength of the cured nanocomposites, which increases as the degree of exfoliation of the MMT is improved. The best protocol for toughening the TGAP/MMT nanocomposites is by the incorporation of 1 wt% BF_3·MEA into the clay galleries of nanocomposites containing 2 wt% MMT.

Keywords

nanocomposite; exfoliation; pre-conditioning; mechanical properties; homopolymerisation; epoxy; layered silicate; differential scanning calorimetry; nanostructure; montmorillonite

Introduction

Epoxy resins constitute a well-known family of thermosetting polymers that have been used widely and over a period of many years in various industrial fields such as coatings, high-performance adhesives and other engineering applications, because of their many desirable properties. However, the cured epoxy resin exhibits low fracture toughness, poor resistance to crack initiation and growth, and low impact strength. Many studies have been made over the past decades to find ways for toughening the epoxy matrix, for example by the addition of a second phase such as rigid or elastomeric particles. More recently, nanoclay fillers, which have both a high aspect ratio (200-1000) and high modulus (170 GPa), have emerged as a new approach for the improvement of the mechanical performance, including the toughness and impact resistance, of the cured epoxy matrix [1-3]. Furthermore, these clays have attracted considerable attention because of their low cost and ready availability.

In addition, the possibility of achieving with nanoclays the same degree of reinforcement as obtained with microscopic fillers but with a much lower filler content is particularly attractive for applications in which the density of the composite materials is important, for example in the aerospace and automotive industries. This requires that the idealised structure of the polymer layered silicate nanocomposite be developed from that of a conventional composite or microcomposite, in which the clay acts as a conventional filler, to that of an exfoliated nanocomposite, in which the individual clay layers are distributed uniformly in the matrix in order to maximise the surface contact between clay and matrix and to inhibit the propagation of cracks. In essence, this has been the goal of much of the research in this area in recent years, and is also addressed in the present paper.

The unmodified nanoclay, such as montmorillonite (MMT), consists of stacks of silicate layers, each of the order of 1 nm thick, and is naturally hydrophilic and hence unsuitable for use as a filler in most of the commonly used epoxy resins, which are hydrophobic. Consequently, the montmorillonite clay is commonly modified organically by an ion exchange process in which the cations are replaced by, for example, quaternary ammonium ions with long alkyl chains. This not only makes the clay organophilic but also increases the spacing between the clay layers, which facilitates the intercalation of the epoxy resin in the preparation of the epoxy-clay nanocomposites. In order to accomplish the desired improvement in mechanical properties of these nanocomposites, it is necessary for the clay layers to be further separated and dispersed homogeneously throughout the polymer matrix, in a process referred to as exfoliation [4, 5], when the epoxy-clay mixture is cured. However, achieving a highly exfoliated nanostructure in these epoxy layered silicate nanocomposites has proven difficult, and it is common to refer to “partial” exfoliation or to consider the nanostructure to be exfoliated when the *d*-spacing of the clay layers cannot be detected by Small Angle X-ray Scattering (SAXS), which normally implies layer separations greater than about 8 nm [6-10]. Very large layer separations is not the only reason for the absence of diffraction peaks, however, as has been noted by several authors [11-13], and consequently

it is important that nanostructural characterisation by Transmission Electron Microscopy (TEM) should also be made.

For epoxy-clay nanocomposites, it has been suggested that, in order to maximise the degree of exfoliation, the intra-gallery epoxy homopolymerisation reaction which takes place between the clay layers should occur before the extra-gallery cross-linking reaction of the epoxy resin with the curing agent [14-16]. This hypothesis is supported by some observations made for the epoxy-clay system based upon the bi-functional epoxy diglycidyl ether of bisphenol-A (DGEBA) and organically modified montmorillonite [17]. When this system was cured with a polyoxypropylene diamine, a marked shoulder appeared on the high temperature flank of the exothermic cure reaction, indicating that a reaction, interpreted as being the intra-gallery homopolymerisation, was occurring after the extra-gallery cross-linking reaction. As a consequence, the cured nanocomposite in this case was poorly exfoliated, indicated by the existence of scattering peaks in the SAXS results. When the same epoxy-clay system was cured with an $-NH_2$ terminated hyperbranched polyethyleneimine, however, this shoulder was not present, suggesting that the intra-gallery reaction was occurring simultaneously with the cross-linking reaction [18]. At the same time, the SAXS results showed no scattering peaks, suggestive of a much better degree of exfoliation.

In contrast, for layered silicate nanocomposites based on a tri-functional epoxy resin, triglycidyl *para*-amino phenol (TGAP), and with the same MMT clay, two distinct reactions were observed in the isothermal cure reaction with 4,4-diamino diphenyl sulphone (DDS) as the curing agent: the first was attributed to the epoxy homopolymerisation reaction taking place within the clay galleries, while the second was attributed to the bulk cross-linking reaction in the extra-gallery regions [19, 20]. The justification for the assignments of these reactions is considered further in the present paper. On the basis of the above hypothesis, therefore, this system therefore appears to afford a mechanism for improved exfoliation in these epoxy-clay nanocomposites, and in earlier work we investigated separately the effect of the preparation procedure on the nanostructure of these cured nanocomposites. The different preparation procedures used were: (i) pre-conditioning of the resin-clay mixture before the addition of the curing agent [19]; (ii) suitable selection of the isothermal cure temperature [20]; and (iii) incorporation of an initiator of cationic homopolymerisation within the clay galleries [21].

In the present work, for each of these different preparation procedures, for which the results have been presented separately in earlier publications [19-21], we make a comparison of the cure reaction kinetics, monitored by differential scanning calorimetry (DSC), and the degrees of exfoliation as identified by nanostructural characterisation techniques such as Small Angle X-ray Scattering (SAXS) and Transmission Electron Microscopy (TEM), in order to clarify the mechanisms responsible and the preparation conditions required for the exfoliation of these epoxy polymer layered silicate

nanocomposites. In addition, we further include the results of new experiments which show how the enhancement in the impact strength of the cured nanocomposites can be correlated with the improved exfoliation in the nanostructure.

Experimental

Materials

The epoxy resin, TGAP, with trade name Araldite MY0510 (Huntsman Advanced Materials) and an epoxy equivalent between 95-106 g/eq, the curing agent, 4,4-diamino diphenyl sulphone (DDS), with trade name Aradur 976-1 (Aldrich), the organically modified montmorillonite (MMT), with trade name Nanomer I.30E (Nanocor Inc.) consisting of 70-75 wt% montmorillonite and 25-30 wt% octadecylamine, with a cation exchange capacity (CEC) of 92 meq/100 g, and the boron trifluoride monoethylamine complex, BF_3·MEA, (Sigma-Aldrich) as the cationic initiator for the homopolymerisation reaction, were all used without further purification.

Moulds

Samples for the mechanical tests were cured in open moulds which had been machined from Teflon. For the dynamic mechanical analysis, the mould consisted of a cylindrical block with four cylindrical cavities, approximately 10 mm diameter and 11 mm in depth, with a slight taper to facilitate the removal of the cured samples. For the impact tests, the mould consisted of a rectangular block with nine separate rectangular cavities, approximately 25×12×2.5 mm. In each case, the block was clamped to a rigid base-plate (circular for the dynamic mechanical tests, rectangular for the impact tests) which could be removed in order to extract the cured samples. The cured samples could be removed from the moulds without the need for the previous application of any release agent. Each of these moulded samples was then machined to the required final dimensions for the different mechanical tests.

Samples for transmission electron microscopy were cast into a flat embedding mould (Pelco®), made of silicone rubber and with overall dimensions 105×70×7 mm deep. This mould contained 24 numbered tapered troughs, 6×13×3 mm deep, designed such that the sample is easily accommodated into the ultramicrotome holder.

Sample preparation

The preparation of the nanocomposites was made according to three different procedures, which are detailed as follows and are illustrated schematically in Figure 1.

Figure 1. Schematic illustration of the different nanocomposite preparation procedures

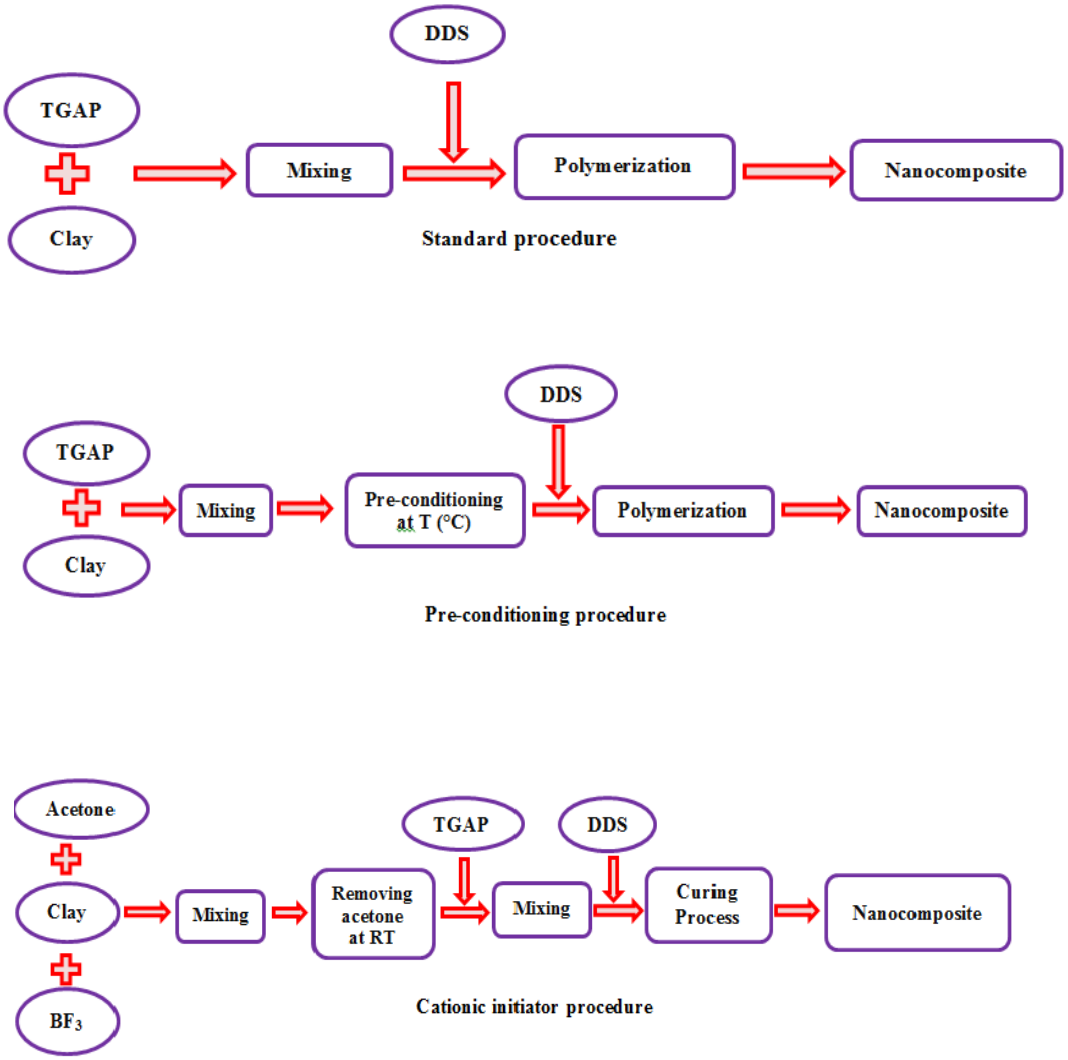

Standard procedure

For the standard procedure, the TGAP epoxy resin and the clay were mixed together by mechanical stirring at a speed of ~200 rpm for approximately 4 h. The proportions of clay used were 2 wt% and 5 wt% MMT with respect to the TGAP weight. The curing agent, DDS, was then added to the TGAP/MMT mixture in a proportion of 52 wt% and mixed by hand for 5-7 minutes on a hot-plate at 80 ºC. This proportion of DDS corresponds to an excess molar epoxy ratio (1:0.85), as recommended by the resin manufacturer. The mixture was finally degassed in a vacuum chamber (Heraeus RVT360)

for approximately 10 min at room temperature and 100 Pa pressure, and the mixture was then either poured into the appropriate mould for the subsequent machining of the mechanical test samples or used for taking small samples for scanning in the DSC. For the mechanical test samples, the standard cure schedule consisted of two isothermal steps in an air-circulating oven: first at 150 ºC for 3 h or at 180 ºC for 1.5 h, followed by a post-cure at 210 ºC for 2 h.

Pre-conditioning procedure

For the pre-conditioned samples, mixtures of TGAP epoxy resin and either 2 wt% or 5 wt% MMT were mixed by mechanical stirring and were then stored at either room temperature (RT) or at a higher temperature (40 ºC, 60 ºC, 80 ºC), using a thermostatic bath (Techne, TE-8D). In the present work we show the results for samples pre-conditioned by storage at 40 ºC for 78 and 67 days, for proportions of 2 wt% and 5 wt% MMT, respectively. Following this pre-conditioning treatment, the required amount of DDS was added to the TGAP/MMT mixtures, according to the epoxy equivalent (*EE*) of the TGAP, determined by titration [22], in order to give an excess epoxy ratio (mass ratio 1:0.52). The mixture was then degassed under vacuum at room temperature as above, poured into the moulds, and subjected to the same cure schedule as described above for the standard procedure.

Cationic initiation procedure

For the samples in which cationic homopolymerisation is initiated in the clay galleries, the MMT and BF_3·MEA were first mixed together, using acetone as a solvent, in various proportions such as to give 0.5 wt% and 1 wt% of BF_3·MEA and 2 wt% and 5 wt% of MMT, both with respect to the TGAP content, in the final nanocomposite. The acetone was then removed by evaporation at room temperature over a period of about one day. The resulting mixture, ground to a fine powder, was then dispersed in the TGAP by high shear mechanical mixing (Polytron, PT1200C, Kinematica AG) at room temperature before being degassed under vacuum as above. This TGAP/MMT/BF_3·MEA mixture was then heated on a hot-plate to 80 ºC and the DDS was added to give an excess epoxy ratio (mass ratio 1:0.52). Finally, the mixture was poured into moulds as required and cured according to the following schedules, different from those used for the samples prepared by the standard and pre-conditioning procedures: (i) 110 ºC for 1 h, 125 ºC for 6 h; (ii) 100 ºC for 2.5 h, 150 ºC for 2 h; (iii) 100 ºC for 2.5 h, 180 ºC for 1 h. Each of these cure schedules was followed by a post-cure at 210 ºC for 2 h.

Samples were prepared according to one or more of the above procedures for a variety of purposes: to follow and analyse the curing kinetics by DSC; to examine the nanostructure of the cured nanocomposites by SAXS and TEM; and to determine the dynamic mechanical properties and, in

particular, the impact strength of the cured nanocomposites in order to see whether the impact strength can be correlated with the nanostructure. A summary of the various compositions that were prepared specifically for the purposes of the impact testing and based on these procedures is given in Table 1.

It should be noted that not all of these samples listed in Table 1 were studied here by DSC, SAXS and TEM; for those that were used here for these purposes, their composition and preparation conditions will be clearly stated when the results are discussed in a later section.

Table 1. Sample identification for different compositions and preparation conditions of TGAP/clay nanocomposites prepared for impact testing

Composition (numbers in brackets represent wt%)	**Cure profile (ºC)**			**Sample identification**
	Step 1	**Step 2**	**Step 3**	
TGAP/DDS(52)	150	----	210	no clay; reference
TGAP/MMT(2)/DDS(52)	150	----	210	2%, 150 ºC
TGAP/MMT(2)/DDS(52)	180	-----	210	2%, 180 ºC
TGAP/MMT(2)+BF_3·MEA(0.5)/DDS(52)	110	125	210	2%+0.5%BF_3, 125 ºC
TGAP/MMT(2)+BF_3·MEA(0.5)/DDS(52)	100	150	210	2%+0.5%BF_3, 150 ºC
TGAP/MMT(2)+BF_3·MEA(0.5)/DDS(52)	100	180	210	2%+0.5%BF_3, 180 ºC
TGAP/MMT(2)+BF_3·MEA(1)/DDS(52)	110	125	210	2%+1%BF_3, 125 ºC
TGAP/MMT(2)/DDS(52), pre-conditioned 40 ºC, 78 days	150	-----	210	2%, pre 40 ºC
TGAP/MMT(5)/DDS(52)	150	-----	210	5%, 150 ºC
TGAP/MMT(5)/DDS(52)	180	-----	210	5%, 180 ºC
TGAP/MMT(5)+BF_3·MEA(0.5)/DDS(52)	110	125	210	5%+0.5%BF_3, 125 ºC
TGAP/MMT(5)+BF_3·MEA(1)/DDS(52)	110	125	210	5%+1%BF_3, 125 ºC
TGAP/MMT(5)/DDS(52) pre-conditioned 40 ºC, 67 days	150	-----	210	5%, pre 40 ºC

Differential scanning calorimetry (DSC)

The calorimetric curing experiments were carried out using a conventional DSC (DSC821e, Mettler-Toledo) equipped with a sample robot and Haake EK90/MT intracooler. All experiments were performed with a flow of dry nitrogen gas at 50 mL/min. The data evaluation was performed with the STAR^e software, and the instrument was calibrated for both heat flow and temperature using indium. Sample masses were typically in the range 8 to 10 mg, weighed on a microbalance and encapsulated in sealed standard aluminium pans with a lid. After mixing, samples were immediately inserted into the DSC furnace, which was previously heated to the appropriate isothermal cure temperature, whereupon the curing experiment was immediately started. The isothermal cure experiments were made at the various temperatures indicated in Table 1 above.

For the calorimetric determination of the glass transition temperature, a stochastic temperature modulated DSC method, TOPEM (Mettler Toledo DSC823e), was used [23, 24]. The TOPEM instrument was equipped with an intracooler (Julabo FT400) and was calibrated for both heat flow and temperature using indium. Scans were made over a temperature range from 100 ºC to 285 ºC at 2 K/min, with temperature pulses of amplitude ±0.5 ºC and a switching time range of 15−30 s, and with a flow of dry nitrogen gas at 50 mL/min. Sample masses for this technique were typically in the range 10 to 15 mg, encapsulated in sealed standard aluminium pans with a lid. The glass transition temperatures were determined from the sigmoidal change in the so-called quasi-static specific heat capacity, c_{p0}.

Nanostructural characterisation

Small angle X-ray scattering (SAXS) and transmission electron microscopy (TEM) were both used to characterise the nanostructure of the nanocomposites. X-ray diagrams were obtained using a Bruker D8 Advanced diffractometer, measurements being taken in a range of $2\theta = 1^o$ to 8^o with copper Kα radiation (λ=0.1542 nm). The power settings were 50 kV and 40 mA. For all the samples, the scans were made with steps in 2θ of 0.02^o and with a time of 10 seconds for each step. The intercalation of the epoxy resin into the clay galleries was determined for the resin-clay mixtures in the form of viscous liquids; the sample was spread in a thin layer on the sample holder, and the viscosity is such that no significant settling of the clay layers will take place during the scan. For the cured nanocomposites the scattering diagrams were obtained for samples in the form of powder after ball-milling (Retsch model MM 400) the bulk samples using 20 mm diameter steel balls and a frequency of 20 Hz for a period of 4 minutes. The powder samples were packed into the appropriate sample holder to form a sintered disc.

Transmission Electron Microscopy was carried out with a High Resolution TEM Jeol Jem-2011 electron microscope, with a resolution of 0.18 nm at 200 kV. The TEM samples, previously prepared by casting the nanocomposite into the specific mould described earlier, were cut with a Leica EM UC7 ultramicrotome using a diamond knife (Diatome), to give a thickness of approximately 50 nm. The ultrathin sections were left floating on water and were picked up and mounted on a 400 mesh carbon coated grid.

Mechanical property measurements

The storage modulus (G'), loss modulus (G'') and the mechanical loss factor ($\tan \delta = G''/G'$) were determined as a function of temperature and frequency by dynamic mechanical analysis (DMA) using the Mettler-Toledo model DMA861[e] in shear mode. Samples in the form of thin discs, approximately 6 mm diameter and 2 mm thickness, were machined from the moulded cylinders. DMA measurements were made over a range of frequencies (0.1, 0.3, 1, 3, 10, 30,100 and 300 Hz) and at 2 °C/min heating rate over the temperature range from 50 ºC to 285 °C.

The impact tests were performed at room temperature using a Zwick Izod impact tester 5110 according to ASTM D4508-05 (2008) on rectangular specimens, machined to 25×12×2.5 mm from the bulk moulded samples. The impact tester had a hammer of energy 0.545 J, and a minimum of eight specimens were tested for each composition.

After impact testing, the fracture surfaces of the impact samples were observed using a scanning electron microscope (SEM, Jeol 5610) with an accelerating voltage of 15 kV and a spot size of 20, using secondary electron imaging. Before making the SEM observations, the fracture surfaces were sputtered with a thin layer of gold, between 10 and 15 nm thick, using a Baltec DSC005 sputter coater.

Results and Discussion

Thermal analysis by DSC

When prepared by the standard procedure described above, these nanocomposite systems using the tri-functional epoxy resin TGAP as the matrix material have previously been shown to be predisposed to exfoliate in view of the rapid intra-gallery reaction that takes place before the bulk cross-linking reaction [19-21]. This is illustrated in Figure 2 for TGAP/MMT/DDS samples with 5 wt% clay and cured isothermally at different temperatures, where the two overlapping reactions are clearly seen. The curing reactions for epoxy resins are complex, particularly in the presence of organically modified MMT, and have been discussed quite extensively elsewhere [17, 22, 25]. The several possible reactions include the reaction of the epoxide groups first with the primary amine and then with the

secondary amine, and etherification catalysed by the tertiary amine and/or by the onium ion of the organically modified MMT. In the isothermal cure of the TGAP/DDS system without any clay, a single bell-shaped peak is found [26, 27], shown in Figure 2 for the isothermal cure temperatures of 150 ºC and 180 ºC, which can be modelled as an autocatalytic reaction [20]. The rapid initial reaction that occurs in the same system with clay, TGAP/MMT/DDS, can therefore be attributed to the presence of the clay.

In order to maximise the degree of exfoliation of the clay layers, it is of interest that as much as possible of the first reaction should occur before the extra-gallery cross-linking reaction creates a rigid matrix around the clay particles. By deconvoluting these cure curves into two separate peaks, it was possible to determine the heat of reaction associated with each, and it was found that the magnitude of the first peak increased as the isothermal cure temperature increased, as also it did as the clay content was increased [20], this latter observation again supporting the hypothesis that the first peak is associated with an intra-gallery reaction. It would be anticipated, therefore, that the degree of exfoliation obtained in these nanocomposites would increase with the isothermal cure temperature, and this is indeed observed, as will be shown further below.

Figure 2. Isothermal cure of TGAP/MMT/DDS system: samples containing 5 wt% MMT at the temperatures of 150 ºC (light purple, dash-dotted), 165 ºC (blue, long dash), and 180 ºC (light green, full); samples without MMT at the temperatures of 150 ºC (dark purple, short dash) and 180 ºC (dark green, dotted). Exothermic direction is upwards

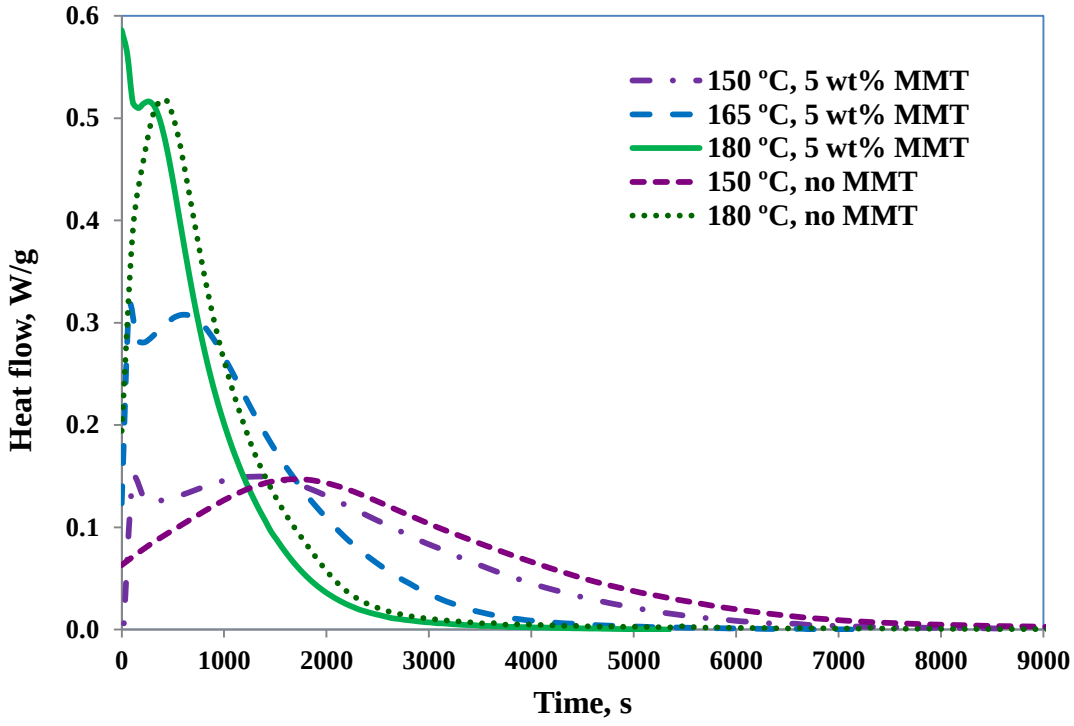

The intra-gallery reaction can also be promoted by the procedure of pre-conditioning, the second preparation procedure described above, which allows the homopolymerisation of the epoxy resin to take place within the clay galleries, catalysed by the onium ion of the organically modified clay. It is clear that a homopolymerisation reaction takes place during pre-conditioning, not only because the epoxy equivalent (understood as epoxy equivalent weight) and the glass transition temperature of the epoxy/clay mixture both increase, but also because the rapid first peak that was seen in the isothermal cure of TGAP/MMT/DDS nanocomposites did not appear if the resin-clay mixture had been pre-conditioned before the addition of the curing agent [19]. This is illustrated in Figure 3 for a sample that has been pre-conditioned for 109 days at room temperature before cure, compared with the cure of a fresh resin-clay mixture under the same conditions, where it can be seen that the initial peak has disappeared for the pre-conditioned sample. Although this procedure is slightly impractical, in that it requires storage of the resin-clay mixtures for relatively long times before the addition of the curing agent, it would be anticipated that pre-conditioning would result in an improved degree of exfoliation in the cured nanocomposite when compared with nanocomposites prepared by the standard procedure. This is because the intra-gallery reaction can proceed unhindered by any cross-linking reaction of the surrounding matrix. As will be shown below, the degree of exfoliation obtained by pre-conditioning the resin-clay mixture is indeed better than that for nanocomposites prepared by the standard procedure.

Figure 3. Comparison of isothermal cure curves at 150 ºC for TGAP/MMT/DDS nanocomposites containing 5 wt% clay, with (purple curve, dashed line) and without (red curve, full line) pre-conditioning. Exothermic direction is upwards

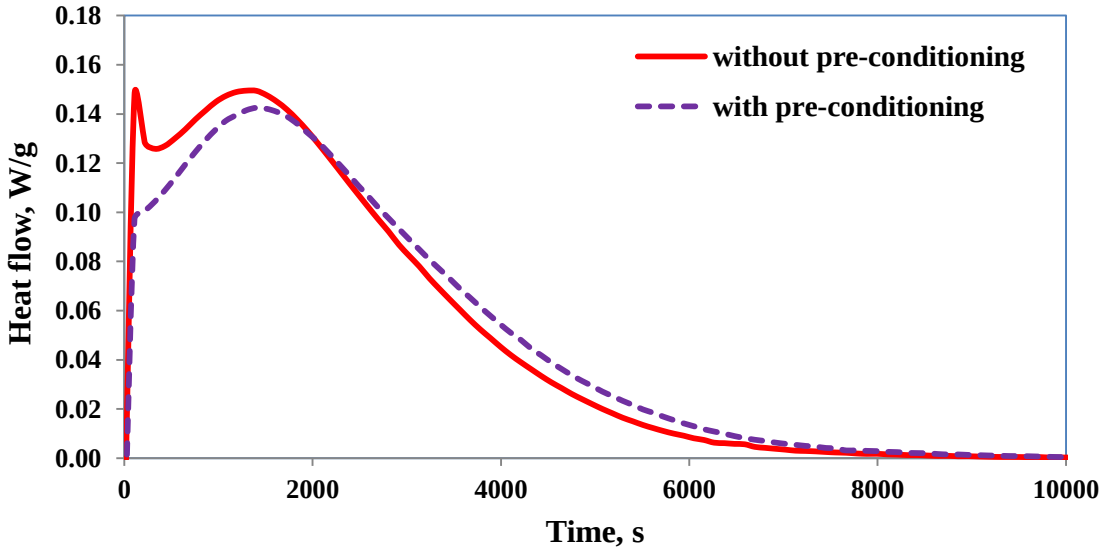

It might be argued that storage of the reactive resin, TGAP, for long periods of time, particularly at elevated temperatures, would lead to changes in the reaction kinetics even without any clay in the system. As a control experiment, the TGAP was stored for 14 days at 80 ºC, and the glass transition temperature of the resin alone was determined before (−39.4 ºC) and after storage (−37.7 ºC). This small increase of 1.7 ºC in T_g reflects a loss of epoxy groups, equivalent to a small increase in the epoxy equivalent [19], which would result in a small change in the reaction kinetics when cured with DDS. However, these changes are insignificant when compared with the changes that occur during pre-conditioning in the presence of organically modified MMT: storage at 80 ºC of the TGAP/MMT system with 5 wt% MMT for 15 days or of the system with 2 wt% MMT for 13 days leads to changes in T_g of 27.1 ºC and 23.7 ºC, respectively, much larger than the 1.7 ºC change for the resin without clay. Indeed, after storage for 2 years at room temperature the T_g of the TGAP increases to only −37.0 ºC. It can be concluded that the pre-conditioning effects observed here are associated almost entirely with the presence of the clay.

As an alternative to the somewhat impractical pre-conditioning procedure, we proposed earlier that the intra-gallery reaction could be promoted instead by incorporating an initiator of cationic homopolymerisation within the clay galleries before mixing the resin with the clay and adding the curing agent [21]. The preparation procedure described further above did indeed incorporate the initiator, BF_3·MEA, into the clay galleries, as was demonstrated by SAXS, resulting in fact in a decrease in the layer *d*-spacing, from 2.1 nm for the organically modified MMT to 1.3 nm, as shown in Figure 4. This can probably be attributed to the interchange of the monoethylamine of the BF_3 complex with the octadecyl ammonium salt of the organically modified MMT, and is therefore indicative of the presence of BF_3·MEA within the clay galleries. Despite this reduction in the *d*-spacing, when the TGAP epoxy was mixed with this "initiated" clay, the resin intercalated into the clay galleries and caused the *d*-spacing to increase to 4.4 nm, a larger separation than the *d*-spacing of 3.5 nm found for the TGAP intercalated directly into the organically modified MMT [21].

It might be argued that there remain some traces of the solvent in the sample after the procedure used for the incorporation of the BF3·MEA into the clay galleries, and that this might affect the reaction kinetics. As a check on this possibility, TGAP/MMT/DDS samples with 5 wt% MMT and without any BF_3·MEA were prepared by the solvent method [22, 25] and then cured isothermally at 165 ºC for 2 h. It transpires that there is very little difference in the reaction kinetics compared with the standard preparation procedure: the first, very rapid, reaction which is associated with intra-gallery homopolymerisation has a peak heat flow after about 30 s for the solvent-prepared sample in comparison with about 20 s for the standard sample, while the main cross-linking peak remains essentially unchanged, and the total heat of reaction is reduced from 651 J/g for the standard sample to

624 J/g for the solvent-prepared sample. These small differences could be attributed to the better dispersion of the clay in the resin which occurs for the solvent preparation method [22, 25], which allows easier access of the resin to penetrate the clay galleries, and hence promotes homopolymerisation, with a corresponding decrease in the total heat of reaction. Accordingly it is concluded that the solvent is indeed eliminated after the preparation procedure involving acetone, and that any small effects observed can be attribute to enhanced intra-gallery homopolymerisation.

Figure 4. SAXS scattering diagrams for the organically modified MMT clay (green dashed line) and for the MMT intercalated with BF_3·MEA (red solid line)

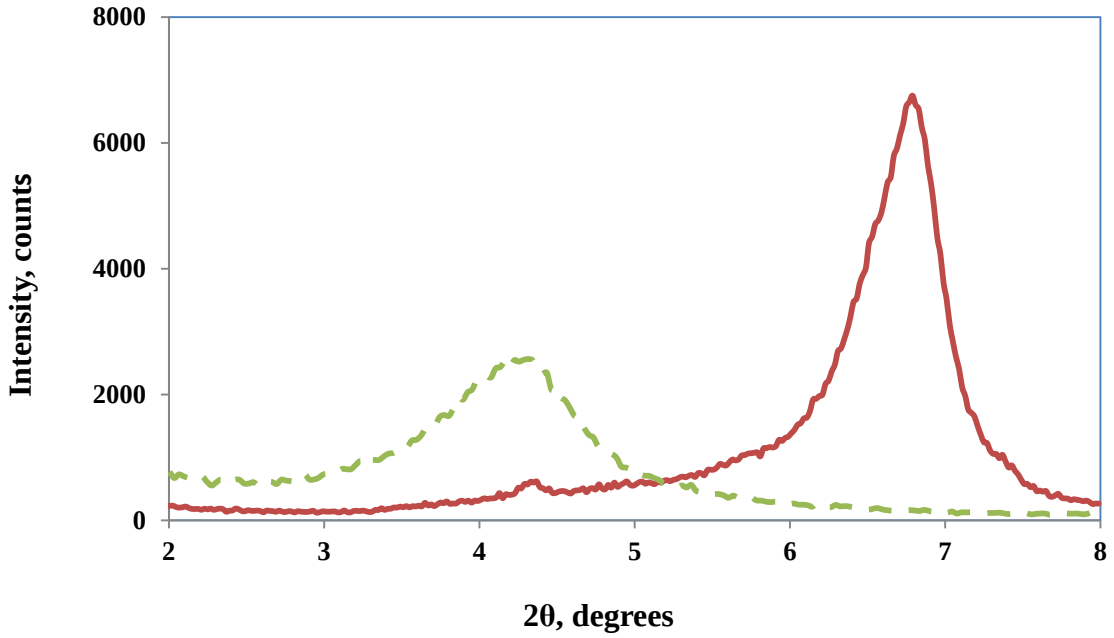

It should be pointed out that it is unlikely that all the BF_3·MEA enters the clay galleries, and hence that some may remain outside the galleries and be able to catalyse an extra-gallery homopolymerisation reaction. This is more likely to occur to a greater extent the higher is the proportion of BF_3·MEA used. The consequence of this would be that, particularly for the higher BF_3·MEA content, the extra-gallery reaction would lead to a more rigid matrix material surrounding the clay tactoids, which would inhibit the exfoliation process. This is a possible explanation for why, despite the anticipated greater extent of intra-gallery homopolymerisation reaction for the higher BF_3·MEA content, improved exfoliation was not always observed by TEM for the BF_3·MEA content of 1% compared with 0.5% [21]. The effect of the BF_3·MEA content is discussed later in respect of the impact tests.

In order to examine further the possible effect of BF_3·MEA on the cure of these nanocomposite systems, the TGAP/DDS system without any clay was cured isothermally after introducing 1 wt% of BF_3·MEA in order to catalyse a homopolymerisation reaction. At the isothermal cure temperature of 150 ºC, for which the TGAP/DDS system has an exotherm with a peak heat flow of less than 0.2 W/g

occurring after more than 1000 s (see Figure 2, for example), the TGAP/DDS system with BF_3·MEA has a peak heat flow at least an order of magnitude larger, and occurring almost instantaneously. Similar observations were made for cure at the much lower isothermal cure temperature of 120 ºC. It can be concluded that a significant presence of BF_3·MEA outside the gallery regions would accelerate the extra-gallery reaction to such an extent that the exfoliation of the clay layers by the intra-gallery reaction would be severely inhibited. The fact that this does not happen suggests that there is, in fact, hardly any BF_3·MEA outside the clay galleries, in other words that the procedure adopted for introducing the initiator into the clay galleries has been very effective.

The cure schedule for this system in which BF3·MEA is incorporated into the clay galleries was designed such that, in a first step at a relatively low temperature of 100 ºC or 110 ºC, only the cationically initiated homopolymerisation reaction between the clay layers would take place, the temperature being too low for any significant amount of cross-linking reaction to occur. In the second step, once the first reaction is complete, the system was isothermally cured at a higher temperature, for example 150 ºC or 180 ºC, and then finally post-cured at 210 ºC. An illustration of the reaction taking place during the first cure step is shown in Figure 5. Here it can be seen that very little homopolymerisation occurs at 100 ºC, whereas at 120 ºC not only much more homopolymerisation but also some cross-linking occurs, seen as the broad shoulder at long times. Consequently, in order to maximise the amount of homopolymerisation that occurs, without any significant cross-linking reaction, the temperature for the first step in this procedure was usually selected as 110 ºC, though some samples were prepared with 100 ºC for this temperature (see Table 1).

Figure 5. DSC scans for the isothermal cure of TGAP/DDS/MMT (5 wt%) with 1 wt% initiator (BF_3·MEA) at different temperatures: 100 ºC (orange, full line) and 120 ºC (pink, dashed line). Exothermic direction is upwards

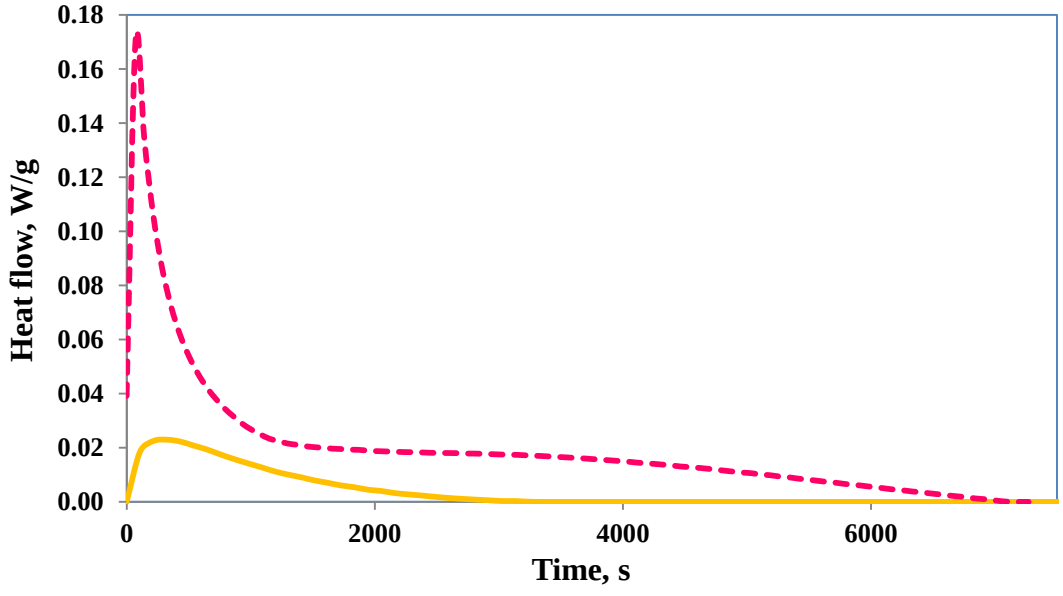

Nanostructural characterisation

The SAXS diffractograms for all the samples prepared by the standard and pre-conditioning procedures showed no scattering peaks in the range of 2θ between 1.2º and 8º, indicating that there was no regular layer stacking with a *d*-spacing less than about 8 nm. An illustration is given in Figure 6a, for the particular case of a nanocomposite with 5 wt% MMT prepared by the standard procedure with an isothermal cure temperature of 180 ºC, and a similarly featureless scattering pattern was found for the pre-conditioned samples. Consequently, nanocomposites prepared by these two procedures are clear candidates for presenting an exfoliated nanostructure, and should be studied by TEM, as will be shown below. For the samples prepared by the cationic initiation procedure, a very small scattering peak was often observed at 2θ close to 6.5º, corresponding to a *d*-spacing of approximately 1.3 nm. An example is given in Figure 6b for the particular case of a nanocomposite with 2 wt% MMT and 0.5 wt% BF_3·MEA, cured isothermally first at 100 ºC and then at 150 ºC, where the small peak at 6.5º is shown on an enlarged scale in the inset. This *d*-spacing is the same as that for the MMT/BF_3·MEA mixture before the intercalation of the epoxy resin into the clay galleries, and indicates that for a very small proportion of these "initiated" clay particles the epoxy resin does not intercalate into the clay galleries. This will be confirmed later by TEM.

Figure 6. Typical SAXS diffractograms for nanocomposites: (a) for sample 5%, 180 ºC; (b) for sample 2%+0.5%BF_3, 150 ºC. The inset shows the small peak at 6.5 nm on an enlarged scale

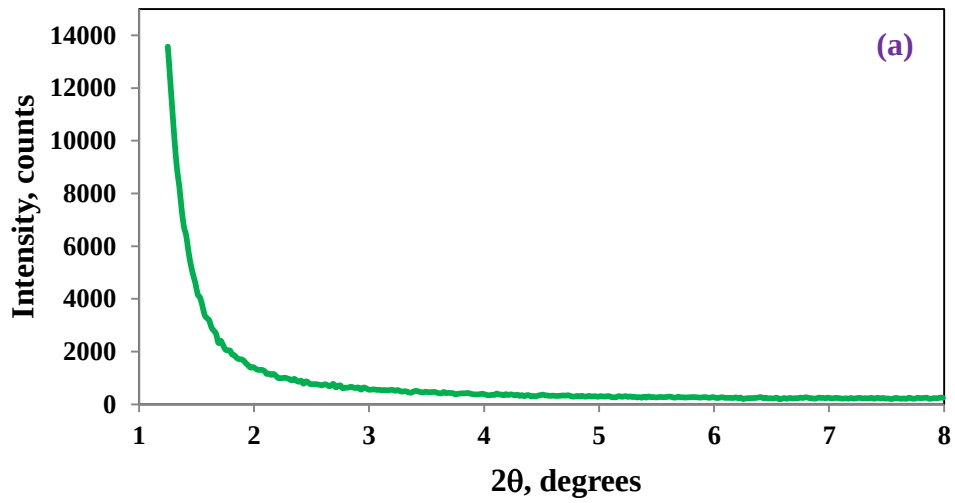

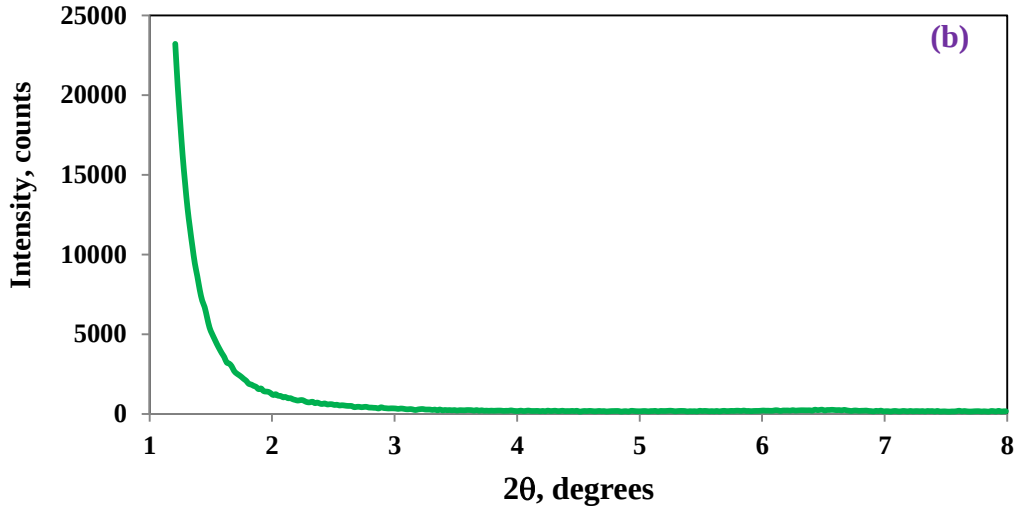

The TEM studies of the nanocomposites prepared by the different procedures revealed significant differences in the nanostructures, which can be correlated with the preparation procedures and with the thermal analysis of the cure process. As regards the standard preparation procedure, Figure 7 shows the nanostructure for two different isothermal cure temperatures, 150 ºC and 180 ºC, for samples with 5 wt% clay. It can be seen that both nanocomposites display a certain degree of exfoliation: even though some clay layers are still in register, the majority are separated by more than 8 nm, the maximum *d*-spacing detectable by SAXS, and are reasonably dispersed in the epoxy matrix. The separation and dispersion of the layers appears greater in the sample cured isothermally at the higher temperature, in agreement with the earlier observation from DSC that the higher isothermal cure temperature resulted in a greater contribution from the intra-gallery homopolymerisation reaction.

Figure 7. TEM micrographs for samples prepared by the standard procedure: (a) 5%, 150 ºC and (b) 5%, 180 ºC. The scale bar is 20 nm in each case

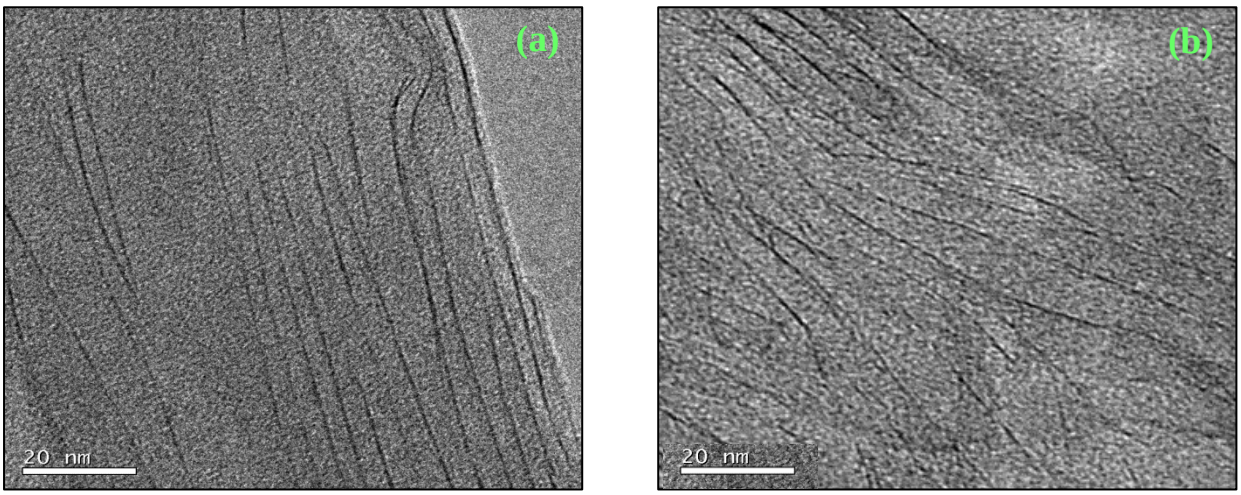

For the pre-conditioning procedure, the TEM micrographs show, for example for a sample with 2 wt% clay pre-conditioned at RT for 225 days shown in Figure 8, that the degree of exfoliation was improved by pre-conditioning. Here it can be seen that there are very few clay layers visible, they are no longer in register, and that they are rather well separated and distributed throughout the matrix, indicating a significantly better degree of exfoliation than for samples prepared by the standard procedure, illustrated in Figure 7.

Figure 8. TEM micrograph for a sample with 2 wt% MMT, prepared by pre-conditioning at RT for 225 days. The scale bar is 20 nm

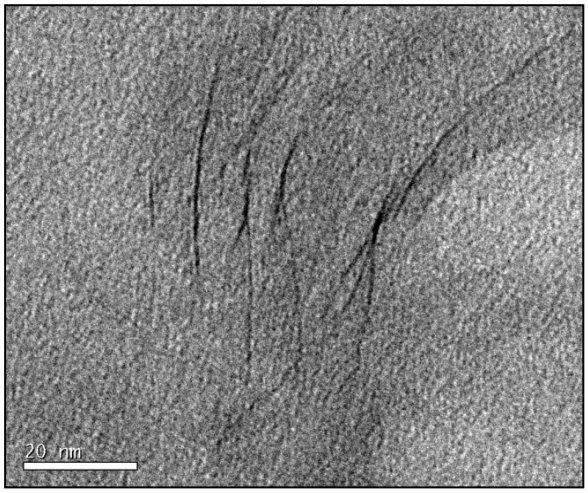

To illustrate the nanostructure of the samples prepared by the cationic initiation procedure, for which the extent of clay layer separation and the uniformity of their distribution is difficult to distinguish unequivocally from those for the pre-conditioned samples, we show first some TEM micrographs at lower magnification in order to indicate how the dispersion and size of the clay agglomerates is improved by this procedure, and how it compares also with the standard preparation procedure. In Figure 9 are shown the TEM micrographs at low magnification for samples with 5 wt% clay prepared by the three procedures: (a) standard, (b) pre-conditioning, and (c) cationic initiation. It can be seen that, for the standard procedure, some clay agglomerations remain after cure, the one shown here being of the order of 10 μm in size. For the pre-conditioned sample, Figure 9b, the agglomerations are much smaller, of the order of 2 μm in size, with several of these agglomerates dispersed throughout the matrix. In comparison, the cationic initiation procedure using BF_3·MEA results in a significant reduction in the number of clay agglomerations, and generally that these agglomerates are also smaller; the largest agglomerate in Figure 9c is about 2 μm in size, and the few other agglomerates are much smaller.

Figure 9. TEM micrographs at low magnification for samples with 5 wt% clay prepared by: (a) standard procedure, 180 ºC; (b) pre-conditioning, 63 days at RT; and (c) cationic initiation with BF_3·MEA, 5%+0.5%BF_3, 150 ºC. The scale bar is 5 µm in all cases

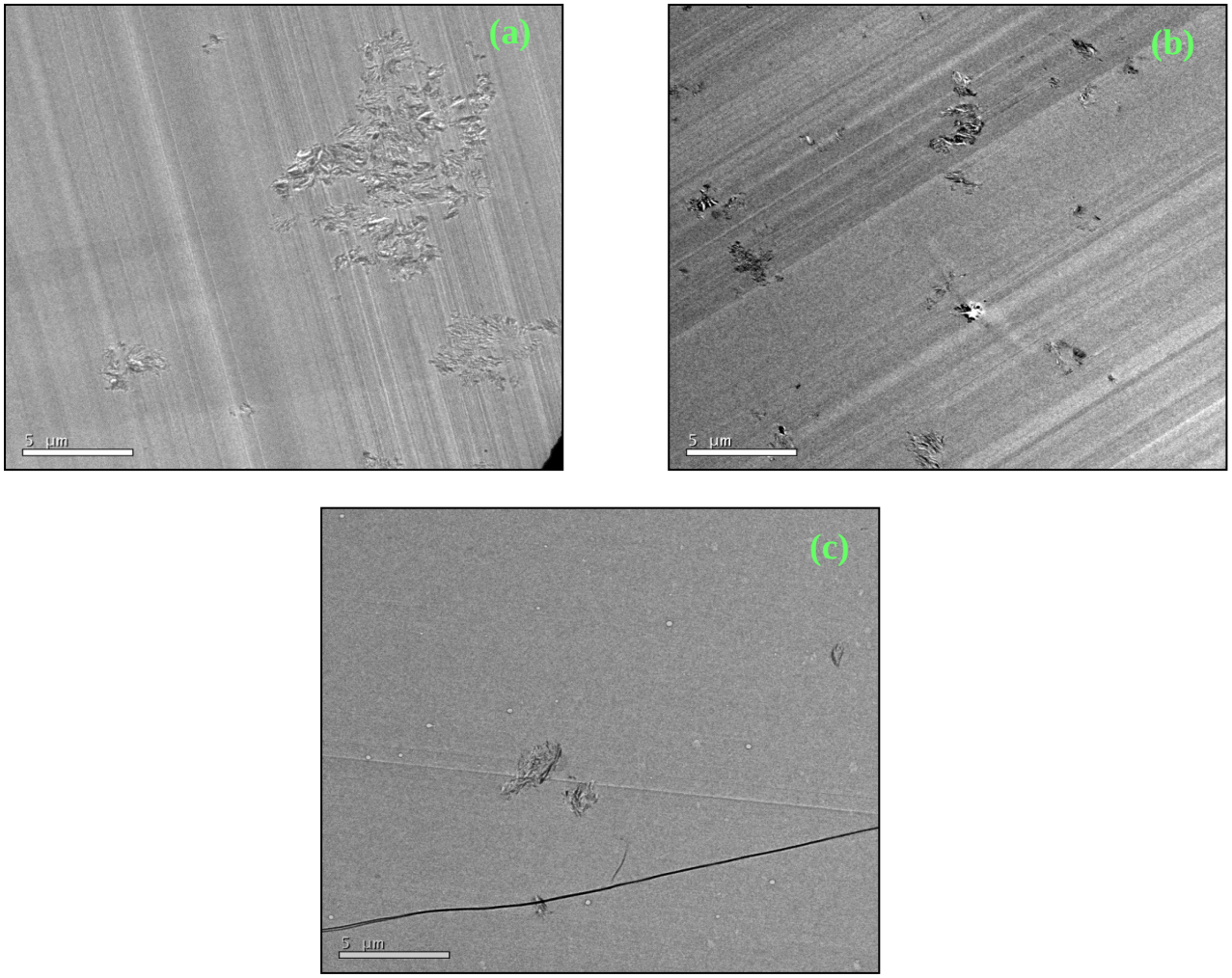

Although, as suggested above, the size and dispersion of the clay agglomerates is much improved by the BF_3 preparation method, there still clearly remain some agglomerates, which in fact tend to be rather dense in comparison with the other preparation methods. This is illustrated by means of higher magnification TEM micrographs, such as that shown in Figure 10. Here, only a small part of the area towards the left of the micrograph contains stacked layers, with a high degree of exfoliation elsewhere. The layers which are stacked, however, have a *d*-spacing of only about 1.3 nm. These layers correspond to those discussed earlier, in the section on SAXS, where it was pointed out that for this preparation method the epoxy resin fails to intercalate into some of the clay tactoids in which the BF_3·MEA has previously been intercalated, with the consequence that these layers remain with the separation of about 1.3 nm which they have before mixing this "cationically initiated" clay with the epoxy.

Figure 10. TEM micrograph at high magnification for sample with 5 wt% clay prepared by cationic initiation with 1% BF_3·MEA and cured isothermally at 180 ºC. The scale bar is 20 nm

The identification and comparison of the nanostructures corresponding to the different preparation procedures by means of TEM, however, particularly at high magnification but also to a certain extent at low magnification, remains a somewhat subjective approach. This technique necessarily examines only a selected part of the overall sample, and even though the micrographs illustrated in Figures 7 to 10 are considered to be representative and characteristic of the complete nanostructure, the observations made here should be supported by measurements of a property which depends on the global nanostructure. For these purposes, the dynamic mechanical properties and the impact resistance have both been determined and are discussed below.

Dynamic mechanical properties

From the dynamic mechanical analysis (DMA) results, tan δ was determined for the nanocomposites prepared by the different procedures, and the dependence on temperature for a frequency of 1 Hz is shown in Figure 11. The maximum in tan δ, for example at a frequency of 1 Hz, is often taken as the dynamic glass transition temperature, T_g, determined mechanically. More correctly, though, since this is frequency dependent, it is better to refer to this as the temperature of the α-relaxation, and so henceforth this temperature is denoted here as T_α. Thus it can be seen that T_α decreases for all the nanocomposites relative to the reference TGAP/DDS system without any clay. The decrease is

relatively small, however, except for the two nanocomposites prepared by the pre-conditioning procedure and for sample 2%, 180 ºC, this last appearing somewhat anomalous.

Figure 11. Tan δ as a function of temperature, at a frequency of 1 Hz, for different TGAP/clay nanocomposites, as indicated

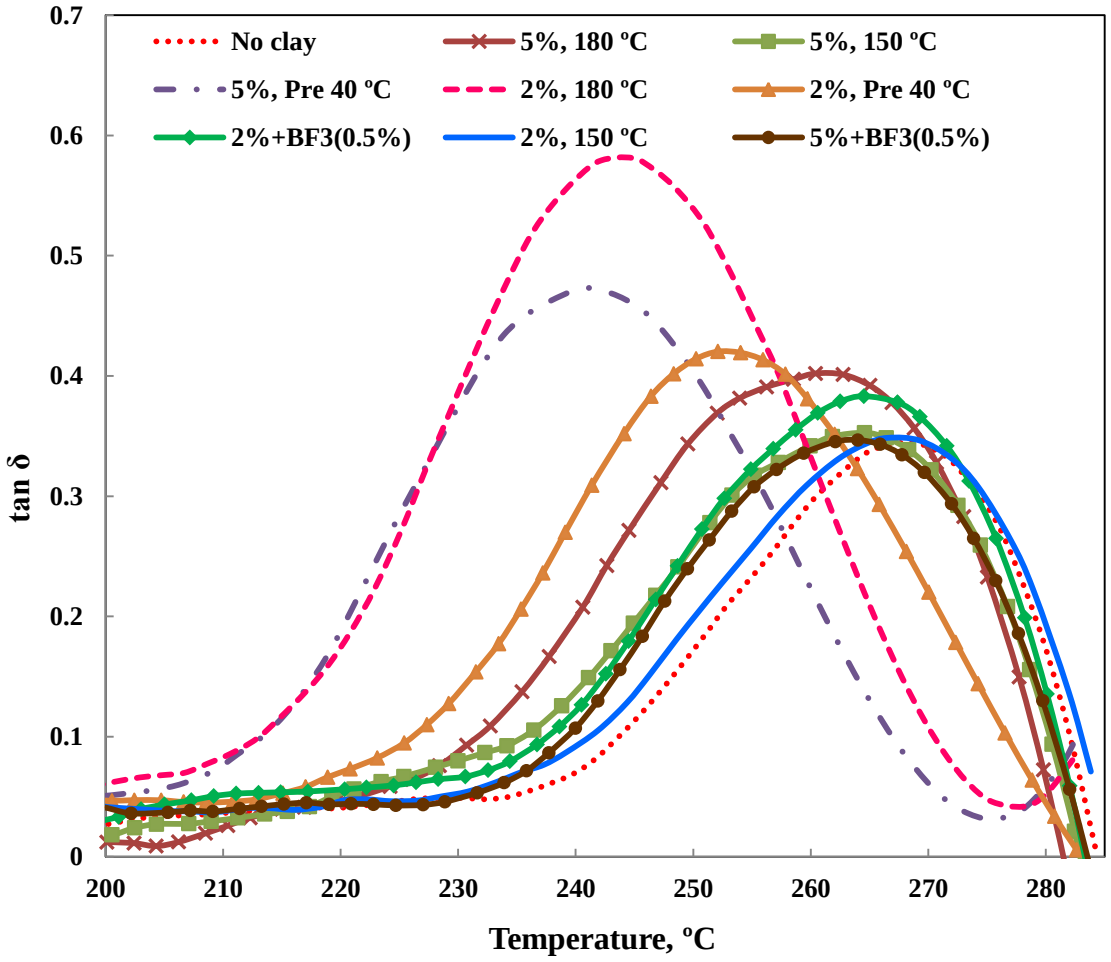

On the other hand, for filled systems such as the present PLS nanocomposites, the effect of the clay reinforcement will be more effective in the rubbery region than in the glassy region, and as a consequence there will be a corresponding effect on the location of the tan δ peak. It would therefore be interesting to examine also how the loss modulus depends on frequency and nanocomposite preparation method. Figure 12 shows the loss modulus curves for the nanocomposite sample TGAP/MMT(5)/DDS(52), for which the clay content is 5 wt%, the sample having been cured isothermally at 150 ºC and then post-cured at 210 ºC.

Figure 12. Loss modulus as a function of temperature, for the frequencies indicated in the insert, for the TGAP/MMT/DDS nanocomposite with 5 wt% clay content

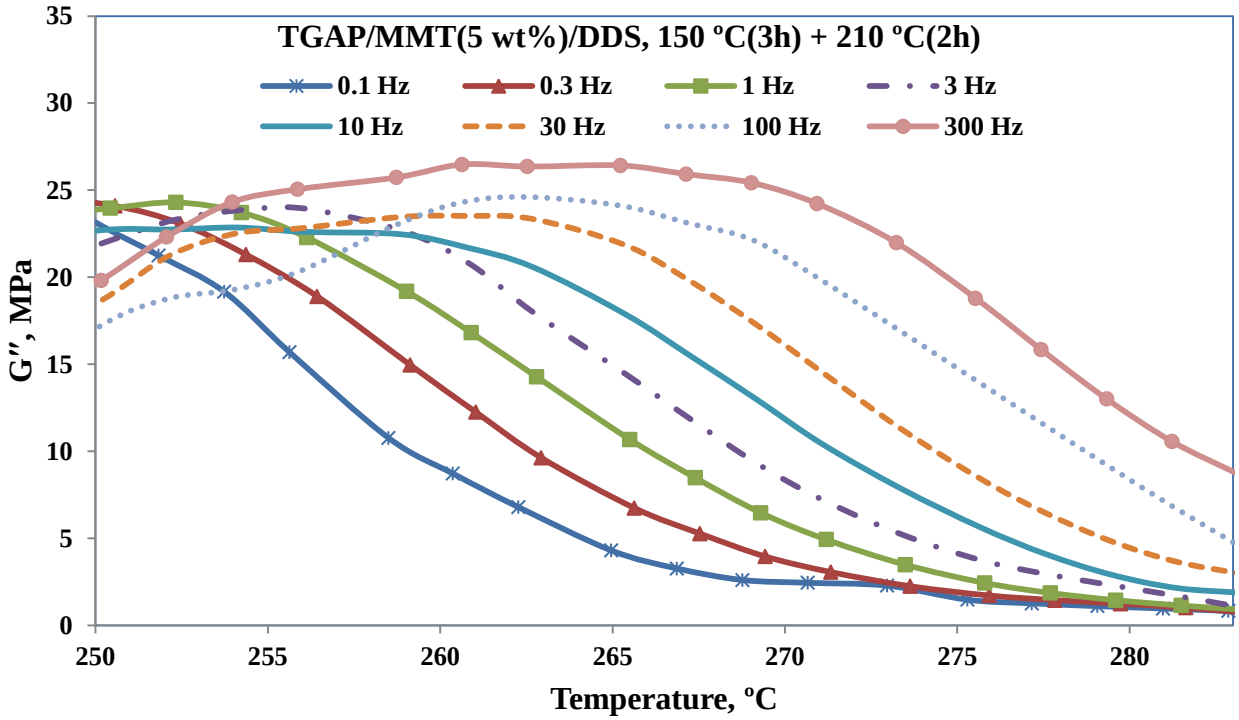

From the frequency dependence of the tan δ peaks in Figure 11 for each nanocomposite, over the full range of frequencies studied, the apparent activation energy for the α-relaxation can be determined. There is considerable variation with the different preparation procedures for the nanocomposites, but it does not appear to be systematic. In fact, using a uniform probability plot, the values of the activation energy are acceptably described by a uniform distribution. Based on the maximum likelihood estimation method, and a confidence limit of 95%, the interval of 800 ± 200 kJ/mol is obtained.

Likewise, the activation energy can be determined from the loss modulus curves in Figure 12. For these curves, the peak was less well defined than was the high temperature flank of the relaxation, and hence the activation energy is determined from the temperature shift with frequency for this region. The results are plotted as log(frequency) versus inverse temperature in Figure 13 for the sample for which the results are shown in Figure 12 as well as for another nanocomposite sample, TGAP/MMT(2)/DDS(52), for which the clay content is 2 wt%, this sample also having been cured isothermally at 150 ºC and then post-cured at 210 ºC. From the slope of the best-fit straight lines in Figure 13, the activation energies of 970 kJ/mol and 892 kJ/mol are obtained for the 2 wt% and 5 wt% samples, respectively. Both of these values fall within the 95% confidence interval for the value found from the tan δ peak, from which we conclude that, in this particular case, the activation energy is the same whether the determination of T_α is made from tan δ curves or from loss modulus data.

Figure 13. Plot of log(frequency) versus inverse temperature for the frequency shift of the loss modulus curves, for two TGAP/MMT/DDS nanocomposite systems: red squares, 5 wt% clay content; blue rhombus, 2 wt% clay content

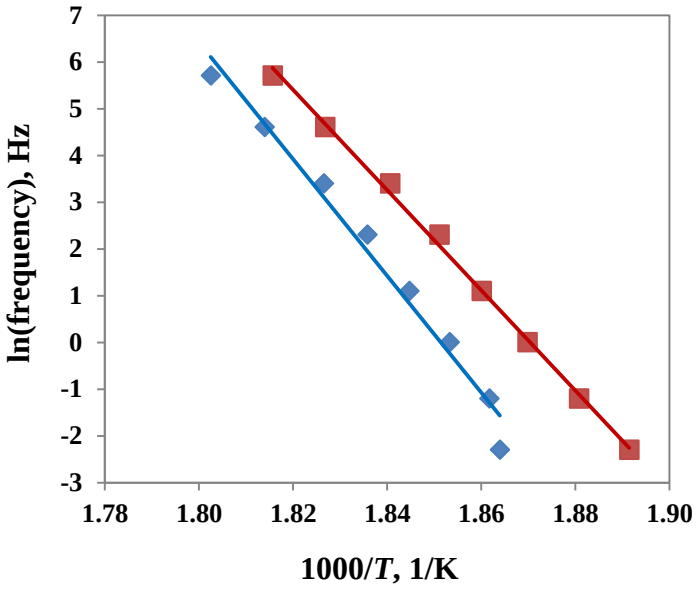

A certain decrease in T_α for the nanocomposites in comparison with the TGAP/DDS reference is not unexpected, as such a reduction on the addition of clay has often been observed before in other nanocomposite systems [7, 17, 28] for which the T_g was determined calorimetrically. In this respect, it is interesting to compare the values of T_α obtained by DMA with the dynamic T_g values obtained by a temperature modulated DSC technique, TOPEM, shown earlier to be convenient for the determination of T_g in these highly cross-linked systems [19-21, 27]. The dynamic glass transition temperatures for the TOPEM measurements were taken from the step change in c_{p0}, the quasi-static specific heat capacity, which can be associated with a frequency of about 4 mHz [29]. The comparison is shown in Figure 14.

Figure 14. Variation of the dynamic glass transition temperature (or T_α) with preparation procedure, obtained by two different techniques: DMA at 1 Hz (green rhombus) and TOPEM at 4 mHz (pink squares)

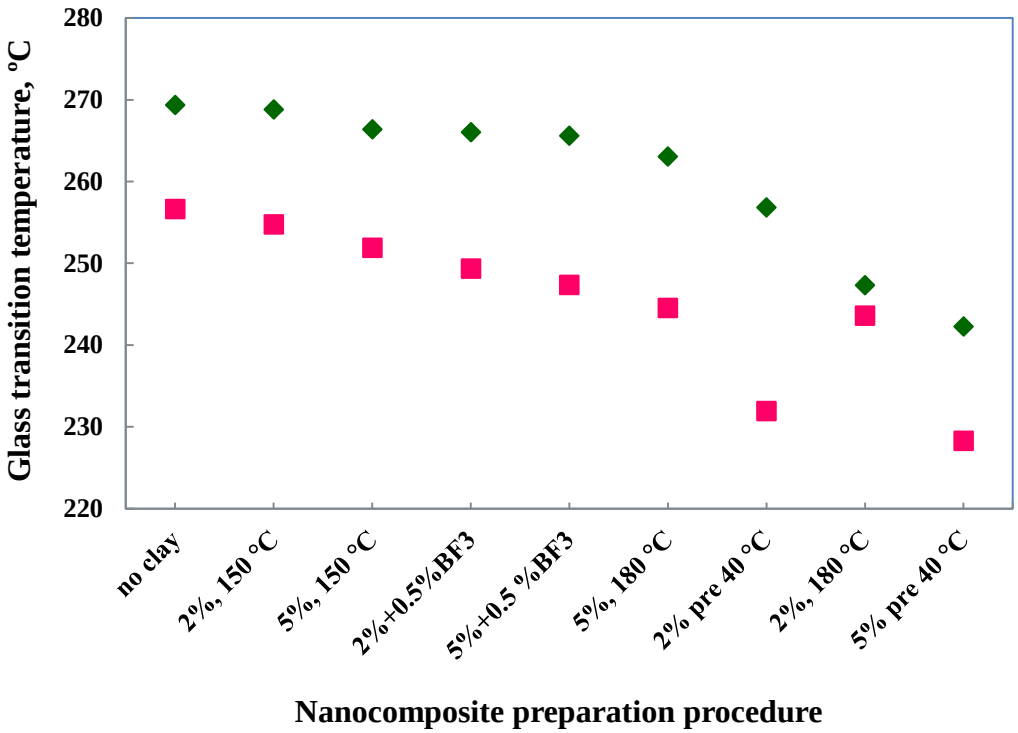

It can be seen from Figure 14 that the DMA values for T_α are systematically greater than the TOPEM values, except for the result for sample 2%, 180 ºC which again appears "anomalous", as it did in Figure 11. The systematic difference between the mechanical and calorimetric α-relaxation temperatures is a consequence of the different frequencies at which T_α is determined. Over the whole range of nanocomposites in Figure 14, the average difference is about 16 ºC, which corresponds to the same activation energy of 800 kJ/mol that was found earlier from the frequency dependence of the tan δ peaks. The slight decrease in T_α with the addition of clay is evident from this figure, as also is the more significant decrease for the preparation procedure involving pre-conditioning, which can be explained on the basis of the significant amounts of homopolymerisation which occur during pre-conditioning, resulting in a reduced cross-link density in the epoxy network.

Very little systematic correlation could be found between the storage modulus, evaluated in the glassy region at 50 ºC, and the preparation procedure. The sample 2%, 180 ºC prepared by the standard procedure again presents a somewhat anomalous behaviour, with a modulus more than 30% higher than the reference. In contrast, the nanocomposites prepared by the pre-conditioning procedure displayed lower values of storage modulus than the reference, particularly sample 2%, pre 40 ºC, for which the storage modulus was reduced by almost 50%. This is presumably related to the greater extent of homopolymerisation in these nanocomposites, noted above also in respect of their T_α values, which results in a less cross-linked network structure. In the other nanocomposites, which all have the same modulus as the reference, within experimental error, it is likely that there is a competition

between the effect of the clay, which is to increase the modulus, and the effect of homopolymerisation, occurring in all these systems to a greater or lesser extent, which is to reduce the modulus. As a consequence no significant or systematic variations are observed.

Impact tests

The values of the impact strength, together with the standard deviations, of the nanocomposites prepared by the different procedures are collected in Table 2. It can be seen that the impact strength of the nanocomposites is increased relative to the reference for all the preparation methods, except for two samples with 5 wt% clay content, namely 5%, 150 ºC and 5%, 180 ºC, which have approximately the same values as the reference. In fact, the impact strengths of all the nanocomposites with 5 wt% clay are less than those of the corresponding 2 wt% nanocomposite. This can be explained on the basis of the better dispersion of the clay agglomerates in the nanocomposites with the lower clay content, an effect often observed previously, and to which the impact resistance is particularly sensitive. We therefore concentrate on the results for the 2 wt% nanocomposites in order to study the influence of the preparation procedure.

Table 2. Values of the impact strength for different TGAP/clay nanocomposites with 2 wt% and 5 wt% MMT

Preparation procedure	**Impact strength (kJ/m^2)**	
	No clay	
Reference	1.40 ± 0.18	1.40 ± 0.18
	2 wt% clay content	**5 wt% clay content**
150 ºC	1.60 ± 0.20	1.34 ± 0.15
180 ºC	1.70 ± 0.38	1.31 ± 0.10
pre 40 ºC	2.10 ± 0.33	2.04 ± 0.32
+0.5%BF_3, 125 ºC	2.34 ± 0.24	1.54 ± 0.23
+0.5%BF_3, 150 ºC	2.50 ± 0.90	-------
+0.5%BF_3, 180 ºC	2.17 ± 0.56	--------
+1%BF_3, 125 ºC	2.91 ± 0.53	2.65 ± 0.22

For the nanocomposites prepared by the standard procedure, it can be seen that there is a slight increase in the impact strength as the isothermal cure temperature increases, though the change is not very significant in the light of the magnitude of the standard deviation. Nevertheless, this increase is consistent with the earlier observations from both DSC and TEM, the former showing that for cure at 180 ºC the contribution of the intra-gallery homopolymerisation reaction is greater than that for cure at

150 ºC, while the latter showed that the *d*-spacing appeared greater for isothermal cure at the higher temperature.

A significantly greater increase in the impact energy, by 50% relative to the reference, is obtained for the preparation procedure involving pre-conditioning of the resin/clay mixture at 40 ºC. This procedure ensures an extensive amount of intra-gallery homopolymerisation reaction, which leads to an improved degree of exfoliation as was shown in Figure 8, in accordance with these impact results. In fact, almost the same value of impact energy is found for the 5 wt% nanocomposite also. This might be explained by the fact that pre-conditioning also improves the dispersion of the clay agglomerations, in particular reducing their size, which would imply that, after pre-conditioning, there would be less deterioration in the impact strength in the 5 wt% nanocomposites caused by the inferior clay agglomerate dispersion in comparison with the 2 wt% nanocomposites.

The greatest increase in impact energy for the 2 wt% nanocomposites, by over 100% relative to the reference for the best case, is obtained by the incorporation of BF_3·MEA between the clay galleries. This procedure promotes the intra-gallery reaction, which was shown earlier to lead to fewer and smaller aggregates in the cured nanocomposite (Figure 9). In fact, even the 5 wt% nanocomposite shows a significant increase in impact strength when prepared by the cationic initiation procedure, which demonstrates how effective this procedure is in improving the properties of these nanocomposites.

To examine more closely the relationship between the measured impact strength of these nanocomposites and their respective cross-linked network formations, both the dynamic glass transition temperature, determined calorimetrically by TOPEM, and the impact strength are plotted in Figure 15 as a function of the various preparation procedures. The preparation procedures are arranged in such a way that the impact strength increases from left to right, which can be interpreted in the following way. In order that the addition of clay to the epoxy resin should increase the impact strength, it is necessary for the clay to be exfoliated, and increasing degrees of exfoliation are observed (i) for increased isothermal curing temperatures, (ii) when the resin/clay mixture is pre-conditioned prior to curing, and (iii) when the BF_3·MEA initiator is introduced into the clay galleries. At the same time, there is a trend for the dynamic glass transition temperature to decrease as the impact strength increases, even though there is clearly one result which does not fit this trend, namely that for the pre-conditioned sample. This trend could be understood in terms of an increasing amount of homopolymerisation taking place as the amount of intra-gallery reaction necessary for exfoliation increases, as the glass transition is lower for the homopolymerised network structure. An important corollary to be drawn from this is that the glass transition temperature should not be used as a measure

of the quality of the nanostructure; in the present case, the increased degree of exfoliation for the samples with increased impact strength comes at the expense of a greater degree of homopolymerisation, which necessarily implies a reduction in the glass transition temperature.

Figure 15. Variation of the dynamic glass transition temperature obtained by TOPEM (left hand axis) and impact energy (right hand axis) with preparation procedure for nanocomposites containing 2 wt% clay

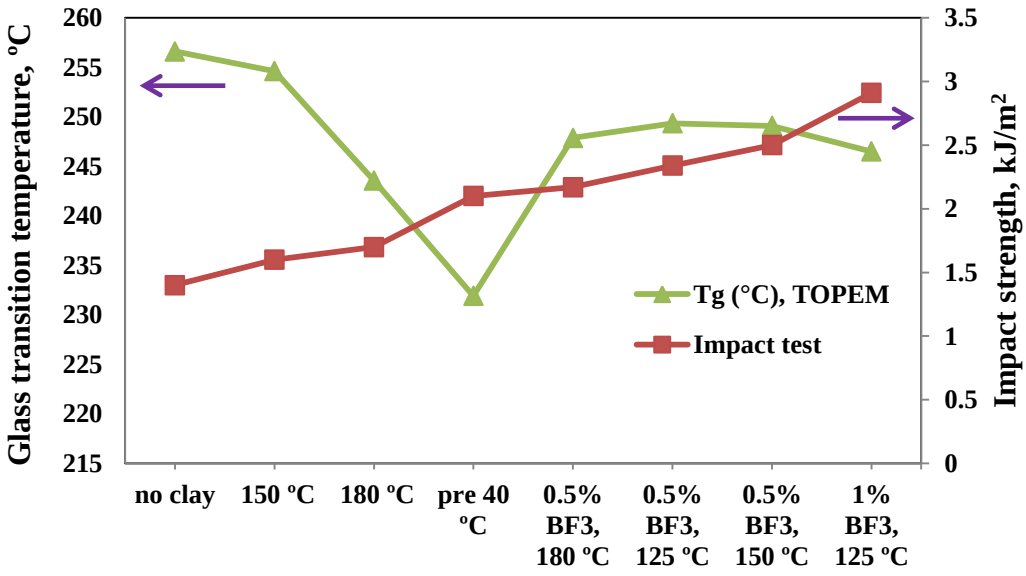

The improvement in the impact strength of these nanocomposites is supported by fracture surface studies by scanning electron microscopy (SEM) after the impact tests. The reference sample, TGAP/DDS without any clay (Figure 16a), shows the typical rather brittle fracture surface, with only a few striations where the crack velocity has increased. The amount of striations in Figure 16b, for the TGAP/MMT/DDS sample cured isothermally at 150 °C, is significantly greater, and the characteristic parabolic shape associated with the divergence of the crack from one plane to another can be seen. The overall appearance, though, is of an essentially planar fracture in both Figures 16a and 16b. On the other hand, the fracture surfaces seen in Figures 16c and 16d, for the pre-conditioned sample and the sample in which the BF_3·MEA initiator was used, respectively, both show a generally much rougher surface. This is consistent with the significantly higher values of impact energy listed in Table 2 for these samples.

Figure 16. SEM micrographs of the fracture surfaces of 2 wt% MMT nanocomposite samples after impact testing: (a) reference, TGAP/DDS without any clay; (b) 2%, 150 ºC; (c) 2%, pre 40 ºC; (d) 2%+1%BF_3·MEA, 125 ºC. Scale bar is 500 µm in all cases

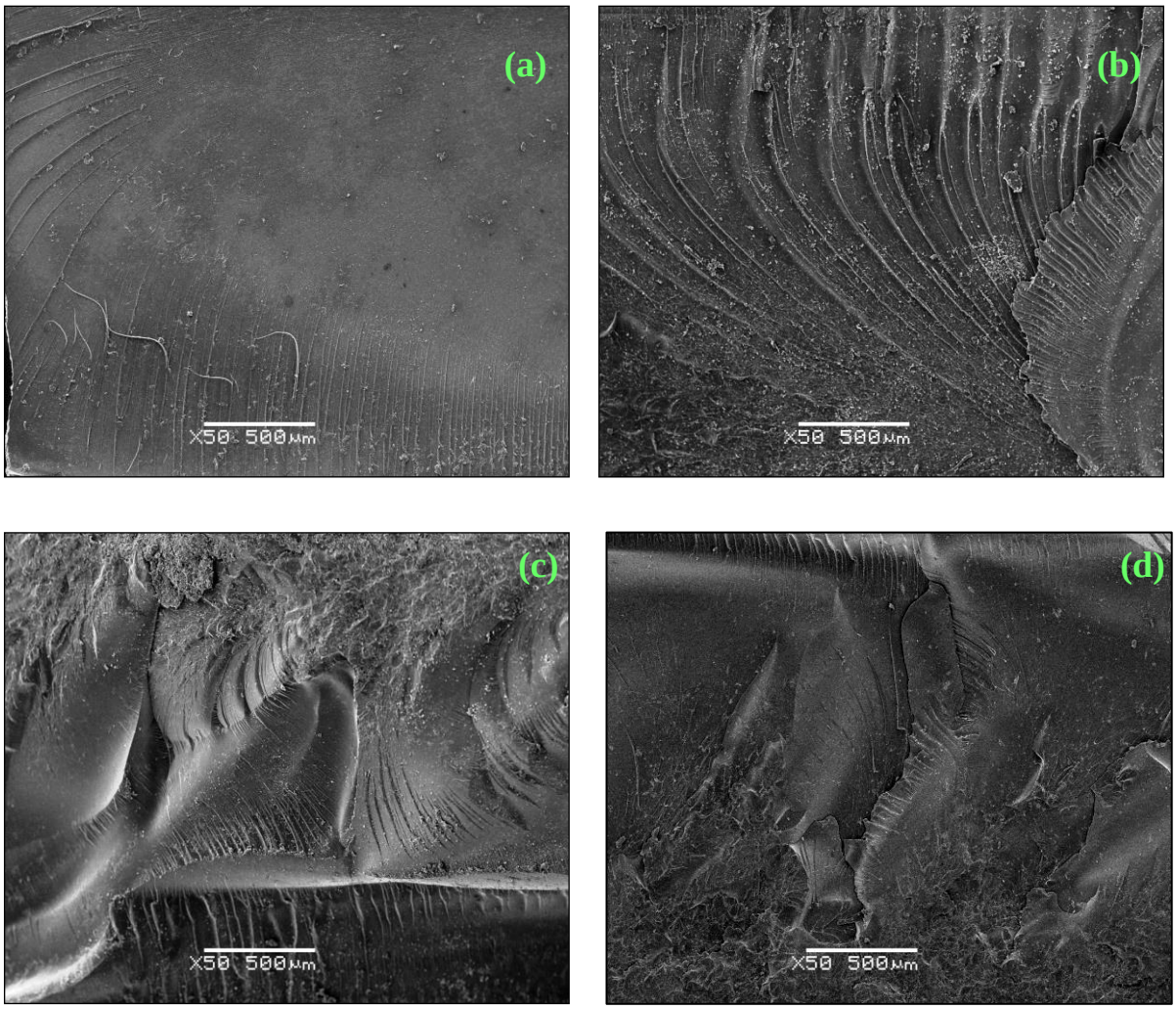

Conclusions

The cure kinetics, nanostructure and mechanical properties of tri-functional epoxy layered silicate nanocomposites, which are fabricated by three different preparation procedures, have been investigated. A clear relationship between features of the cure reaction, the nanostructure identified by SAXS and TEM, and the dynamic mechanical properties and the impact strength has been observed for each of the preparation methods, which permits the identification of the optimum procedure for achieving highly exfoliated nanocomposites. The crucial feature common to all the procedures is the separation of the intra-gallery homopolymerisation from the extra-gallery cross-linking reaction, and in particular the promotion of the intra-gallery reaction such that it occurs to a maximum extent and

before the extra-gallery reaction. The intra-gallery reaction can be promoted by fabricating the nanocomposite by three distinct procedures: (a) by increasing the temperature of isothermal cure; (b) by pre-conditioning the resin/clay mixture before adding the curing agent; and (c) by incorporating an initiator of cationic homopolymerisation into the clay galleries. Each of these procedures improves the degree of exfoliation as identified by TEM, the extent of improvement being best for procedure (c) and least for procedure (a). These improvements in the nanostructure could be anticipated from the cure kinetics observed by DSC, and correlate with the improvements in the impact strength of the cured nanocomposites. It is concluded that the incorporation of an initiator of cationic homopolymerisation into the clay galleries in order to promote the intra-gallery homopolymerisation reaction is an effective procedure for achieving high degrees of exfoliation in the cured nanocomposite.

Acknowledgements

The authors are grateful to Huntsman Corporation for the epoxy resin and curing agent and Nanocor Inc. for the organically modified clay. This work was supported financially by MINECO Project MAT2011-27039-C03-03. F.S. is grateful for a grant from the Agència de Gestió d'Ajuts Universitaris i de Recerca (AGAUR), FI-DGR 2011.

References

1. Becker, O.; Simon, G.P. Epoxy layered silicate nanocomposites. *Adv. Polym. Sci.* **2005**, *170*, 29-82.

2. Tjong, S.C. Structural and mechanical properties of polymer nanocomposites. *Mater. Sci. Eng.* **2006**, *53*, 73-197.

3. Karak, N. Polymer (epoxy) clay nanocomposites. *J. Polym. Mater.* **2006**, *23*, 1-20.

4. Alexandre, M.; Dubois, P. Polymer-layered silicate nanocomposites: preparation, properties and uses of a new class of materials. *Mater. Sci. Eng.* **2000**, *28*, 1-63.

5. Ray, S.S.; Okamoto, M. Polymer/layered silicate nanocomposites: a review from preparation to processing. *Prog. Polym. Sci.* **2003**, *28*, 1539-1641.

6. Brown, J.M.; Curliss, D.; Vaia R.A. Thermoset-layered silicate nanocomposites: quaternary ammonium montmorillonite with primary diamine cured epoxies. *Chem. Mater.* **2000**, *12*, 3376-3384.

7. Becker, O.; Cheng, Y-B.; Varley, R.J.; Simon, G.P. Layered silicate nanocomposites based on various high-functionality epoxy resins: the influence of cure temperature on morphology, mechanical properties, and free volume. *Macromolecules* **2003**, *36*, 1616-1625.

8. Chen, C.G.; Curliss, D. Preparation, characterization, and nanostructural evolution of epoxy nanocomposites. *J. Appl. Polym. Sci.* **2003**, *90*, 2276-2287.

9. Velmurugan, R.; Mohan, T.P. Room temperature processing of epoxy-clay nanocomposites. *J. Mater. Sci.* **2004**, *39*, 7333-7339.

10. Mohan, T.P.; Kumar, M.R.; Velmurugan, R. Rheology and curing characteristics of epoxy-clay nanocomposites. *Polym. Int.* **2005**, *54*, 1653-1659.

11. Giannelis, E.P.; Krishnamoorti, R.; Manias, E. Polymer-silicate nanocomposites: model systems for confined polymers and polymer brushes. *Adv. Polym. Sci.* **1999**, *138*, 107-147.

12. Manias, E. Origins of the materials properties enhancements in polymer/clay nanocomposites. http://raman.plmsc.psu.edu/~manias/PDFs/nano2001b.pdf

13. Morgan, A.B.; Gilman, J.W. Characterization of polymer-layered silicate (clay) nanocomposites by transmission electron microscopy and X-ray diffraction: a comparative study. *J. Appl. Polym. Sci.* **2003**, *87*, 1329-1338.

14. Kornmann, X.; Lindberg, H.; Berglund, L.A. Synthesis of epoxy-clay nanocomposites. Influence of the nature of the curing agent on structure. *Polymer* **2001**, *42*, 4493-4499.

15. Chin, I-J.; Thurn-Albrecht, T.; Kim, H-C.; Russell, T.P.; Wang, J. On exfoliation of montmorillonite in epoxy. *Polymer* **2001**, *42*, 5947-5952.

16. Lan, T.; Kaviratna, P.D.; Pinnavaia, T.J. Mechanism of clay tactoid exfoliation in epoxy-clay nanocomposites. *Chem. Mater.* **1995**, *7*, 2144-2150.

17. Montserrat, S.; Román, F.; Hutchinson, J.M.; Campos, L. Analysis of the cure of epoxy based layered silicate nanocomposites: reaction kinetics and nanostructure development. *J. Appl. Polym. Sci.* **2008**, *108*, 923-938.

18. Shiravand, F.; Fraga, I.; Cortés, P.; Calventus, Y.; Hutchinson, J.M. Thermal analysis of polymer layered silicate nanocomposites: identification of nanostructure development by DSC. *J. Therm. Anal. Calorim.* **2014**, DOI 10.1007/s10973-014-3709-3.

19. Hutchinson, J.M.; Shiravand, F.; Calventus, Y. Intra- and extra-gallery reactions in tri-functional epoxy polymer layered silicate nanocomposites. *J. Appl. Polym. Sci.* **2013**, *128*, 2961-2970.

20. Shiravand, F.; Hutchinson, J.M.; Calventus, Y. Influence of the isothermal cure temperature on the nanostructure and thermal properties of an epoxy-layered silicate nanocomposite. *Polym. Eng. Sci.* **2014**, *54*, 51-58.

21. Hutchinson, J.M.; Shiravand, F.; Calventus, Y.: Fernández-Francos, X.; Ramis, X. Highly exfoliated nanostructure in trifunctional epoxy/clay nanocomposites using boron trifluoride as initiator. *J. Appl. Polym. Sci.* **2014**, DOI: 10.1002/app.40020.

22. Pustkova, P.; Hutchinson, J.M.; Román, F.; Montserrat, S. Homopolymerization effects in polymer layered silicate nanocomposites based upon epoxy resin: implications for exfoliation. *J. Appl. Polym. Sci.* **2009**, *114*, 1040-1047.

23. Fraga, I.; Hutchinson, J.M.; Montserrat, S. Vitrification and devitrification during the non-isothermal cure of a thermoset. A TOPEM study. *J. Therm. Anal. Calorim*. **2010**, *99*, 925–929.

24. Fraga, I.; Montserrat, S.; Hutchinson, J.M. Vitrification and devitrification during the non-isothermal cure of a thermoset. Theoretical model and comparison with calorimetric experiments. *Macromol. Chem*. **2010**, *211*, 57-65.

25. Hutchinson, J.M.; Montserrat, S.; Román, F.; Cortés, P.; Campos, L. Intercalation of epoxy resin in organically modified montmorillonite. *J. Appl. Polym. Sci.* **2006**, *102*, 3751-3763.

26. Varley, R.J.; Hodgkin, J.H.; Hawthorne, D.G.; Simon, G.P. Toughening of a trifunctional epoxy system. II. Thermal characterization of epoxy/amine cure. *J. Appl. Polym. Sci.* **1996**, *60*, 2251-2263.

27. Hutchinson, J.M.; Shiravand, F.; Calventus, Y; Fraga, I. Isothermal and non-isothermal cure of a tri-functional epoxy resin (TGAP): a stochastic TMDSC study. *Thermochim. Acta* **2012**, *529*, 14-21.

28. Miyagawa, H.; Rich, M.J.; Drzal, L.T. Thermal properties of anhydride-cured epoxy/clay nanocomposites. *Polym. Compos*. **2005**, *26*, 42-51

29. Fraga, I.; Montserrat, S.; Hutchinson, J.M. TOPEM, a new temperature modulated DSC technique. Application to the glass transition of polymers. *J. Therm. Anal. Calorim.* **2007**, *87*, 119-124.

Paper VII

Comparative results between three protocols for achieving highly exfoliated epoxy-clay nanocomposites

J.M. Hutchinson, F. Shiravand, Y. Calventus, F. Ferrando

Polimery, in press, 59(9), 2014

COMPARATIVE RESULTS BETWEEN THREE PROTOCOLS FOR ACHIEVING HIGHLY EXFOLIATED EPOXY-CLAY NANOCOMPOSITES

John M Hutchinson, Fatemeh Shiravand, Yolanda Calventus

Universitat Politècnica de Catalunya, Escola Tècnica Superior d'Enginyeries Industrial i Aeronàutica, C/ Colom 11, 08222 Terrassa, Spain

hutchinson@mmt.upc.edu

Abstract

Three different methods of fabricating polymer layered silicate nanocomposites based upon a tri-functional epoxy resin are compared in respect of the nanostructure and impact energy of the cured nanocomposites. The three methods are designed to maximise the amount of intra-gallery reaction that takes place during cure, and this paper examines separately the effects of: (i) increasing the isothermal cure temperature; (ii) preconditioning the resin/clay mixture; and (iii) incorporating an initiator of homopolymerisation within the clay galleries. It is shown that each of these methods increases the degree of exfoliation in the cured nanocomposite, and that this improved nanostructure correlates also with an increase in the impact energy.

Keywords

PLS nanocomposites; exfoliation; epoxy resin; homopolymerisation; differential scanning calorimetry

INTRODUCTION

The idea of obtaining significant reinforcement of polymers at low filler contents by the incorporation of nanoclays has been rather widely investigated since the original conception by the Toyota research group in the early 1990's [1]. In order to accomplish the desired improvement in mechanical properties of these nanocomposites, it is necessary for the clay layers to be separated and dispersed homogeneously throughout the polymer matrix, in a process referred to as exfoliation, which creates a very large polymer-clay interfacial area [2]. For epoxy-clay nanocomposites, this process of exfoliation begins with the intercalation of the resin monomer into the clay galleries, and the subsequent crosslinking reaction is supposed to lead to the desired exfoliated nanostructure. However, achieving a highly exfoliated nanostructure in these epoxy layered silicate nanocomposites has proven difficult, and it is common to refer to "partial" exfoliation or to consider the nanostructure to be exfoliated when the *d*-spacing of the clay layers cannot be detected by Small Angle X-ray Scattering (SAXS), which normally implies layer separations greater than about 8 nm. One problem is related to the relative rates of reaction of the resin in the intra- and extra-gallery regions of the clay. It is generally recognized that, in order to maximise the degree of exfoliation, the intra-gallery reaction should occur before the extra-gallery reaction [3, 4], but this does not occur naturally for nanocomposites based upon DGEBA epoxy and organically modified montmorillonite (MMT) cured with a diamine [5]. One possibility for overcoming this problem is to precondition the intercalated epoxy-clay mixture [6, 7] before adding the curing agent and effecting the crosslinking reaction; this preconditioning procedure results in a homopolymerisation reaction taking place within the clay galleries. On the other hand, it transpires that, during the isothermal cure of such nanocomposite systems based upon a tri-functional epoxy resin cured with a diamine, two distinct reactions occur: the first is the epoxy homopolymerisation reaction taking place within the clay galleries, while the second is

the bulk crosslinking reaction in the extra-gallery regions [8]. This system therefore affords a mechanism for improved exfoliation in these epoxy-clay nanocomposites, and we present here the results of three different ways in which the intra-gallery reaction can be promoted. These are:

(a) preconditioning of the resin-clay mixture;

(b) selection of the isothermal cure temperature;

(c) incorporation of an initiator of cationic homopolymerisation within the clay galleries.

The procedures involved in each of these protocols and the nanostructures and properties obtained are the subject of this paper.

EXPERIMENTAL

The materials used for this study are as follows. The epoxy resin was tri-glycidyl p-amino phenol, TGAP (Araldite MY0510, Huntsman Advanced Materials), with diamino diphenyl sulphone, DDS (Aradur 976-1, Huntsman Advanced Materials), as the curing agent. The organically modified clay was Nanomer I.30E (Nanocor Inc.). The initiator was a boron tri-fluoride mono-ethylamine complex, BF_3·MEA (Sigma Aldrich), which is known to be an efficient initiator for the homopolymerisation of epoxy resins [9].

For the "standard" preparation of the epoxy-clay nanocomposites, mixtures of TGAP and 2 wt% or 5 wt% MMT were first mixed mechanically for approximately 4 hours. For the preconditioning procedure, these mixtures were then stored either at room temperature (RT) or at higher temperatures (40ºC, 60ºC, 80ºC) using a thermostatic bath. After storage for selected periods of time at each temperature, the epoxy equivalent (EE) was determined by titration and the glass transition temperature, T_g, of the mixture was determined by differential scanning calorimetry (DSC). For the curing of the final nanocomposite, the

required amount of DDS was added to the TGAP/MMT mixture, according to the measured EE of the resin and to give an excess epoxy ratio (1:0.85 molar).

To incorporate the initiator into the system, BF_3·MEA and MMT were first mixed together in various proportions (to give 0.5 wt% and 1 wt% for BF_3·MEA, and 2 and 5 wt% for MMT, both with respect to the TGAP content in the final nanocomposite) using acetone as a solvent, which was subsequently removed by evaporation at room temperature over a period of about one day. The resulting mixture, ground to a fine powder, was then dispersed in the TGAP by high shear mechanical mixing (Polytron, PT1200C, Kinematica AG) at room temperature. This TGAP/MMT/BF_3·MEA mixture was then heated on a hot-plate to 80ºC and the DDS was added.

All samples were degassed under vacuum at room temperature for 10-15 minutes before scanning them in the DSC. The calorimetric experiments were carried out using a conventional DSC (DSC821e, Mettler-Toledo) with a flow of dry nitrogen gas at 50 mL/min.

The impact tests were performed using a Zwick Izod impact tester 5110 according to ASTM D4508-05 (2008) on rectangular samples, 25 × 12 × 2.5 mm, with a hammer of energy 0.545 J.

The nanostructure of the cured samples was observed by Transmission Electron Microscopy (TEM) on ultra-microtomed sections using a Jeol JeM-2010 high resolution transmission electron microscope. The fracture surfaces of the impact samples were observed using a Scanning Electron Microscope (SEM, Jeol 5610).

RESULTS AND DISCUSSION

Preconditioned samples

Samples of TGAP/MMT/DDS prepared according to the standard procedure described above and then cured isothermally display two peaks in the DSC curves, as shown in Figure

1. The first peak, which is very rapid, is assigned to the intra-gallery homopolymerisation reaction of the epoxy resin catalysed by the onium ion of the MMT, while the second peak is associated with the crosslinking reaction of the TGAP with the DDS. The reason why the first peak can be assigned to the intra-gallery reaction is evident when the cure curve for the preconditioned sample is compared, as shown also in Figure 1. Here it can be seen that the effect of preconditioning, in this case for 112 days at RT, is to eliminate the first peak and reduce the heat of reaction, measured as the area under the cure curve. This is because a homopolymerisation reaction occurs within the clay galleries during the preconditioning process, in which both the EE and the T_g of the mixture increase [6, 7]. Consequently, for preconditioned samples no further intra-gallery reaction will occur when the DDS is added and the sample is cured isothermally at 150ºC, and the heat of reaction will be reduced because some epoxy groups will have already reacted during preconditioning.

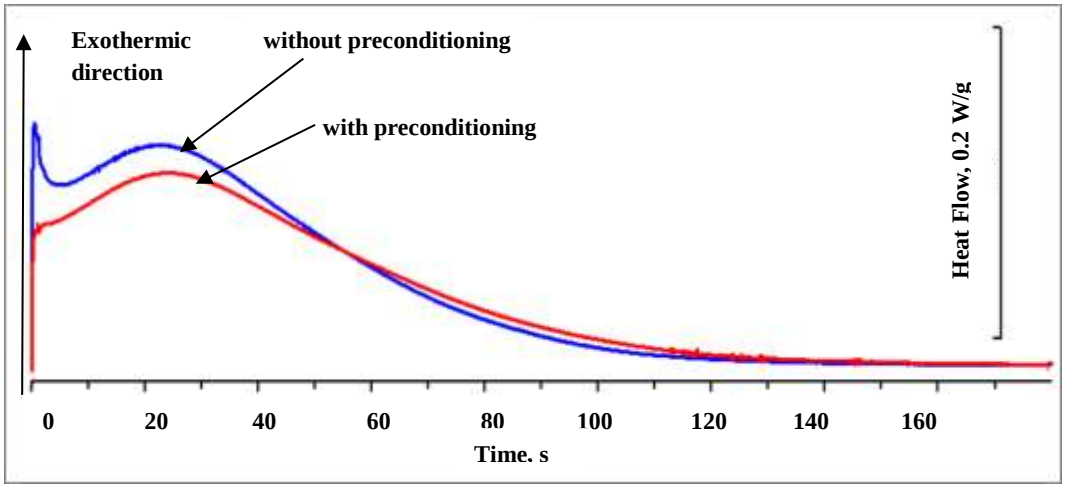

Figure 1. Isothermal cure of TGAP/MMT (5 wt%)/DDS at 150ºC, with and without preconditioning, as indicated.

The occurrence of the intra-gallery reaction before the crosslinking reaction is important for exfoliation. It is clear, therefore, that preconditioning the TGAP-clay mixture before adding

the curing agent helps to promote the intra-gallery reaction and hence should be beneficial for exfoliation. TEM images show that the preconditioning procedure does indeed improve the final nanostructure by producing a greater layer separation and a more random dispersion of the clay layers, as illustrated in Figure 2.

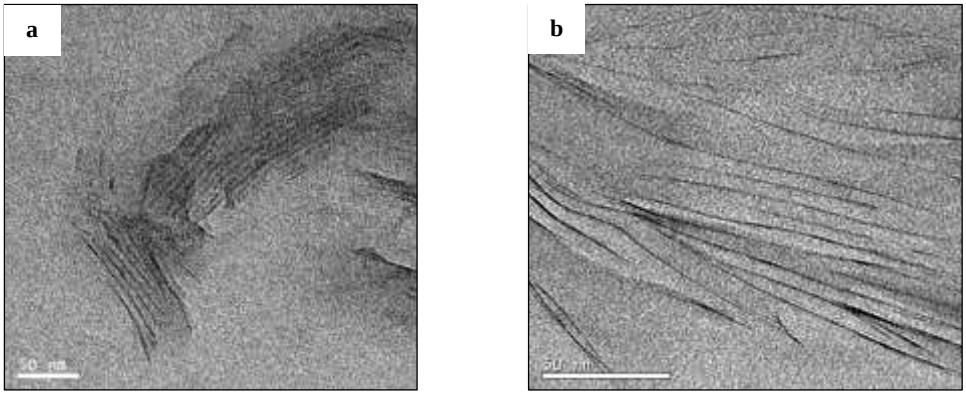

Figure 2. TEM micrographs of cured TGAP/MMT(5 wt%)/DDS nanocomposites: (a) without preconditioning; (b) with preconditioning (scale bar is 50 nm in each case).

Isothermal cure temperature

The effect of the isothermal cure temperature for TGAP/MMT/DDS mixtures prepared by the standard method has been investigated, and is illustrated in Figure 3. It can be seen that, in each case, there is a very rapid first (intra-gallery) reaction, followed by the broader bell-shaped peak corresponding to the crosslinking reaction. As the isothermal cure temperature increases, the crosslinking reaction moves to shorter times, as expected, while the magnitude of the intra-gallery reaction increases. This latter effect can be quantified by deconvolution of the overall curve into two peaks and determining the area under the first peak, which corresponds to the amount of homopolymerisation reaction that has taken place [10]. For example, for the samples and cure schedules in Figure 3, the approximate extent of reaction

within the clay galleries at the different cure temperatures is as follows: 33% at 150ºC, 50% at 165ºC, and 76% at 180ºC.

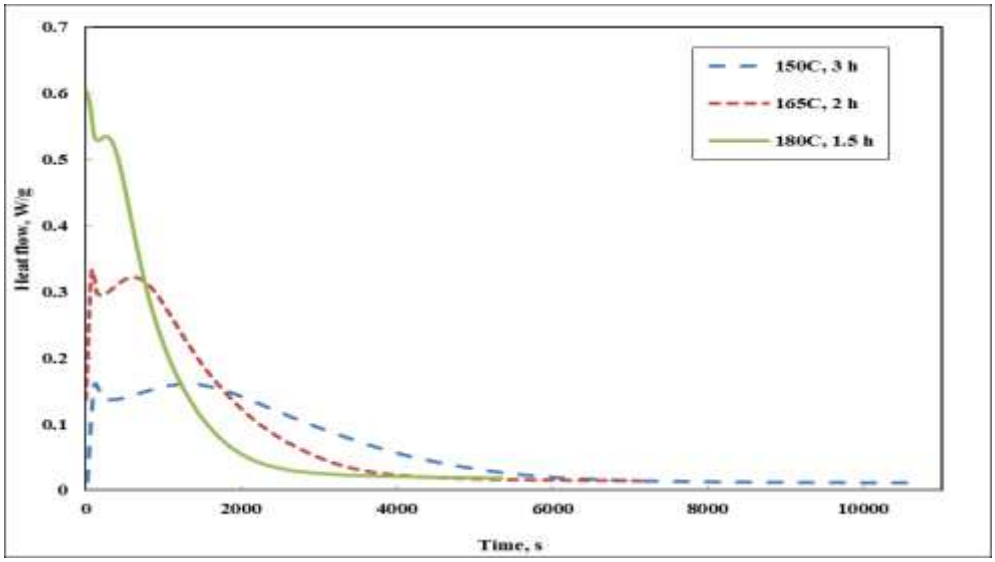

Figure 3. DSC scans for a TGAP/MMT(5 wt%)/DDS mixture prepared by the standard procedure and cured isothermally at the temperatures indicated.

The greater extent of the homopolymerisation reaction that takes place at the higher cure temperature would imply that a greater degree of exfoliation would be expected for cure at 180ºC in comparison with cure at 120ºC. This is indeed the case, as illustrated in Figure 4, where the TEM micrographs show significantly greater layer separations for the higher cure temperature. The same effect was observed by Becker et al [11] for both DGEBA- and TGAP-based nanocomposites.

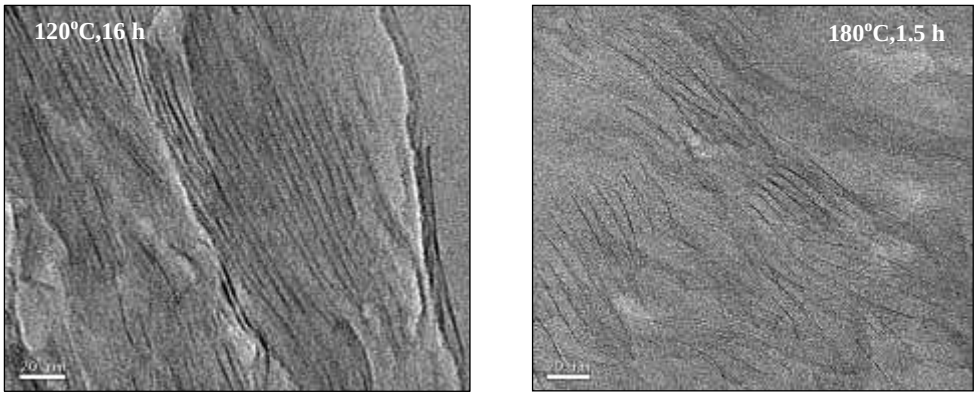

Figure 4. TEM images for TGAP/MMT(5 wt%)/DDS nanocomposites cured isothermally at the different temperatures indicated (scale bar is 20 nm in each case).

Initiator of cationic homopolymerisation

The intra-gallery homopolymerisation reaction can also be promoted by the inclusion of BF_3·MEA as an initiator within the clay galleries. Firstly, the BF_3·MEA is intercalated into the clay galleries by the procedure described earlier. The presence of the BF_3·MEA within the clay galleries is verified by SAXS, which in fact shows that the *d*-spacing decreases, from 2.1 nm for the organically modified MMT to 1.3 nm, which is attributed to the interchange of the mono-ethylamine of the BF_3 complex with the octadecyl ammonium salt of the MMT. This should be compared with an increase in the *d*-spacing to 3.5 nm when the TGAP is intercalated into the MMT [8].

The curing agent, DDS, is then added and the system is cured. Here, the cure schedule must be selected carefully in order to separate the two reactions: the intra-gallery homopolymerisation reaction, now initiated by the BF_3·MEA, and the extra-gallery crosslinking reaction with the DDS. This involves a two-stage schedule. First, the system is cured isothermally at a relatively low temperature, 100ºC or 110ºC, during which the intra-gallery reaction proceeds, allowing the clay layers to separate without any significant crosslinking occurring in the extra-gallery regions. This is followed by an isothermal post-cure at a higher temperature to allow the crosslinking reaction to proceed.

An illustration of the effect of this procedure on the nanostructure can be seen in Figure 5. Here, TEM images at low magnification are shown in order to demonstrate how the incorporation of the BF_3·MEA into the system results in a significantly better dispersion of the clay in the matrix of epoxy resin. Only a single aggregate can be seen in Figure 5a for the sample with initiator, whereas several agglomerations, often somewhat larger, can be seen for the other samples in Figures 5b and 5c.

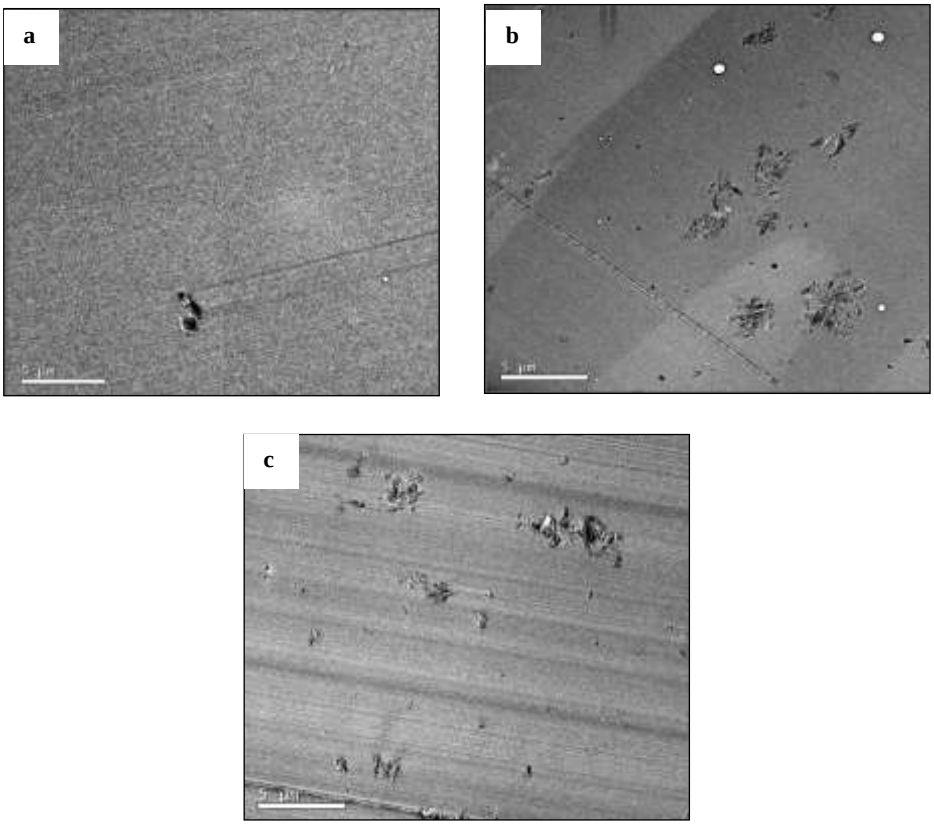

Figure 5. Comparison of TEM micrographs at low magnification for TGAP/MMT(5 wt%)/DDS samples, with and without BF3•MEA initiator: (a) sample with 1 wt% BF3•MEA, cured at 100ºC for 2.5 h, post-cured at 150ºC for 2 h; (b) sample without initiator, cured at 180ºC for 1.5 h; (c) sample without initiator, pre- conditioned at RT for 112 days then cured at 150ºC for 3 h (scale bar is 5 µm for all images).

The low magnification TEM images in Figure 5 serve to illustrate the improved dispersion of the clay when the procedure involving the BF_3·MEA initiator is used. Nevertheless, within the small agglomeration of Figure 5a, for example, there still remains some layer stacking in the clay, as shown in Figure 6, though this occurs to a much smaller extent than in the other preparations. Here it is evident that there are some regions in which the *d*-spacing is as small as 1.3 nm, the spacing of the clay intercalated with BF_3·MEA before the addition of the TGAP.

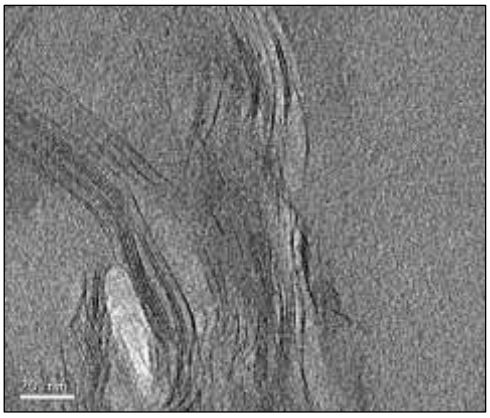

Figure 6. TEM micrograph of TGAP/MMT(5 wt%)/DDS/BF3 nanocomposite post-cured at 150ºC (scale bar is 20 nm).

Impact tests

Although it can be deduced from the TEM images shown above that these three preparation procedures lead, to a greater or lesser extent, to an enhanced degree of exfoliation in the final nanostructure of the cured nanocomposite, these images each nevertheless represent only a small selected part of the overall nanostructure. In this respect it is interesting in addition to determine a bulk property, such as the impact strength, which is strongly dependent on the nanostructure. To this end, the effects of the preparation

procedures described above on the impact energy of cured nanocomposites with 2 wt% MMT are collected in Table 1.

Table 1. Values of the impact strength of epoxy-clay nanocomposites with 2 wt% MMT

Formulation	Impact strength, kJ/m^2	Standard deviation
Reference	1.40	±0.18
TGAP/MMT/DDS, 150ºC	1.60	±0.20
TGAP/MMT/DDS, 180ºC	1.70	±0.38
TGAP/MMT/DDS, preconditioned at 40ºC	2.10	±0.33
TGAP/MMT/DDS/BF_3(0.5 wt%)	2.34	±0.24

The reference material is TGAP cured with DDS without any clay reinforcement; it is evident that the addition of clay increases the impact strength for all the preparation methods used, but that the increase is greater for some than for others. For the standard preparation, isothermal cure at 180ºC increases the impact strength slightly more than does isothermal cure at 150ºC, as anticipated from both the DSC and TEM results, the former showing that more intra-gallery reaction occurs (ref. Figure 3) while the latter shows that the *d*-spacing is greater (ref. Figure 4) the higher is the isothermal cure temperature. An even greater increase in the impact energy, 50% relative to the reference, is obtained when the TGAP/MMT mixture is preconditioned, in this case for 56 days at 40ºC, before curing with the addition of the DDS. This procedure ensures an extensive amount of intra-gallery reaction, which leads to an improved degree of exfoliation (ref. Figure 2), in accordance with these impact results. The greatest increase in impact energy, by nearly 70% relative to the reference, is afforded by the procedure involving the incorporation of BF_3·MEA, in this case in a proportion of 0.5 wt%, into the clay galleries. This procedure promotes the intra-gallery reaction, which was shown to lead to fewer and smaller aggregates in the cured nanocomposite (ref. Figure 5), in accordance with these impact results.

The fracture surfaces after impact, for the same samples as those for which the impact energies were presented in Table 1, have been observed by SEM, and the results are shown in Figure 7 at a magnification of ×50. The reference sample, TGAP/DDS without any clay (Figure 7a), shows the typical rather brittle fracture surface, with only a few striations where the crack velocity has increased. The amount of striations in Figure 7b, for the TGAP/MMT/DDS sample cured isothermally at 150ºC, is significantly greater, and the characteristic parabolic shape associated with the divergence of the crack from one plane to another can be seen. The overall appearance, though, is of an essentially planar fracture in both Figures 7a and 7b. On the other hand, the fracture surfaces seen in Figures 7c and 7d, for the preconditioned sample and the sample in which the BF_3·MEA initiator was used, respectively, both show a generally much rougher surface. This is consistent with the significantly higher values of impact energy listed in Table 1 for these samples.

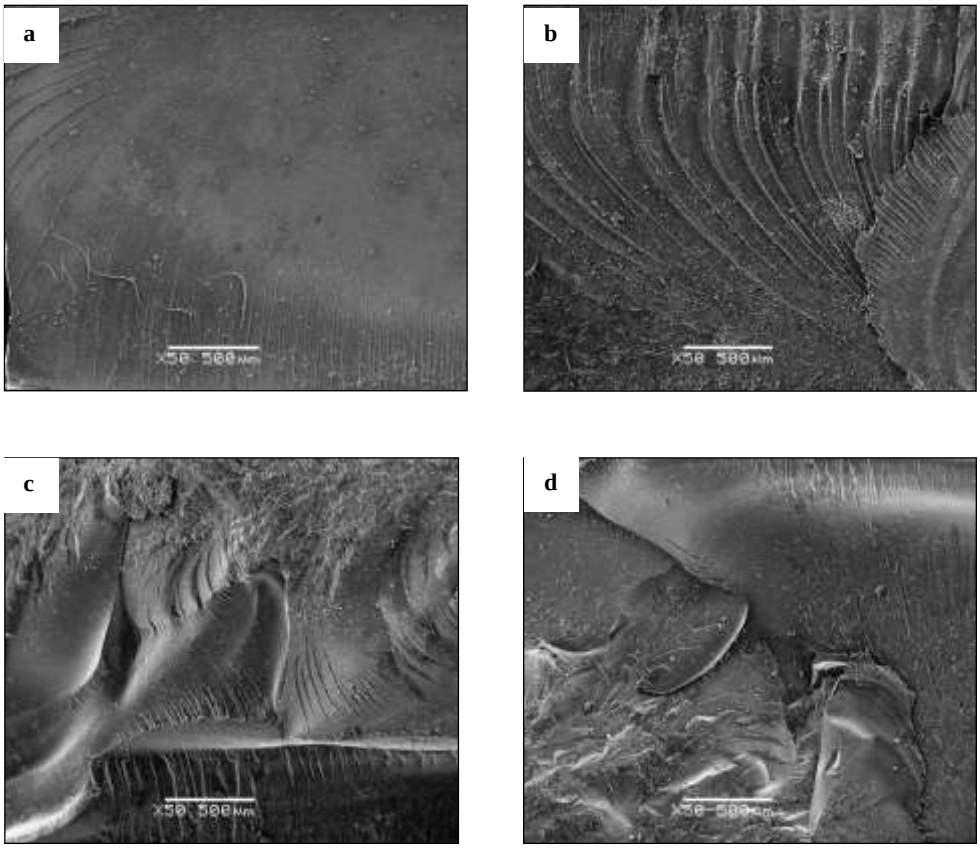

Figure 7. SEM micrographs of the fracture surfaces of 2 wt% MMT nanocomposite samples after impact testing: (a) reference, TGAP/DDS without any clay; (b) TGAP/MMT/DDS cured at 150ºC; (c) TGAP/MMT/DDS preconditioned 56 days at 40ºC; (d) TGAP/MMT/DDS/BF3 (scale bar is 500 μm in all cases).

CONCLUSIONS

The effect on the nanostructure and properties of three different preparation procedures for the fabrication of polymer layered silicate (PLS) nanocomposites based upon a tri-functional epoxy, TGAP, has been investigated: preconditioning of the resin-clay mixture before curing; isothermal cure at different temperatures; incorporating an initiator of cationic homopolymerisation into the clay galleries before intercalation of the epoxy resin and curing. All these procedures promote the occurrence of the homopolymerisation reaction within the clay galleries, which occurs before the bulk crosslinking reaction, and which hence leads to improved exfoliation. The improved nanostructure is observed by TEM and results also in an increase in the impact energy of the cured nanocomposites. The most effective procedure is to incorporate the initiator, a BF_3·MEA complex, into the clay galleries, and represents an important protocol for the achievement of highly exfoliated PLS nanocomposites.

ACKNOWLEDGEMENTS

This work was supported by MINECO Project MAT2011-27039-C03. The authors are grateful to Huntsman Corporation for the epoxy resin and curing agent, and to Nanocor Inc. for the organically modified clay. FS is grateful for a grant from the Agència de Gestió d'Ajuts Universitaris i de Recerca (AGAUR), FI-DGR 2011. We are grateful to the Universitat Rovira i Virgili for providing the facilities for the impact tests.

REFERENCES

[1] Kojima Y., Usuki A., Kawasumi M., Okada A., Kurauchi T., Kamigaito O.: J. Polymer Sci. Part A Polym. Chem. 1993, **31**, 983.

[2] Alexandre M., Dubois P.: Mat. Sci. Eng. 2000, **28**, 1.

[3] Kornmann X., Lindberg H., Berglund L.A.: Polymer 2001, **42**, 4493.

[4] Chin I-J., Thurn-Albrecht T., Kim H-C., Russell T.P., Wang J.: Polymer 2001, **42**, 5947.

[5] Montserrat S., Román F., Hutchinson J.M., Campos L.: J. Appl. Polym. Sci. 2008, **108**, 923.

[6] Benson Tolle T., Anderson D.P.: J. Appl. Polym. Sci. 2004, **91**, 89.

[7] Pustkova P., Hutchinson J.M., Román F., Montserrat S.: J. Appl. Polym. Sci. 2009, **114**, 1040.

[8] Hutchinson J.M., Shiravand F., Calventus Y.: J. Appl. Polym. Sci. 2013, **128**, 2961.

[9] Matejka L., Chabanne P., Tighzert L., Pascault J.P.: J. Polymer Sci. Part A Polym. Chem. 1994, **32**, 1447.

[10] Shiravand F., Hutchinson J.M., Calventus Y.: Polym. Eng. Sci. 2013, DOI#23540

[11] Becker O., Cheng Y-B., Varley R.J., Simon G.P.: Macromolecules 2003, **36**, 1616.

Paper VIII

Thermal analysis of polymer layered silicate nanocomposites: identification of nanostructure development by DSC

J.M. Hutchinson, F. Shiravand, I. Fraga, P. Cortés, Y. Calventus

Journal of Thermal Analysis and Calorimetry, 2014

DOI: 10.1007/s10973-014-3709-3

Appendix A

Study of the effects of different silicate layered clays on thermal properties and final nanostructure of trifunctional epoxy nanocomposites

F. Shiravand, J.M. Hutchinson, Y. Calventus

To be prepared, 2014

Sample preparation

First, TGAP and clays were mixed together by mechanical mixing at about 300 rpm at 5 wt% clay for comparative purposes with respect to TGAP weight for period of 3 H. Then the curing agent, DDS, in a proportion of 52 wt% with respect to the epoxy resin equivalency, as excess epoxy ratio which recommended by the resin manufacturer, were added to TGAP/clay mixture. The mixture was finally degassed under vacuum at room temperature. Then the calorimetric experiments were carried by using conventional differential scanning calorimeter (DSC).

Study the TGAP/clay mixture behaviour

Table 1 shows the basal spacing of three different types of silicate layered clay; Nanomer I.30 (MMT), Cloisite 30B and Nanofil SE 3000. These values were determined from the diffraction peak in the SAXS pattern. Though these clays have different *d*-spacing, they have same *d*- pacing which is about 3.54 nm when the TGAP intercalated into their galleries.

Table 3: Values of the *d*-spacing that were obtained from the SAXS patterns for different silicate layered clays

Clay type	Peak degree: 2θ,°	*d*-spacing, nm
Nanomer I.30	$2\theta = 4.2°$	d= 2.1 nm
Cloisite 30B	$2\theta = 4.75°$	d= 1.86 nm
Nanofil SE 3000	$2\theta = \begin{cases} 2.55° \\ 4.75° \\ 7.125° \end{cases}$	$d = \begin{cases} 3.45\ nm \\ 3.74\ nm \\ 3.72\ nm \end{cases} \longrightarrow d_{ave} = 3.6\ nm$

Before study the cure behaviour of the TGAP/DDS system in the present of these clays, it is better that study the effects on these clays on the TGAP before adding any curing agent. So TGA/DSC technique was used. During non-isothermal scan of these mixtures, one peak appears at high temperature. The peak temperature of this peak for Closite and Nanofil is around the same value as pure TGAP which is about 330^{o}C. Hence, this peak is attributed to the thermally accelerated TGAP homopolymerisation. Whereas the peak temperature of about 300^{o}C for the Nanomer mixture implied that the anion ion in the clay structure is capable to initiate the TGAP homopolymerisation in less temperature and make TGAP more stable. This fact affects on the thermal resistance of TGAP. As shown in Figure 1, the highest and lowest decomposition temperatures are associated to the TGAP/MMT mixture and pure

TGAP, respectively. And the thermal resistance of the TGAP with Cloisite and Nanofil is laid between these two thresholds; TGAP/MMT mixture and pure TGAP which TGAP/Cloisite decomposed in higher temperature than TGAP/Nanofil.

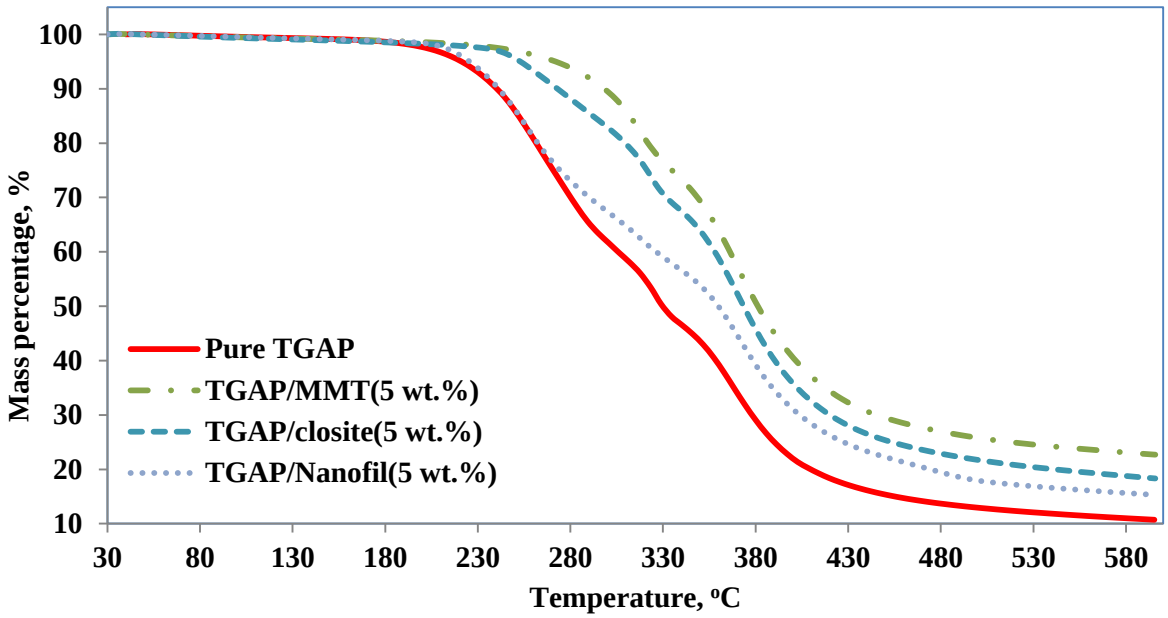

Figure 1. TGA thermograph of the mixture of the TGAP with three types of the clay with 5 wt %

In respect of the exfoliation, the quality of clay dispersion is important which influences on the final nanostructure. Therefore, two procedures can be considered, the first one is studying the size, number and distribution of the clay agglomeration and the second one is following the clay dispersion during the pre-conditioning procedure by means of the optical microscopy. Figure 2 shows that the best quality of the clay dispersion belongs to the Nanofil which dispersed through the bulk of the sample and the poorest dispersion is found when use the Nanomer that can detect the visible area of the resin without clay. In addition, by tracing the dispersion behaviour of clay, it can be understood that the Nanofil dispersion which is initially the best deteriorates with pre- conditiong process at all temperature. Likewise, the Cloisite dispersion also improved at all temperature but not to the same extent as for Nanomer. It is also noted that the glass transition and epoxy equivalent varied with pre-conditiong time as the same trend as Nanomer but not rapidly.

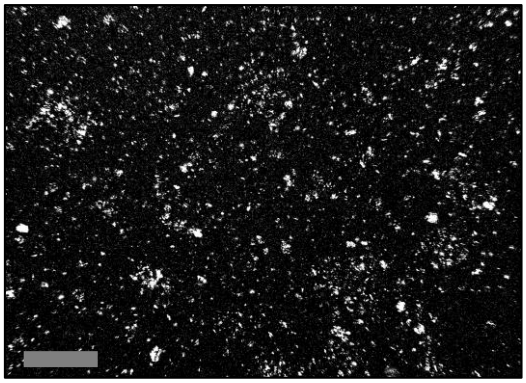

TGAP/Cloisite 30B (5 wt %)

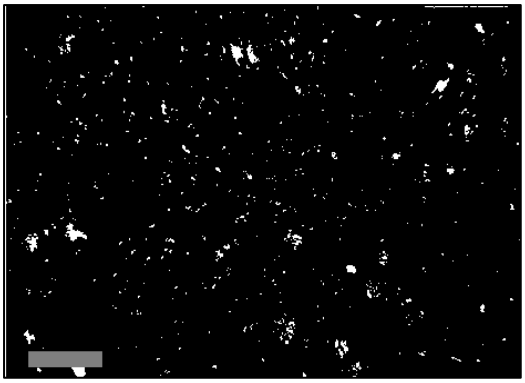

TGAP/Nanomer I.30 (5 wt %)

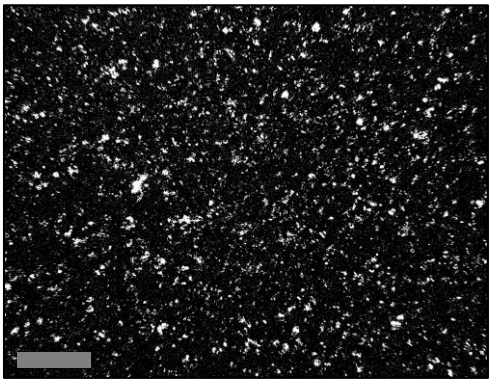

TGAP/Nanofil SE 3000(5 wt %)

Figure 2. Optical microscopy images of clay dispersion in the epoxy resin after 3 H mechanical mixing. Scale bar is 100μm.

Study the TGAP/DDS/Clay system

Figure 3 shows the isothermal cure behaviour of these TGAP/clay mixtures at 165^{o}C for 2 H. For the TGAP/Nanomer system, clearly can be detect two peaks that the 1st peak is referred to the intra-gallery reaction that immediately followed by the 2nd peak which is ascribed to the cross-linking reaction. in contrast, at same isothermal cure ,165^{o}C, neither the TGAP/Cloisite nor the TGAP/Nanofil system shows such first peak and just displays the broads bell peak which is attributed to the extra-gallery reaction; cross-linking reaction. As expected from the previous results, the Cloisite and Nanofil cannot afford to initiate the intra-gallery reaction namely TGAP homopolymerisation neither in high cure temperature like 180^{o}C or high clay loading like 10 wt %.

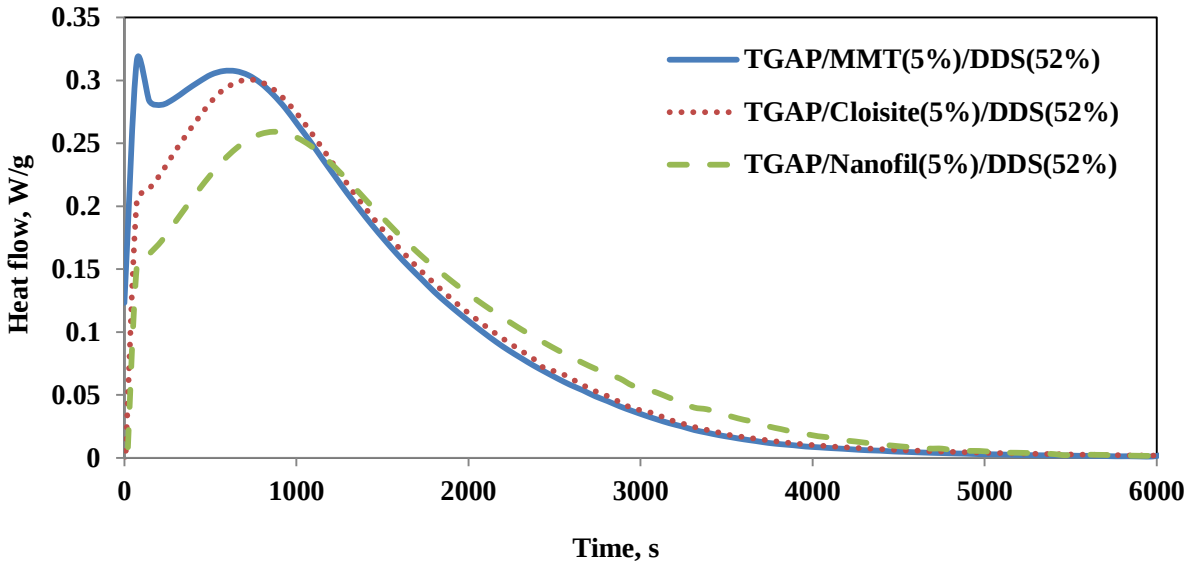

Figure 3. Isothermal DSC scan at 165°C for 2 H for three different type clay in TGAP/clay (5 wt %)/DDS (52 wt%) system.

Moreover, Figure 4 shows that the lowest glass transition temperature and vitrification time is related to the Nanomer system due to the catalyze effects of Nanomer on TGAP homopolymerisation reaction that leads to the less cross-linked density in the final network.

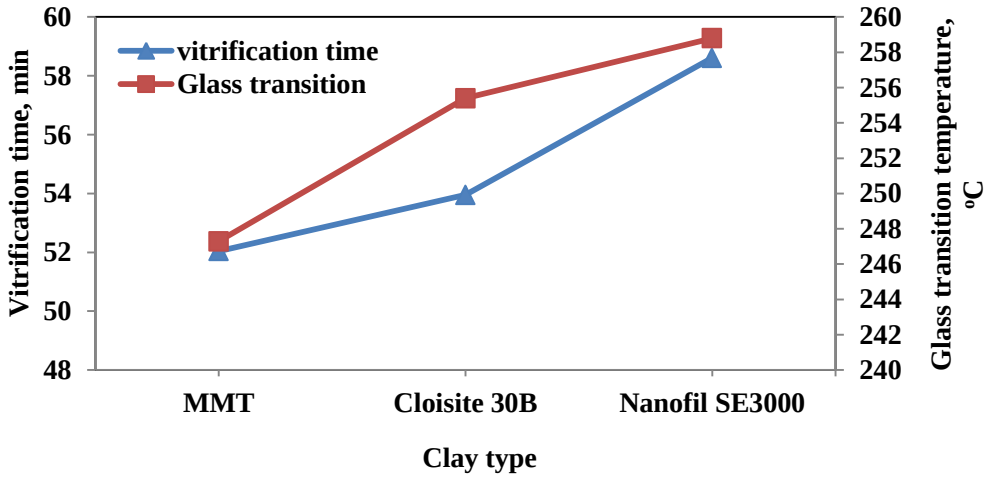

Figure 4.The glass transition temperature and the vitrification time of the three different epoxy nanocomposites as followed: TGAP/MMT (5 wt %) /DDS (52 wt %), TGAP/Cloisite (5 wt %) /DDS (52 wt %) and TGAP/Nanofil (5 wt %) /DDS (52 wt %) that cured isothermally at 165°C for 2 H versus clay types.

As results, we expect that the final nanostructure of the Nanomer appears to be exfoliated relative to the Cloisite and Nanofil systems. So the nanostructure for these systems is examined by the SAXS. The SAXS pattern, Figure 5, displays the small shoulder around 2.53°, which is corresponding to about 3.5 nm *d*-spacing, for the Cloisite and Nanofil systems

and no peaks appears for the Nanomer system between 1.15 nm to 8 nm. These results imply that for the Nanomer system, there is no regular layer stacking in nanostructure. As expected, the Nanomer system shows improvement in the degree of exfoliation due to the intra-gallery homopolymerisation occurs before the extra- gallery reaction so there is enough time to increase the clay basal spacing before the matrix became rigid and highly cross-linked that was confirmed by SAXS.

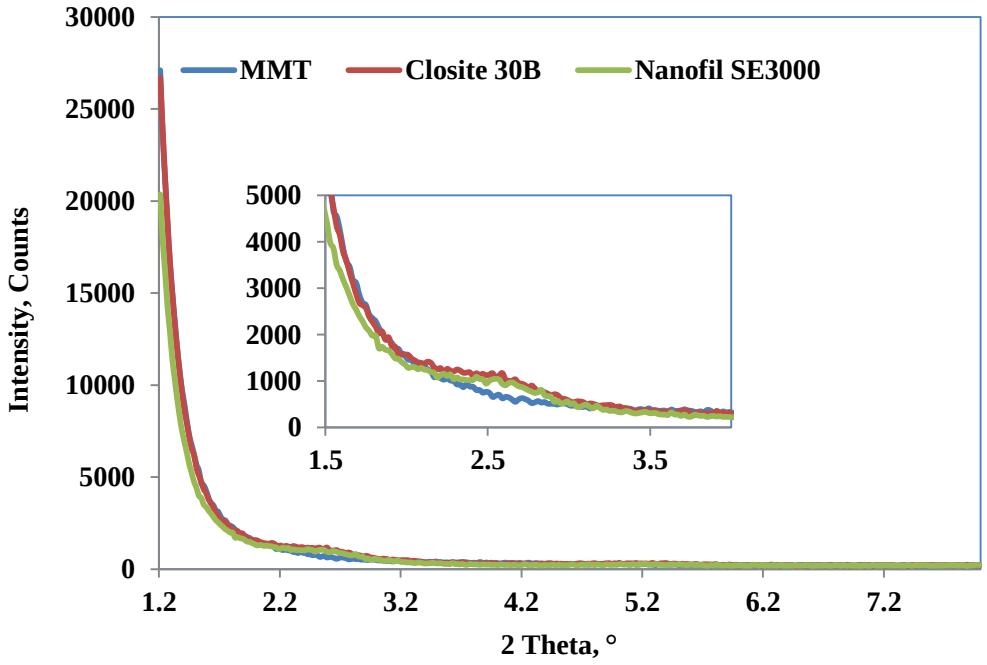

Figure 5. SAXS pattern for the three different nanocomposites as follow: TGAP/DDS(52 wt %)/MMT(5 wt %), TGAP/DDS(52 wt %)/Cloisite (5 wt %) and TGAP/DDS(52 wt %)/Nanofil(5 wt%) which cured isothermslly at 165°C for 2 H

Conclusion

The Nanomer presents the best possibilities for achieving a highly exfoliated epoxy-clay nanocomposite rather than the Cloisite and Nanofil because of two reasons as follow: the dispersion of Nanomer in resin with pre-conditioning procedure improves and the first rapid peak as intra-gallery reaction appears before the cross-linking reaction during the isothermal curing process which is necessary to promote exfoliation that is in accord with the SAXS pattern. Therefore, it can be concluded that the increment of exfoliation degree depends on the type of clay in TGAP based nanocomposites that leads to detectable peak as intra-gallery reaction in DSC scan.

Appendix B

Study of the cure behaviour of tri-functional epoxy/hyperbranched polyethylenemine nanocomposites

F. Shiravand, J.M Hutchinson, Y. Calventus

To be prepared, 2014

TGAP/Lupasol mixtures preparation

The TGAP and Lupasol were mixed in various proportions (a) stoichiometric composition (epoxy: Lupasol mass ratio 1:0.372, molar ratio 1:1); (b) excess epoxy composition (epoxy: Lupasol mass ratio 1:0.316, molar ratio 1:0.850); (c) excess Lupasol composition (epoxy: Lupasol mass ratio 1:0.441, molar ratio 1:1.185). These mixtures were prepared by mixing the TGAP and Lupasol together in an ice bath at 0°C to prevent any polymerisation from occurring in this highly reactive system before taking small samples for studying the curing process in the calorimeter. It is note that just the excess lupasol composition was used for the isothermal experiments.

Study the cure behaviour

The TGAP/Lupasol system, without any clay, exhibits two peaks during the non- isothermal cure process, with characteristics which depend on the composition of the mixture: excess epoxy, stoichiometric ratio or excess Lupasol. Typical results are shown in Figure 1 for DSC scans over the temperature range from 0ºC to 290ºC at 5ºC/min for each of these compositions. The two peaks which are well separated in the temperature scale since the 1^{st} peak occurs in low temperature at about 90^{o}C and being about same magnitude for excess Lupasol and excess epoxy composition and the other one (2^{nd} peak) occurs just more than 250^{o}C which is particularly depended on the composition. On the other hand, the stoichiometric composition shows the slightly smaller 1^{st} peak at the same temperature of about 90^{o}C, but a much larger 2^{nd} peak at higher temperature of about 310^{o}C.

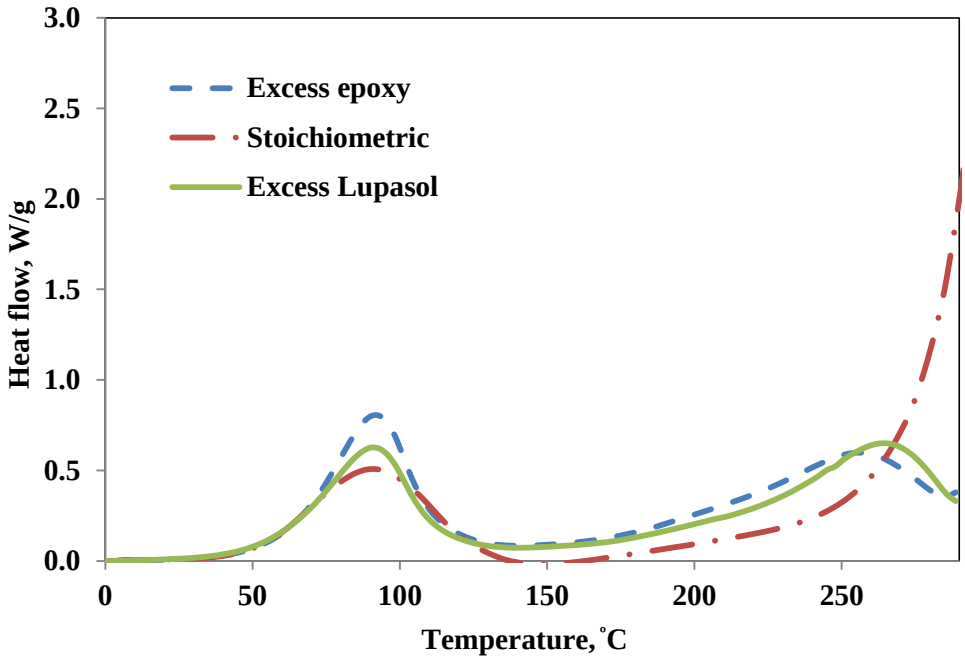

Figure 1. Non-isothermal scans from 0ºC to 290ºC at 5ºC/min for the TGAP/Lupasol system with different compositions

Although, for distinguishing the identification of these two peaks, some further information are required but the early assumption based on the Lupasol structure is considered as following:

- The 1st peak, which occurred in low temperature, is nominated as the cross-linking reaction between the primary amines in Lupasol structure and epoxy groups and peak temperature is essentially constant for all the Lupasol compositions and varying only slightly in intensity.
- The 2nd peak, which occurred in high temperature, is due to the TGAP homopolymerisation which accelerated by tertiary amines which is embedded in the Lupasol molecule structure and also occurs in approximately the same temperature range as the homopolymerisation reaction in the TGAP/DDS system.

In terms of confirming these interpretations, we obtain these data; firstly, the glass transition temperature of different TGAP/Lupasol composition, as shown in Figure 1, which is obtained from the 2nd scan of DSC is roughly around 140°C that shows the system is less cross-linked and also, implies that the network structure would be different in contrast of the our earlier work which is related to the curing of TGAP with DDS. Secondly, the heat of reaction for the

1st peak is roughly 40kJ/ee except the system with stoichiometric ratio which is about 21kJ/ee so it can be concluded that this system has low cross-link density structure which leads to reduction in glass transition temperature. Therefore, the first assumption which associated the 1st peak to cross-linking reaction is indeed correct.

In order to distinguish the 2nd peak identification, it is useful to study the effect of initiator like 1MI (1- methylimidazole, 99%, Acros Organics) on this system as tertiary amine agent, which is accelerated the homopolymerisation reaction. It can be found that the addition of 3 wt% 1MI to the TGAP leads to occur the all TGAP homopolymerisation at lower temperature about 143°C when the system heated non-isothermally at 10°C/min heating rate. As shown in the Figure 2, addition of 3 wt% 1MI to the TGAP/Lupasol system with excess Lupasol composition shifted the 2nd peak along temperature axis and has no effects on the 1st peak. It means that the 2nd peak appears as shoulder at lower temperature around 114°C. Therefore, the second peak is correctly attributed to the TGAP homopolymerisation which initiated by the tertiary amine in Lupasol structure and also, the difference in peak temperature in these two systems is due to the difference in heating rate during dynamic scan. Generally, the peak temperature during the non-isothermal cure shifted to the higher temperature by increasing the heating rate and their difference is usally between the 15-30°C.

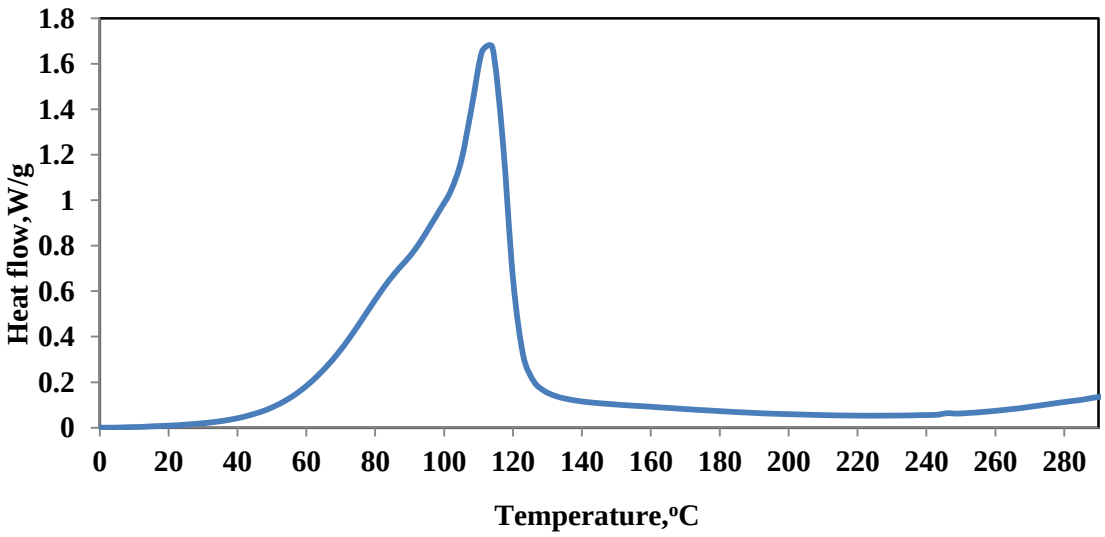

Figure 2. DSC dynamic scan of the TGAP/Lupasol (44.1%) /IM (3%) from 0-290°C with 5 °C/min heating rate

Another issue which is highlighted here, the tertiary amine in 1MI structure is more activated than the tertiary amine in Lupasol structure so 1MI provides an alternative reaction

pathway for homopolymerisation which is different from the route that was provides by Lupasol. So, the homopolymerisation reaction in the present of the 1MI take place in lower temperature and Furthermore, different large number of the amines group; primary, secondary and tertiary amines, in Lupasol structure make the polar denteric interaction which leads to activate the tertiary amines at higher temperature as initiator for the homopolymerisation reaction.

Although, the identification of every peak is found, but the main question remains of why two widely separated peaks appear in dynamic cure. Referring to the Lupasol chemical structure, it can be understand that the Lupasol is highly branched structure and also the TGAP has nonlinear structure so the possibility of being strong molecular interaction increases between them that leads the difficulty in molecular motion. On the other hand, it seems that the restriction in mobility is the main reason for exhibiting such cure behaviour. For clarifying this idea, we tested the cure tendency of the TGAP with another curing agent that has a similar linear chemical structure of Lupasol; DETA (Diethylenetriamine, Aldrich) as shown in Figure 3. It is noted that the Lupasol is Hyperbranched polymer which is produced from repeating of this chain.

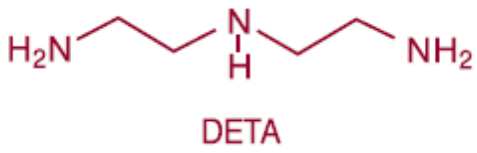

Figure 3. The chemical structure of the DETA (Diethylenetriamine)

The dynamic cure scan of the TGAP/DETA with stoichiometric ratio of the curing agent (mass ratio TGAP: DETA, 1:0.206) displays only the single peak with 91 kJ/ee as the heat of reaction as shown in Figure 4. Moreover, Santiago et al [Thermochimica Acta, 526, pp. 9-21, 2011] reported only one peak appeared during the non-isothermal cure of the DGEBA, either with DETA or Lupasol which is different from what happens for TGAP system. Thus the cross-linking reaction in the TGAP/Lupasol system is inhibited by mobility restriction because of the molecular interaction of reactants; TGAP and Lupasol.

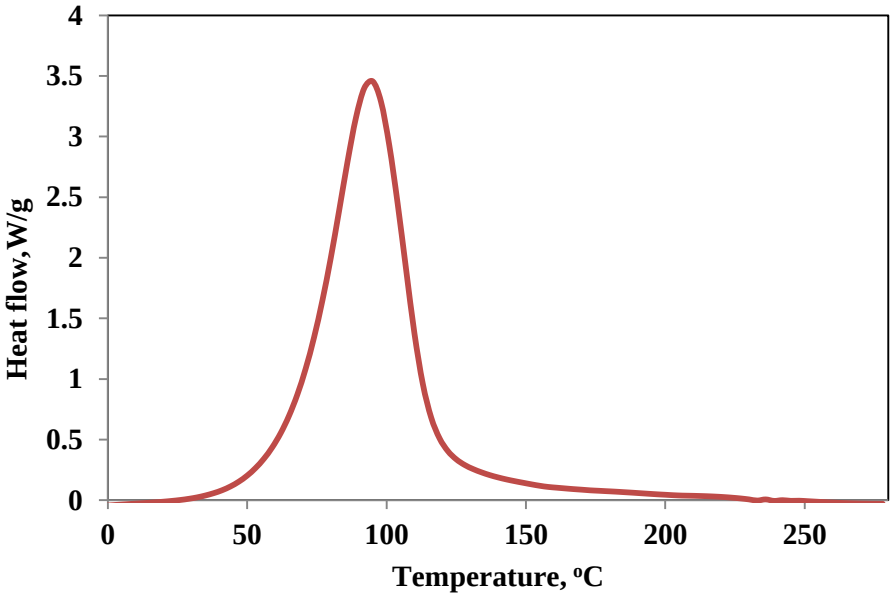

Figure 4. The DSC dynamic scan of TGAP/DETA (20.6 wt%) with heating rate of 10°C/min.

Considering these results and compare them with our previous results, non-isothermal cure of TGAP/DDS system, it can be understand that two widely separated peaks appears in the dynamic scan of TGAP/Lupasol system whereas TGAP/DDS system exhibit the composite curve which is deconvoluted into 2 peaks; cross-linking and tertiary amine catalysed homopolymerisation. This discrepancy in cure kinetic of these systems is due to use of the different hardener for curing the tri functional epoxy resin, one of them is aromatic amine; DDS, and the other one is hyperbranched polyethyleneimine, Lupasol.

Furthermore, the heat of the cross-linking reaction in excess epoxy composition for the TGAP/Lupasol system is around 40kJ/ee which is much less than the TGAP/DDS system, about 74kJ/ee. This fact indicates that the TGAP/Lupasol system cannot cross-link to the nearly the same extent as the TGAP/DDS system because of restricting in the mobility of reactants which leads to reduction in the T_g from 216^{o}C for TGAP/DDS system to 140^{o}C for TGAP/Lupasol system.

The isothermal cure experiments of the TGAP/Lupasol shows the same behaviour as non-isothermal scan. It means that the first scan shows one peak when the curing process is done at low temperature like 50, 70, 80 and 90^{o}C and in the dynamic scan after the isothermal scan, two separated peaks appears that the 1st peak at low temperature is related to the residual heat of the reaction and the 2nd peak at higher temperature is associated to the TGAP homopolymerisation which accelerated by tertiary amines. This fact shows that again the

cross-linking reaction is inhibited by mobility restriction. As results, the low heat of the reaction and glass transition temperature is also found which is attributed to the less cross-linked density of final network.

In summary, the TGAP/Lupasol cross-linking reaction occurred at the low temperature whether the system cured isothermally or non- isothermally and also the restriction in mobility does not allow that the cross-linking reaction occurred completely which leads to low heat of the reaction and glass transition temperature in both cases. In TGAP/Lupasol system, the homopolymerisation reaction which initiated by tertiary amine of lupasol structure occurs as separated peak at high temperature.

Cure behaviour of TGAP/Lupasol/MMT system

TGAP/Lupasol mixtures preparation

Two different procedures were used depending on whether the clay was mixed first with the Lupasol or with the epoxy resin based on the excess Lupasol content, as following:

- Sample I. the Lupasol and MMT were first mixed together on a hotplate at 52ºC. An elevated temperature was required because the Lupasol is very viscous at room temperature (RT), but the temperature must not exceed 80ºC as this can result in damage of the Lupasol structure. At 52ºC the viscosity of the mixture decreased and the clay was easily dispersed in the Lupasol, after that the TGAP was added to the mixture and they are mixed together in an ice bath to prevent polymerization.
- Sample II. For these samples, the TGAP and MMT were first mixed together at room temperature (RT), and then the Lupasol was added to the mixture and they are mixed together in an ice bath to prevent polymerization.

Study the cure behaviour

The results in the previous section show that the cross-linking reaction occurred at lower temperature than the homopolymerisation in this system without clay. In the other word, it cannot be seen any homopolymerisation reaction until very high temperature. Though, the addition of the clay make another possibility for occurring the homopolymerisation reaction which catalysed by the onium ion of the MMT but we show in our earlier work that the intra-gallery reaction in the TGAP/DDS/MMT system takes place at high temperature like 150^{o}C. Therefore, the cross-linking reaction occurs before the intra-gallery reaction in the TGAP/Lupasol/MMT system due to the low curing temperature of cross-linking reaction. So,

this fact does not lead to the exfoliation as the clay layers are already embedded in a relatively rigid matrix. On the other word, we believe that the isothermal DSC scan at higher temperature shows a single rapid peak that means the cross-linked network inhibited the intra-galley reaction occurs. Therefore, we expect that the final nanostructure is hardly exfoliated and we cannot reach to the acceptable exfoliation in this nanocomposite. Figure 5 presents the typical isothermal scan of the TGAP/MMT/Lupasol system at 90^{o}C.

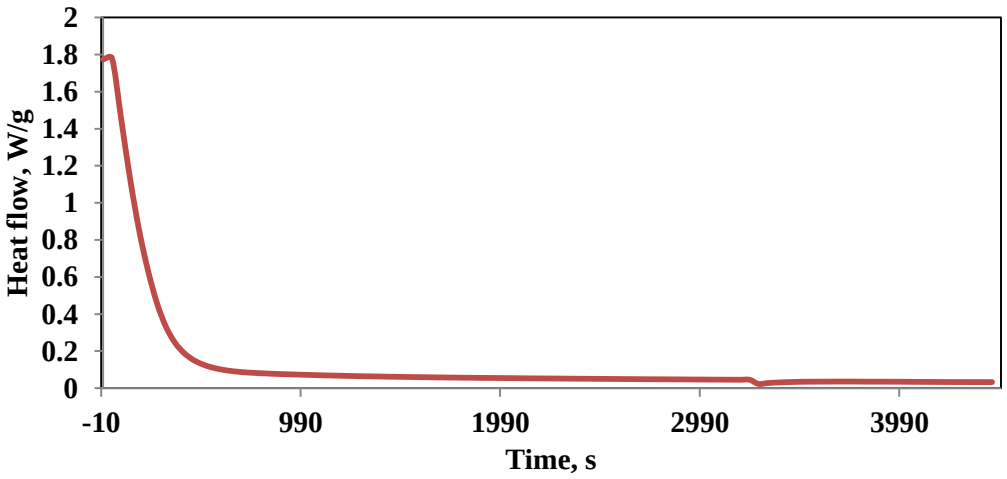

Figure 5. Isothermal scan for the [TGAP/ [MMT (5 wt %) +Lupasol (44.1wt. %)] at 90^{o}C for 75 min.

However, it is interesting to study the clay dispersion in this system so two different sample preparations are considered: sample I and Sample II. Figure 6 shows that the MMT is dispersed into the Lupasol bulk better than TGAP bulk. In the other hand, sample I shows the large number of empty areas of clay in bulk so the clay disturbed through the bulk more uniformly by using the sample I. Hence, we use the sample I preparation due to quality of clay dispersion for study the nanocomposite structure. Also, the pre-conditioning procedure leads to inversed effect on the quality of the clay dispersion which leads to increase significantly size of the clay agglomerations.

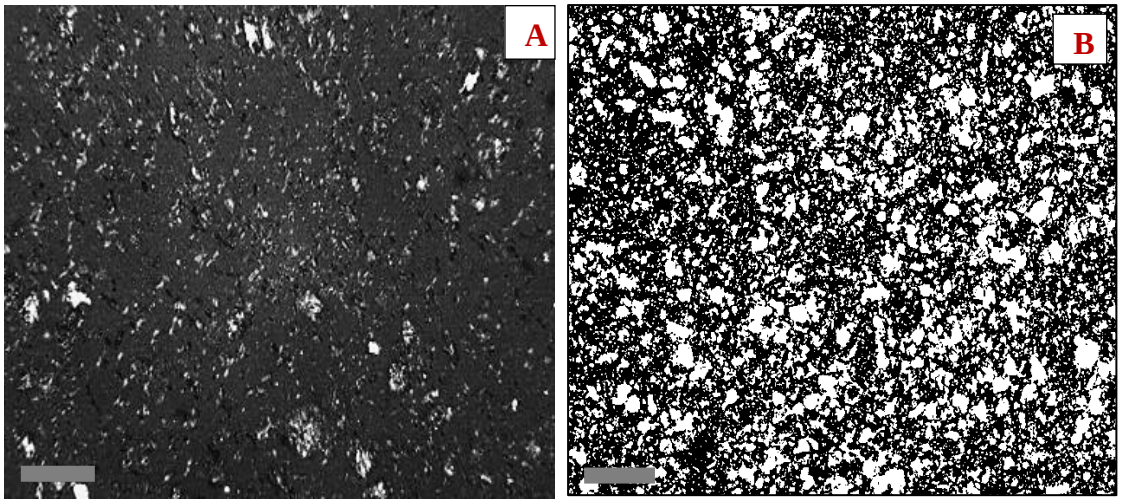

Figure 6. Optical images for: A) dispersion of 5 wt% MMT in TGAP after 3 H mixing at RT; B) dispersion of the 5 wt% MMT in Lupasol after mixing at 52ºC for 5 H. Scale bar is 100µm.

Furthermore, SAXS results show that the *d*-spacing of clay decreases from 2.1 the organically modified MMT to 1.6 nm in the intercalated state for sample I. This reduction in the *d*-spacing can probably be attributed to the interchange of the lupasol groups with the octadecyl ammonium salt of the organically modified MMT.

The nanostructure quality of the sample I studied by means of SXAS and TEM. Although, no diffraction peak can be detectable for this sample in SAXS graph for small range of 2θ which implies that there is no layer stacking with *d*-spacing less than 8 nm in nanostructure. This is not adequate evidence to display the nanostructure is exfoliated so the TEM experiment must be used to support the SAXS results. As shown in Figure 7 many big agglomerations can be observed in bulk of sample and there are hundreds clay layers with narrow *d*-spacing stick together in ordered arrangement. As results, the final nanostructure is poorly exfoliated due to the intra-gallery homopolymerisation occurs after cross-linking reaction in the matrix.

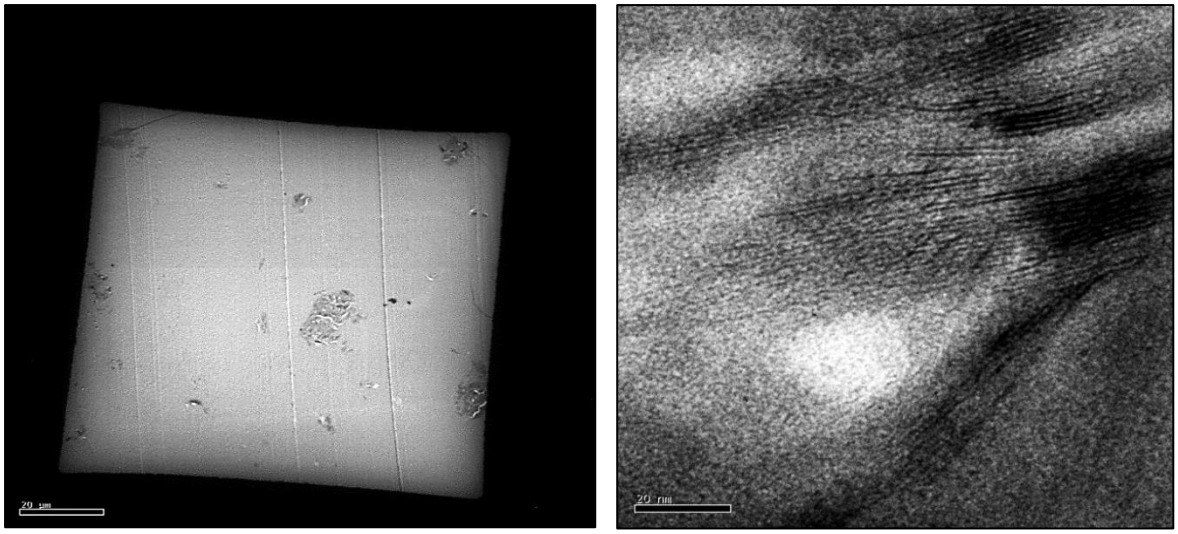

Figure 7. TEM micrographs for nanocomposite sample I with TGAP/Lupasol (44.1 wt.%)/MMT (5 wt.%) that cured isothermally at 70^{o}C for 2 H; scale bar is 20 nm.

Conclusion

In summary, during the non-isothermal scan of the TGAP/Lupasol system, two quite separated peaks exhibits; as cross-linking reaction (1st peak) in low temperature and homopolymerisation reaction (2nd peak) in high temperature which are depended on the Lupasol composition particularly 2nd peak. Also, results shows that the difficulty in molecular motion restricted the cross-linking reaction when compared the cure behaviour of this system with counterpart system TGAP/DETA. The same results are also obtained for the isothermal scan of the TGAP/Lupasol system.

Moreover, the optical microscopy images show that the Dispersion of the clay in Lupasol is better than the TGAP in spite of decreasing in the *d*-spacing about 1.6 nm. Also, TEM images show that the quality of final nanostructure is poor in respect of the exfoliation. This case came from the relative rate of the intra- gallery reaction to extra- gallery reaction. It means that the intra-gallery in this system occurs after the extra-gallery reaction that is the significant issue in terms of exfoliation process. This case leads to low degree of exfoliation in fully cured nanostructure.

Appendix C

The effect of an OH-terminated hyperbranched (polyester amide) on the cure behaviour of a the tri-functional epoxy layered silicate nanocomposite

Sample preparation

The mixtures were prepared by adding the various portions of Hybrane (5, 10, 20 wt. % HBH) into the epoxy resin then the mixtures were heated at 40oC until the Hybrane was dissolved and became clear then the nanofiller, MMT(5 wt. %) and curing agent, DDS (52 wt. %) were added to the resin-Hybrane mixture, the sample was degassed hence was ready for experiments that were carried out by using a conventional calorimeter, DSC821e (Mettler-Toledo), and a temperature modulated DSC technique, TOPEM® (DSC823e, Mettler-Toledo). All the samples cured isothermally at different temperatures, T_c (1350, 150, 165, 180^{o}C) with different cure time, t_c (6h, 3h, 2h, 1.5h, respectively).

Study the isothermal cure behaviour

Typical isothermal scan, obtained by DSC, for TGAP/Hybrane/MMT/DDS system was shown in the Figure 1. It can be found that the addition of the Hybrane to the TGAP/DDS/MMT system accelerates the epoxy-amine reaction due to the catalytic effect of hydroxyl group in the Hybrane structure so the cross-linking reaction occurs in less time in contrast the system without Hybrane. Also, Figure 1 shows that the increase in the Hybrane content up to 20 wt% leads to shift the intra-gallery reaction along time axis until completely disappeared. In the other hand, the cross-linking reaction completely overlapped the intra-gallery reaction. It means that the exfoliation process cannot take place significantly due to simultaneously occurring the intra and extra-gallery reaction. Hence, we expect the final nanocomposite is poorly exfoliated relative to the system without clay.

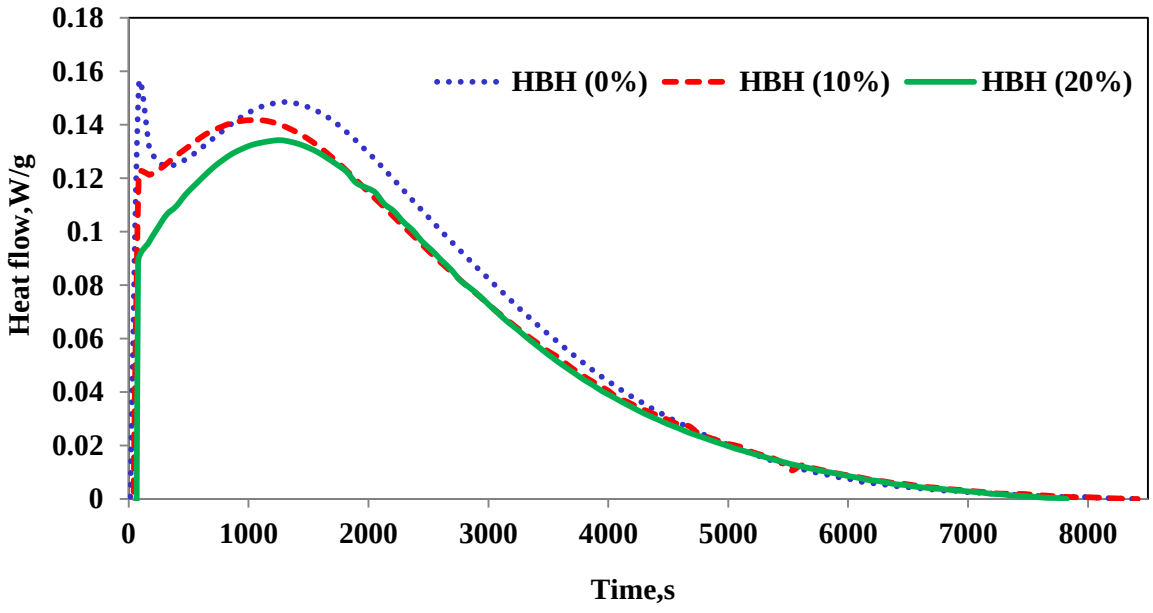

Figure 1. Isothermal DSC scan at 150°C (3 H) for three different samples: TGAP/MMT (5 wt %) /DDS, TGAP/MMT (5 wt %) /DDS/Hybrane (10 wt %), TGAP/MMT (5 wt %) /DDS/Hybrane (20 wt %)

In order to reach the same extent intra-gallery reaction as the system without the Hybrane, we incorporated the Hybrane into the clay layers with solvent such as ethanol and then the same procedure for ample preparation was done as before. As shown in the Figure 2, the magnitude of the intra-gallery reaction is the same as the system without Hybrane.

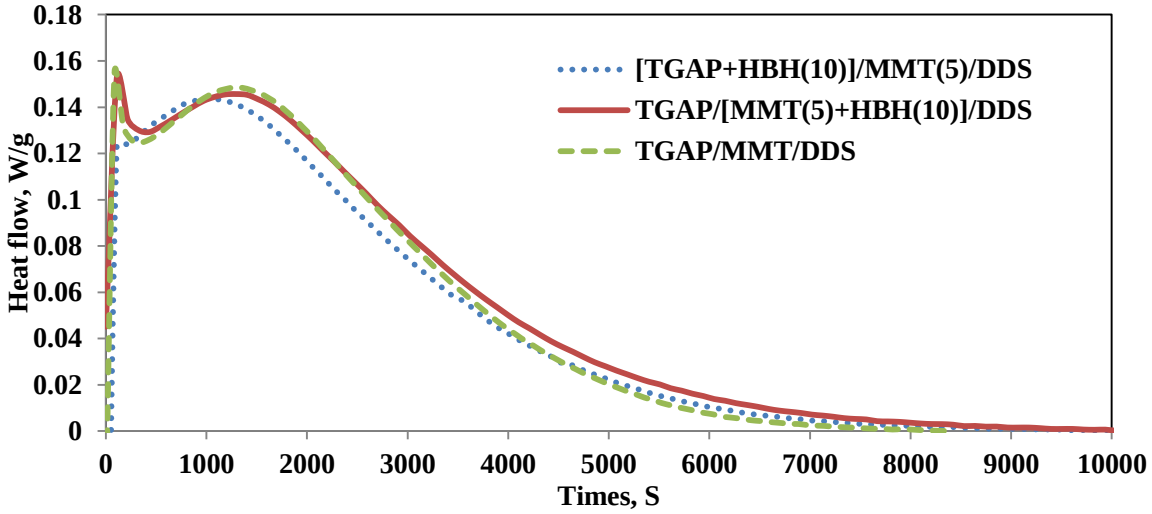

Figure 2. Isothermal scan at 150°C for 3 H of two different mixing methods for the TGAP/MMT (5 wt.%)/Hybrane (10 wt.%)/DDS system and system without Hybrane with clay content 5 wt.%.

Furthermore, it can be noticed from Figure 3a and 3 b that the magnitude of the intra-gallery reaction is depended on the cure temperature and Hybrane loading. These results are obtained from the isothermal experiments, as shown in below. It means that the area under intra-gallery reaction increases until 165°C and intra-gallery reaction completely disappears at higher temperature than 165°C and also, Hybrane loading cannot be exceeded more or less than 10 wt % due to the intra- gallery reaction. Hence, the best cure temperature and Hybrane content for obtaining the more intra-gallery reaction must be 165°C and 10 wt %, respectively. Also, the one glass transition can be detected for TGAP/[MMT+Hybrane]/DDS system that decrease to about 238.5°C due to the increase in the mobility of the network structure. The single glass transition temperature is attributed the single phase morphology for the final nanostructure which is confirmed with TEM later.

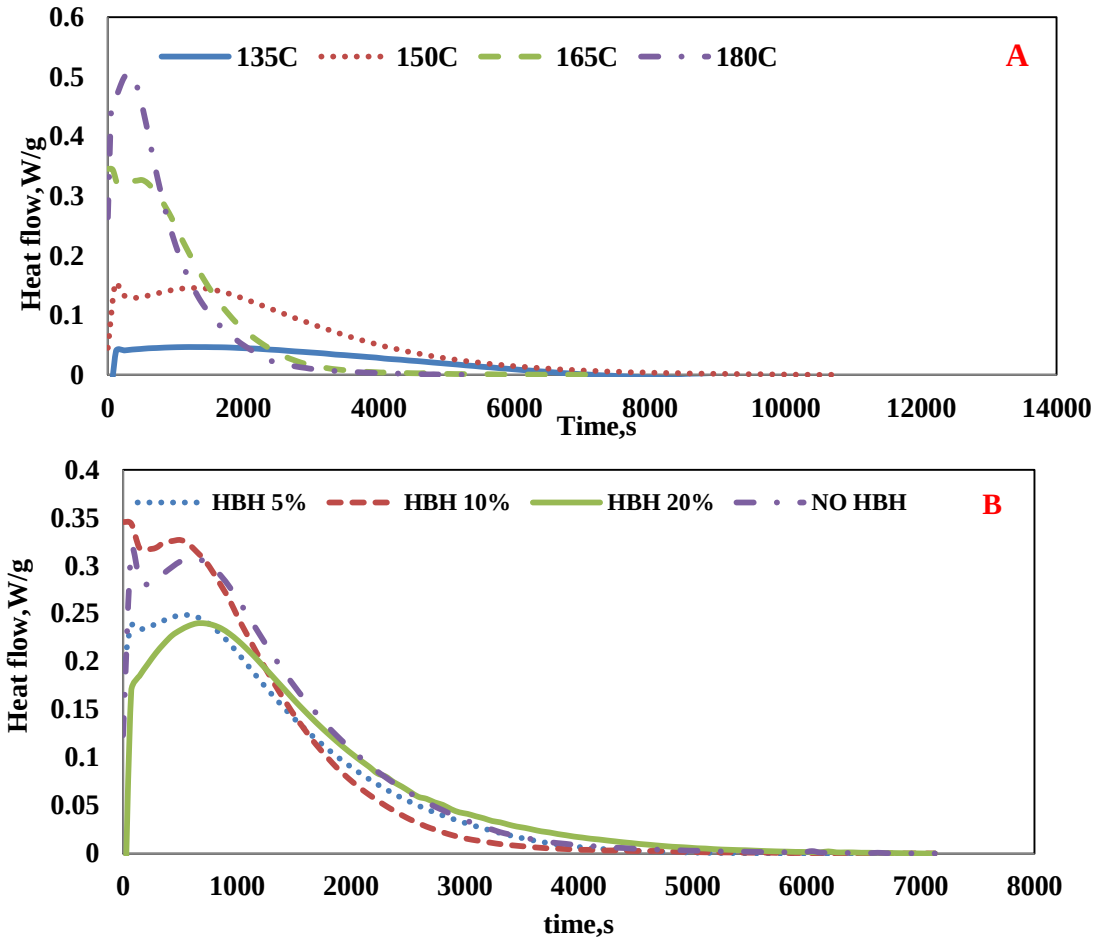

Figure 3. (A) Effects of cure temperature on intra-gallery reaction on the TGAP/ [MMT (5 wt %) +Hybrane (10 wt %)]/DDS. (B) Isothermal DSC scan of the TGAP/MMT (5 wt %) +Hybrane (0, 5, 10 and 20 wt %) /DDS (52 wt %) at 165^{o}C

The quality of the final nanostructure was studied by TEM. Figure 4 shows that hundreds clay layers with narrow *d*-spacing stick together in ordered arrangement as big agglomeration with more than 5 μm size in low magnitude in contrast of the sample without Hybrane that cured in high temperature like 180^{o}C (Paper III) which has agglomerations in small size (less than5μm) with wide *d*- spacing between clay layers that places in disordered arrangement. As results, the incorporation of Hybrane in TGAP- clay based nanocomposite leads to poorly exfoliated structure.

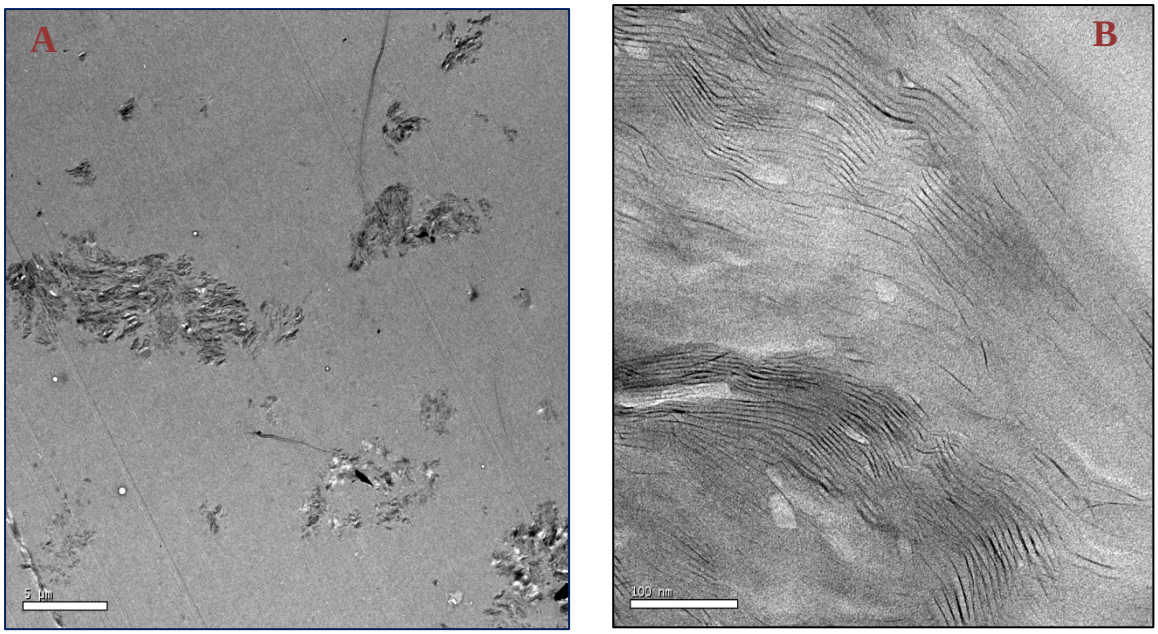

Figure 4.TEM micrographs of TGAP/MMT (5 wt %) +Hybrane (10 wt %) /DDS (52wt %) that cured isothermally at 165^{0}C for 2 H; A: scale bar is 5µm. B: the scale is 100 nm.

Conclusion

It can be finally concluded that the Hybrane H 1500 initiated the cross-linking reaction through proton- accepter of the end hydroxyl groups and also leads to retard the intra-gallery reaction. Furthermore, the magnitude of the intra- gallery reaction is depended on the cure temperature and Hybrane loading which are determined as 165^{o}C and 10 wt % , respectively. Also, this ternary system (TGAP-clay nanocomposite in corporation of Hybrane H 1500) does not show the exfoliation as well as the sample without Hybrane which is confirmed by TEM pictures. Hence, there is limitation to increase the exfoliation degree or generally toughening of the TGAP based nanocomposite by means of the Hyperbranched polymer due to the type of the epoxy and Hyperbranched polymer and rate of the intra-gallery reaction.